ORYX 2.0

A PLANETARY EXPLORATION MOBILITY PLATFORM

Robotics & Intelligent Vehicles Research Laboratory

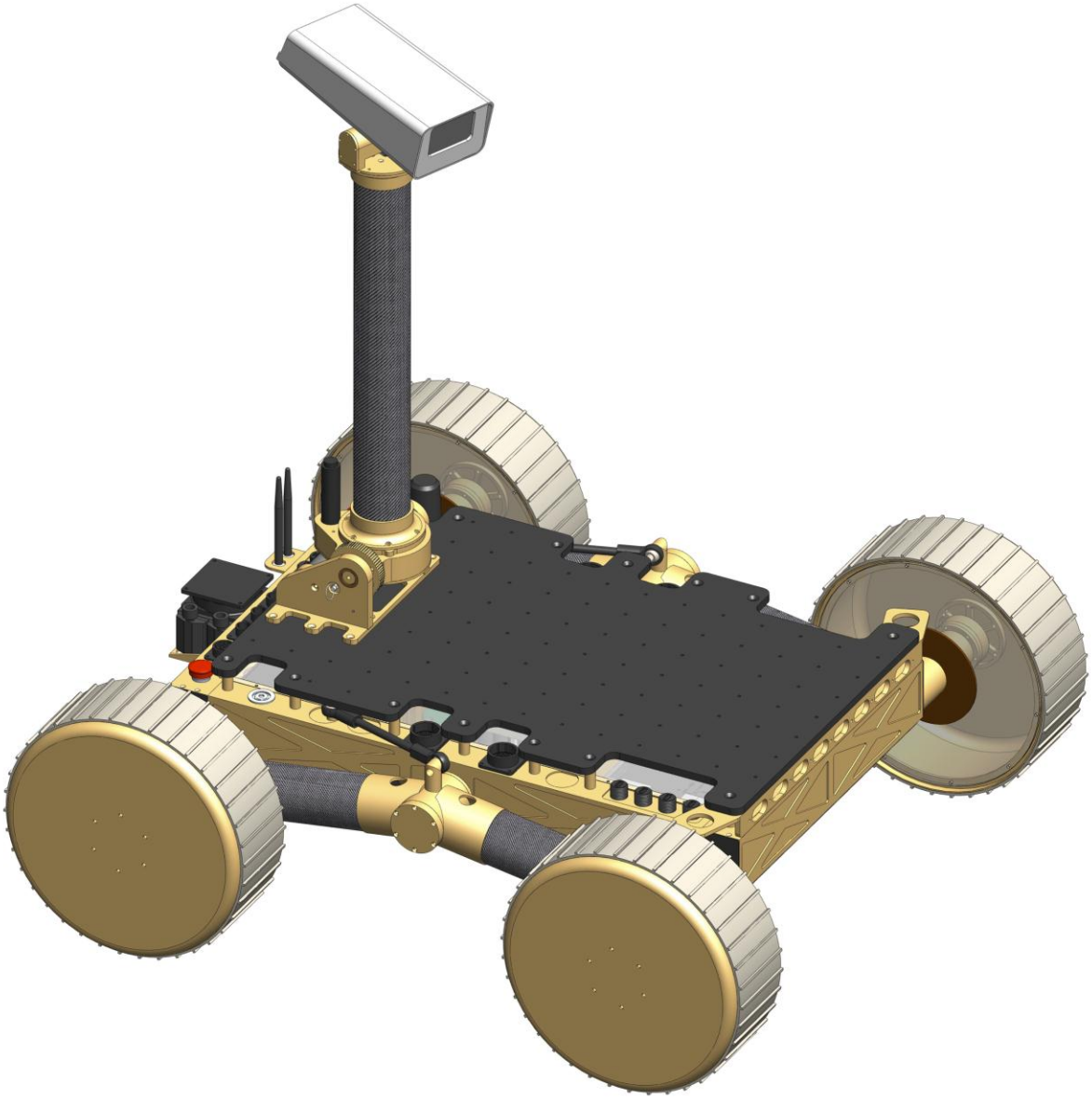

AUTHORS

Joseph L. Amato
Jon J. Anderson
Thomas J. Carlone
Michael E. Fagan

KEYWORDS

1. WPI Robotics
2. Planetary Rover
3. Passive Averaging Suspension
4. Robot Operating System (ROS)
5. NASA RASC-AL Robo-Ops

ORYX 2.0:
A Planetary Exploration Mobility Platform

A Major Qualifying Project Report
submitted to the Faculty of
WORCESTER POLYTECHNIC INSTITUTE
in partial fulfilment of the requirements for the
Degree of Bachelor of Science
by

Joseph L. Amato
Jon J. Anderson
Thomas J. Carlone

A Major Qualifying Project Report
submitted to the Faculty of
WORCESTER POLYTECHNIC INSTITUTE
in partial fulfilment of the requirements for the
Degree of Bachelor of Arts
by

Michael E. Fagan

Date: April 26, 2011

Report Submitted to:
Professor Taskin Padir, Advisor, WPI
Professor Kenneth Stafford, Advisor, WPI

ABSTRACT

ORYX 2.0 is a modular mobility platform designed for operation on rough terrain to facilitate space related technology research and Earth based exploration missions. Currently there are no low-cost rovers available to academia or industry, making it difficult to conduct research and testing related to surface exploration. ORYX 2.0 fills this gap by serving as a platform that can operate in analog Martian or lunar environments, and can withstand harsh Earth conditions while also providing users with many features to simplify payload integration. A standard mechanical and electrical interface aids in this process, and the use of Robot Operating System (ROS) provides a common software architecture for research platforms. A passive kinematic averaging suspension provides excellent mobility over obstacles in addition to improving stability and even weight distribution. The rover chassis is sealed to provide all electronics with environmental protection from dust and water. Extended field testing was done to evaluate both the mobility aspects of the rover and its ability to integrate and transport payloads. Mobility performance far exceeded expectations, with ORYX 2.0 climbing obstacles up to three times its intended limits. Multiple teleoperated field testing trials on a variety of terrains validated the rover's ruggedness and ability to operate soundly over long periods. Lastly, a sample payload in the form of a deployable camera boom was designed, built, and tested in order to demonstrate the effectiveness of payload integration features.

ACKNOWLEDGEMENTS

We would like to thank our project advisors; Taskin Padir, Kenneth Stafford, and Brad Miller, for their constant support. We would also like to thank those who supported this work through financial sponsorship and the donation of services and components, including NASA's Software, Robotics and Simulation Division, JSC; National Institute of Aerospace; Worcester Polytechnic Institute; Maxon Precision Motors, Inc.; Linemaster Switch Corporation; InterSense, Inc.; The Mathworks Inc.; Axis Communications; Barnstorm Cycles; Tesla Motors; and igus inc. Without the generous support of these corporate sponsors this project would not be possible.

TABLE OF AUTHORSHIP

	Author
Abstract	Carlone
Acknowledgements	Carlone
1. Introduction	Carlone
2. Background	Carlone
2.1 Recent Rovers and their Missions	Carlone
2.1.1 NASA's Mars Rovers	Carlone
2.1.2 Google Lunar X-Prize and Red Rover	Carlone
2.2 Rover Mobility as the Common Problem	Fagan
2.2.1 Rover Suspension Systems	Fagan
2.2.2 Rover Hazard Avoidance	Amato
2.3 Analog Testing in Harsh Earth Environments	Anderson
2.3.1 NASA's Rock Yard and Mars Yard Facilities	Anderson
2.3.2 NASA's Analog Field Tests	Anderson
2.3.3 Ruggedness Requirements for Harsh Earth Environments	Fagan
2.3.4 NASA's Competitions as Analog Tests for New Technologies	Amato
3 Design Requirements & Specifications	Carlone
4 Design and Analysis	Carlone
4.1 Mobility	Carlone
4.1.1 Chassis Design and Rocker Differencing Suspension	Carlone
4.1.2 Wheel Design	Carlone
4.1.3 Drive Motor Selection	Carlone
4.2 Electronics and Communications	Anderson
4.2.1 Selecting the Main Computer	Anderson
4.2.2 Battery Selection and the BMS	Fagan
4.2.3 Power Distribution	Fagan
4.2.4 Communications Hardware	Fagan
4.3 Diagnostic Systems	Anderson
4.3.1 Temperature Monitoring	Anderson
4.3.2 Slope Monitoring	Carlone
4.3.3 Battery Management	Fagan
4.4 Software Architecture	Amato
4.4.1 ROS Framework	Amato
4.4.2 Software Design and ROS Nodes	Amato
4.5 Payload Interface	Carlone
4.5.1 Payload Hardware Interface	Carlone
4.5.2 Deployable Vision Payload	Carlone
4.6 Matlab Simulation and Velocity Controller	Carlone
4.6.1 3D Kinematic Model	Carlone
4.6.2 Feed Forward Velocity Control	Carlone
4.6.3 Matlab Simulation Results	Carlone
5 Subsystem Testing and Validation	Carlone
5.1 Temperature Testing	Carlone

LIST OF FIGURES

LIST OF TABLES

ACRONYM REFERENCE TABLE

ACRONYM	MEANING
ANSI	American National Standards Institute
ARC	Ames Research Center
ATHLETE	All Terrain Hex Limbed Extra Terrestrial Explorer
BMS	Battery Management System
CMU	Carnegie Mellon University
D-RATS	Desert Research and Technology Studies
GUI	Graphical User Interface
IEC	International Electrotechnical Commission
IMU	Inertial Navigation Unit
ISO	International Standards Organization
JPL	Jet Propulsion Laboratory
JSC	Johnson Space Center
MER	Mars Exploration Rover
MIL-STD	Military Standard issued by the US Department of Defense
MSL	Mars Science Laboratory
MQP	Major Qualifying Project
NASA	National Aeronautics and Space Administration
NEMA	National Electrical Manufacturers Association
NIA	National Institute of Aeronautics
RASC-AL	Revolutionary Aerospace System Concepts - Academic Linkage
ROS	Robot Operating System
SEV	Space Exploration Vehicle
WPI	Worcester Polytechnic Institute

Table of Contents

1 INTRODUCTION

The high costs and dangers associated with space exploration have led NASA and other private enterprises to pursue planetary research through the use of unmanned robotic systems. Continued interest in lunar, Martian, and deep-space exploration has created a demand for many surface rovers, for a variety of research purposes. With the moon, much of the interest lies within its potential reserves of frozen water, methane, and ammonia, which have the potential to be converted into fuels (Neal, 2009). These moon-made fuels may greatly reduce the costs of future space exploration, by reducing the amount of fuel that needs to be transported from Earth. The moon's potential abundance of Helium-3 is another area of key interest, as it may be used as a fuel for clean fusion power plants on Earth (Blewett, Ouyang, & Zheng, 2008). Similarly, interest in Mars stems from our desire to learn more about its environment and potential to support life and future colonization.

While there are many reasons to explore the moon and Mars, few have had enough economic potential to gain direct interest from the private sector. Due to the high cost of space exploration, most missions to date have been conducted by NASA and other government-supported organizations. However, the continually decreasing cost of technology and economic potential in natural resources has led some private companies to pursue space transportation and exploration as a core business. For example, Astrobotic Technology, Odyssey Moon, and Armadillo Aerospace are just a few companies that are developing rovers and landers for different space missions. While companies like these have made progress in the commercialization of space exploration, the inherently high costs continue to hinder economic feasibility.

There are many factors contributing to the high cost of space exploration. Launch vehicle costs are the most substantial barrier to private enterprise. While the cost associated with getting materials to space varies largely based on the size and capacity of the rocket, some estimates show that it costs about $10,000 per kg to get material into Low Earth Orbit (LEO) (Wilcox, 2006). However, some evidence suggests that the costs of planetary exploration are even higher. For example, the company Astrobotic Technology currently has a launch agreement to send their lunar rover to the moon, and is offering to integrate third-party payloads on their lander or rover. Companies and government organizations have the opportunity to add payloads, such as scientific equipment or mini-rovers, at the cost of $1,800,000 per kg (Astrobotic, 2011). This large difference in price between getting material to LEO versus the surface of the moon shows how prohibitive the costs of planetary exploration can be.

These high launch costs mean that all space vehicles and space-related technologies must be thoroughly tested on Earth, before they make the expensive journey to space. Whether it is NASA's space shuttle, a robotic arm for the international space station, or a surface exploration rover, all components and systems are tested in analogous Earth environments. For planetary exploration rovers these analog tests are normally conducted in harsh Earth environments such as

the deserts of Arizona or the frozen tundra of the Arctic. Places like these are also used to test the ruggedness of the rovers and their resistance to large temperature swings. They also have similar terrain to the Mars or the moon, making them ideal for testing the rover's mobility. While this type of analog testing is very useful, it is not without its own high costs.

The need to develop specialized high-fidelity systems capable of operating in harsh earth environments typically leads to longer development timelines and greater expenditures. While specific applications will always require unique designs, there are many commonalities in planetary rovers. Issues such as mobility, navigation, and vision, may differ slightly between missions but are largely the same in most scenarios. Given these fundamental characteristics of many planetary rovers we believe that a modular and ruggedized system meeting these basic requirements would aid in the process of developing space-ready technology. There are currently many mobile research platforms available, yet few are designed to operate in the harsh earth environments that are often used for planetary surface rover testing. By creating a rover that is suitable for these types of environments, our goal is to facilitate the development of rovers and their related technologies, in addition to lowering development costs. We also hope that the platform developed can be tested and improved upon, to potentially serve as a model for a rover that could go to the moon or Mars in the future.

Our mission is to design, develop, and test a rover to serve as a research platform, suitable for testing planetary surface exploration technologies in harsh earth environments. The design will focus on incorporating features that are believed to be essential for most planetary exploration missions including:

1. Mobility and basic navigation
2. Tele-operation and intuitive user controls
3. Low mass and small form-factor

The rover will also aim to be low cost, ruggedized, and modular to allow for easy additions of custom or Commercial-Off-The-Shelf (COTS) hardware components. It will also have sufficient computing power and standard I/O ports to support a variety of additional payloads. The goal is to provide a platform that can be easily used for the development, testing, and validation of space exploration technology, both hardware and software.

2 BACKGROUND

This chapter will begin by reviewing some past space exploration rovers as well as rovers currently in development. It will discuss specific missions along with the corresponding design features and capabilities, specifically relating to mobility and navigation, that made these rovers successful in meeting their objectives on the Martian or lunar surface. Next, specific features of these rovers are discussed in order to learn more about the types of technologies that are often used on exploration rovers. Both hardware and software design choices are reviewed, as they relate to the mobility challenges of ground compliance and hazard avoidance. Lastly, research into analog testing presents what is currently being done by NASA and others to validate planetary rovers on Earth. A variety of harsh Earth environments are examined for their suitability in analog testing based on how well they represent certain aspects of the Martian and Lunar environments. A few NASA sponsored competitions are also reviewed, as they can often provide unique opportunities for analog testing at NASA facilities.

2.1 Recent Rovers and Their Missions

Much of space exploration can be divided into three categories: a quest to better understand our universe, interest, and economic potential in using natural resources outside our planet, and the future colonization of extra-terrestrial bodies. Furthermore, most interest has been in our moon and Mars, as these planetary bodies are close by, and have environments that are hospitable enough for rovers, and potentially for future colonization.

Our moon has been relatively undisturbed by wind or water for billions of years, making it an attractive place for scientists who are interested in exploring the origins of our solar system or how the sun has varied over time (Neal, 2009). The moon is also very well suited for scientific equipment such as radio observatories or IR telescopes, as it has no atmosphere, instruments such as these can measure signals that would otherwise be disturbed or eliminated on Earth. Reconnaissance missions around the moon have revealed several natural resources such as water, methane, and other volatiles (Neal, 2009). These resources may make it possible to create an outpost or a way to manufacture fuel on the moon. It is likely that future missions to our moon and Mars will require that 85% of total launch mass to be propellant (Wilcox, 2006). This greatly adds to the cost of launches and limits the amount of non-propellant payloads that can be transported. Operating directly from the moon greatly reduces this cost, and can provide a base to send rovers or people deeper into space. Helium-3 is another resource on the moon that has been implanted into the regolith by solar winds over millions of years. If it becomes technologically and economically feasible to transport back to Earth, Helium-3 could prove to be the fuel of the future, given its efficiency in fusion reactors and low residual radioactivity (Blewett, Ouyang, & Zheng, 2008).

Interest in Mars mostly relates to expanding our knowledge of the planet, specifically with

respect to its ability to support a human colony. Learning more about the composition of its atmosphere and soil can tell us whether Mars could potentially support microbial life.

This chapter will review several surface rovers that currently in development and that have already been deployed for Mars and moon exploration missions. We discuss current and past rovers that were created by NASA and private companies in an effort to explore a wide variety of rover types. While each rover has a unique mission, we also look for commonalities in rover design features. The main objective is to understand the types of tasks that rovers are used for and to examine common features that will influence our rover design.

2.1.1 NASA's Mars Rovers

Since 1976, NASA has been exploring the surface of Mars with rovers, starting with the dual landing of Viking 1 and Viking 2 landers (Adler & Manning, 2005). In 1997, The Mars Pathfinder (MPF) lander delivered the Sojourner Rover to the surface successfully. Most recently, in early 2004, NASA again landed two more rovers on Mars, Spirit and Opportunity. For the next mission scheduled in November 2011, NASA will launch the Mars Science Laboratory (MSL) with a rover named Curiosity. Despite the multiple rovers that NASA has sent to Mars, each mission has similar objectives. They are mainly to analyze the chemical composition of the soil and atmosphere to determine if the Martian environment could support microbial life, past or present.

Of the two most recent rovers sent to Mars, Spirit has been unresponsive to communications since August 2010, while Opportunity has remained operational and active. To accomplish their mission each rover is equipped with several scientific instruments, designed to analyze the chemical composition of rocks and soil. Instruments such as the rock abrasion tool, spectrometers, and microscopic imagers are mounted onto the rover's arm were they are positioned to collect and analyze a variety of soil and rock samples from different locations. To safely move to different sampling locations of interest, these rovers employ many autonomous planetary mobility technologies.

Making improvements form past Mars rovers, NASA has continued to develop autonomous navigation to make it easier and quicker to control their rovers, given the relatively large time delays in sending commands. To do this, on-board stereo vision processing was used to develop an image on the environment, which identified positive and negative obstacles relative to the ground plane. Using this data, the rover would calculate the shortest and safest path and then executes the path in 0.5 to 2.0 meter increments, before taking more images and repeating the process (NASA JPL, 2011). This allows NASA to simply command a desired location for their rovers, instead of more conventional teleoperation techniques. Given the increased capabilities of the MER, they were able to process stereo images with 16,000 data points and autonomously navigate at speeds of about 9 mm/second (NASA JPL, 2011). Additionally, the MERs use visual

odometry to supplement their stereo vision and get a more accurate estimate of where they are relative to known objects.

The other main features of the MERs relate to mobility hardware, which allowed them to traverse the Martian terrain with relative ease. In continuation of past Mars rover designs, the rocker-bogie suspension was used. It consists of six wheels and multiple axles that allow the rover to overcome obstacles larger than its wheel diameter. The specialized wheels of the rover are approximately 26 centimeters in diameter and have a unique aluminum flexure structure to connect the hub to the rim of the wheel. These flexure joints act as shock absorbers which help to reduce the shock loads on other components of the rover (NASA JPL, 2011). Each wheel also has small cleats, which have been found to be effective both for soft sandy terrain and in navigating over rocks. An artistic rendering of a MER is shown in Figure 1.

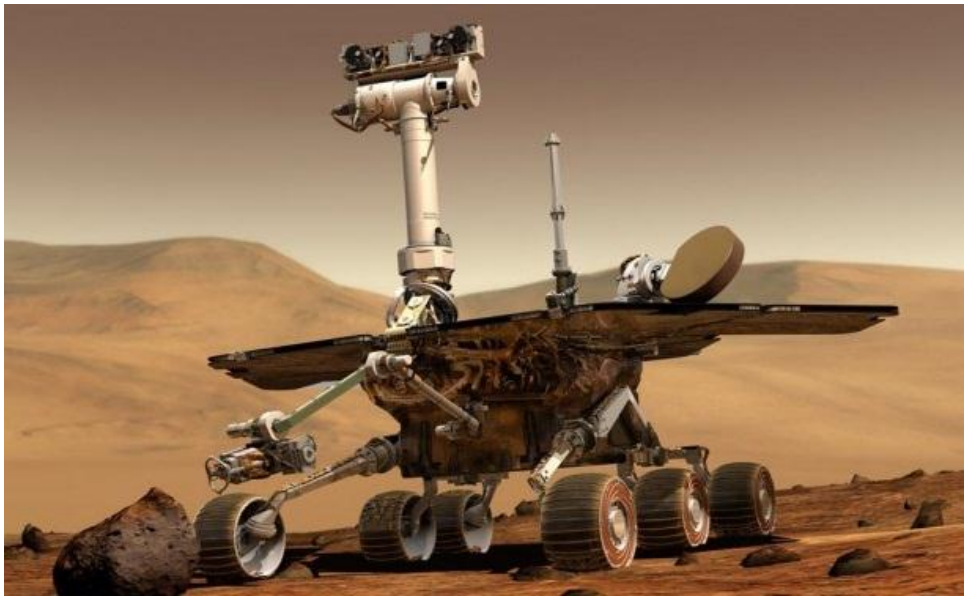

Figure 1: Artistic Rendering of a MER Rover

NASA's newest Mars rover, which is currently en route to Mars, may look very similar to its predecessors; however, its increased size gives it greater mobility and a larger payload of more advanced scientific instruments. With a similar mission of searching Mars for conditions that could support life or preserve a record of past life, Curiosity has a multitude of high-tech sensors. With in-situ instrumentation such as: mineralogy X-ray diffraction, Chemcam, radiation assessment detector, dynamic albedo of neutrons, alpha particle X-ray spectrometer, and a suite of other sample analysis instrumentation, Curiosity is a powerful chemistry laboratory (NASA JPL, 2011).

To transport all of these instruments between sampling sites, Curiosity will be using similar autonomous navigation and path planning as the MER rovers. More memory and processing power combined with newer software that was developed and tested on the MER rovers will give

Curiosity an advantage in terms of its path planning ability. It will also have a three axis inertial measurement unit (IMU), enabling the rover to make precise movements while also monitoring the degree of tilt that the rover is experiencing (NASA JPL, 2011).

To tackle the mobility challenge, the 900kg rover has a very similar 6 wheel rocker-bogie suspension as previous Mars exploration rovers have. The larger size combined with the rocker-bogie suspension allows the rover to go over obstacles 60-75cm higher, which is greater than its wheel diameter of 50cm (JPL & California Institute of Technology, 2009). It can also safely traverse slopes up to 45°, but is limited to 30° slopes by software to ensure a factor of safety (NASA JPL, 2009). Curiosity also has cleated treads that are similar to the MER rovers, which were found to be an optimal solution for Martian terrain. With a top speed of 4cm/sec, it will be the fastest rover sent to Mars; however actual operation speeds are estimated to be around 22mm/sec (JPL & California Institute of Technology, 2009). Figure 2 is a picture of NASA engineers testing Curiosity.

Figure 2: NASA's Curiosity Rover in a Testing Facility

In reviewing NASA's rovers for surface exploration on Mars, mainly MER and MSL, there were many similarities in both their mechanical design and software that enable the rovers to perform on-board path planning. Autonomous planetary navigation combined with hazard avoidance and other self-preservation autonomy makes these rovers excellent platforms to reliably transport and position their scientific instruments. It should also be noted that across all missions to Mars the basic mobility challenge, and the resulting hardware and software solutions, were very similar. The biggest changes between missions have been the size of the rover and the types of scientific instruments it supports. There have also been some changes in the computing power, and methods to generate power as technology has changed to allow for better and lighter solutions.

2.1.2 Google Lunar X-prize and Red Rover

A recent X-prize, sponsored by Google, is encouraging lunar exploration by offering $20,000,000 to the first team to successfully land on the moon, travel at least 500m, and send back video and other data. Currently, 26 teams from around the world are fundraising, planning, and designing robots in an effort to be the first privately funded organization to send a rover to the moon. The large prize money has in essence created another race to the moon; however, this race is between privately funded teams and has become part of the trend towards the commercialization of space exploration.

Astrobotic Technology Inc. is one such company that has founded itself on making space exploration profitable, by delivering payloads and performing robotic services on the moon (Astrobotic, 2011). They are currently in collaboration with Carnegie Mellon University and others, to develop a rover and lander for their first surface lunar exploration mission, which if successful will satisfy the X-prize criteria as well as other objectives. Their robot, called Red Rover, is reviewed here because it is one of the most developed lunar exploration rovers, and will likely be the next rover to land on the moon. Red Rover is designed to be a scout, exploring places such as polar ice fields or skylights into lunar lava tubes. Its goal will be to determine where the interesting locations are, based on its analysis of chemical composition and high resolution 3D images. Some chemical compounds of particular interest are frozen water and Helium-3, which may have the most potential in terms of an economically feasible outpost on the moon.

To facilitate roving about the lunar surface, Red Rover uses a 4 wheel rocker differencing suspension system. This type of passive suspension is based on the rocker-bogie design but is simplified by reducing the number of wheels and free-pivoting axles. It drives the two wheels on each side of the rover together, and thus relies on skid-steering to rotate the rover. For vision, Red Rover has a stereo camera and flash LIDAR which will allow it to make high-resolution terrain maps. While it will likely have some form of on-board autonomous hazard avoidance or path planning it is unclear exactly to what extent, as available information only suggests that the rover will be teleoperated. Figure 3 is a picture of one of the recent prototypes of Red Rover.

Figure 3: Recent Prototype of Red Rover

2.2 Rover Mobility as the Common Problem

One of the most challenging aspects of rover operation in planetary environments is effective mobility. In order for a rover to complete any science tasks, it first must be able to move confidently in unforgiving terrain. This may include both challenging surfaces and wider-scale terrain discontinuities. Surface challenges to rover mobility include fine powders such as lunar regolith, scree fields, and larger rocks. Topographic features such as craters, hills, gullies, and cliffs present different forms of challenges. To complicate the problem further, many planetary environments are not well studied, so rover mobility systems must be flexible to accommodate unknown factors. Effective rover mobility systems combine robust mechanical hardware with sensors and programming to detect impassible terrain.

2.2.1 Rover Suspension Systems

From a mechanical standpoint, the goal of any rover mobility system is to reduce the impact of variable terrain on the rover's ability to traverse a given path. This typically involves a suspension system which allows the rover to travel over certain obstacles in its path as well as absorb shocks and unevenness. All planetary rovers and many Earth-based rover prototypes have incorporated a suspension system as a key aspect of their mobility systems.

The most basic mobility system is the wheel, and an effective wheel design becomes a major part of any rover drive system. Most planetary rovers have used all-metal wheels for their high strength-to-weight ratio. NASA/JPL's 10.5 kilogram Sojourner rover used 13 centimeter one-piece aluminum wheels with sharp stainless steel cleats to climb obstacles and gain traction in soft soil. Sojourner's wheels were rigidly connected to the drive motors with no suspension elements. Sojourner was programmed to climb obstacles up to 6 centimeters under autonomous

control and potentially up to 13 centimeters (1 wheel diameter) in some circumstances (Mars Pathfinder Engineering Team, 1997).

When JPL engineers designed the twin MERs, Spirit and Opportunity, they decided to incorporate suspension into the wheel elements to help accommodate the additional strains of the 180 kilogram rover chassis traversing over obstacles up to 26 centimeters (1 wheel diameter) in height. The single-piece aluminum billet wheels were machined with thin spiral flectures in the hub which absorbed a considerable portion of shock received both during landing as well as planetary operation (Watanabe, 2007). Solimide foam was used to fill gaps in the wheels to prevent foreign object intrusion. Sojourner's stainless steel cleats were replaced with aluminum ribs machined directly into the wheel rim. Additionally, MER's wheels are crowned which allows them to move more easily when steering.

The Mars Science Laboratory is the latest NASA/JPL vehicle to travel to Mars. It has large billet aluminum with thin straight spokes and a zigzag aluminum pattern machined into the outer surface. These 50 centimeter wheels will support the 900 kilogram rover over obstacles up to 75 centimeters in height. Additionally, MSL's wheels will need to support the rover during its final landing, a large shock load. The Mars Science Laboratory plans to drive about 12 kilometers during its mission, most of it autonomously. Figure 4 is a picture showing all three wheels of the various Mars rovers.

Figure 4 : (L-R) MER, Sojourner, and MSL wheels

The next critical member in the rover mobility system is the mechanical geometry connecting the individual wheel and drive modules with the rover chassis. These components are typically articulated to increase the maximum obstacle the rover is capable of traversing, as well as maintain stability on tilted terrain. These mobility systems can also incorporate passive or active suspension elements which help reduce the shock loading experienced by the rover chassis. The two most common methods of articulating mobility systems include rocker bogie and rocker differencing.

The rocker differencing system, primarily used on four-wheeled vehicles, utilizes two large structural elements known as rockers which connect the drive elements on each side of the rover. The two rockers are connected to the rover chassis by a rigid pivot, and are connected to each other through a mechanical linkage. This connection, which may take the kinematic form of a 5-bar linkage or a geared differential, reverses the movement of the two rockers with respect to one another. Thus, if the right hand rocker is raised in the front, the left hand rocker will be raised in the rear. The chassis, suspended in the middle, moves half of the total angular displacement of the two rockers, a characteristic known as pitch-averaging. This is a significant advantage if the rover is traversing sloping terrain or surmounting an obstacle with a single wheel.

While no rover has travelled to another planet with a rocker differencing system, this system has been used on several Earth-based rover platforms, particularly Carnegie Mellon's Scarab rover. This rover uses a 5-bar mechanical linkage to connect the rockers. Additionally, Astrobotic Technologies' Red Rover, a Google Lunar X-Prize competitor, has used both a rocker differencing suspension with a central geared differential and a 5-bar mechanical linkage in various versions.

The most common type of mobility system for Earth-based rovers and the most common mobility system to travel to another planet is the 6-wheel rocker-bogie system. This system, pioneered by JPL in the Rocky series of rovers and ultimately patented, has all the features of a rocker differencing system with the addition of a second, freely pivoting link connecting the rear two wheels, known as a "bogie" after the freely pivoting suspension members used in trains (Wilcox, 2000 and 2001). The additional link supports a central wheel and helps surmount larger obstacles while keeping the overall system mass down (Harrington, 2004). The addition of the bogie also supports flight hardware which must collapse to fit in the size limitations of the launch system. Like a rocker differencing system, the rocker may be connected with either a mechanical linkage or a geared differential system. In the MER rovers, the linkage is connected with a pair of epicyclic gear-sets on either side of the rover chassis. Figure 5 and Figure 6 show the rocker bogie suspension that was used by MSL's Curiosity and Sojourner respectively.

Figure 5: Mars Science Laboratory chassis showing suspension and wheels.

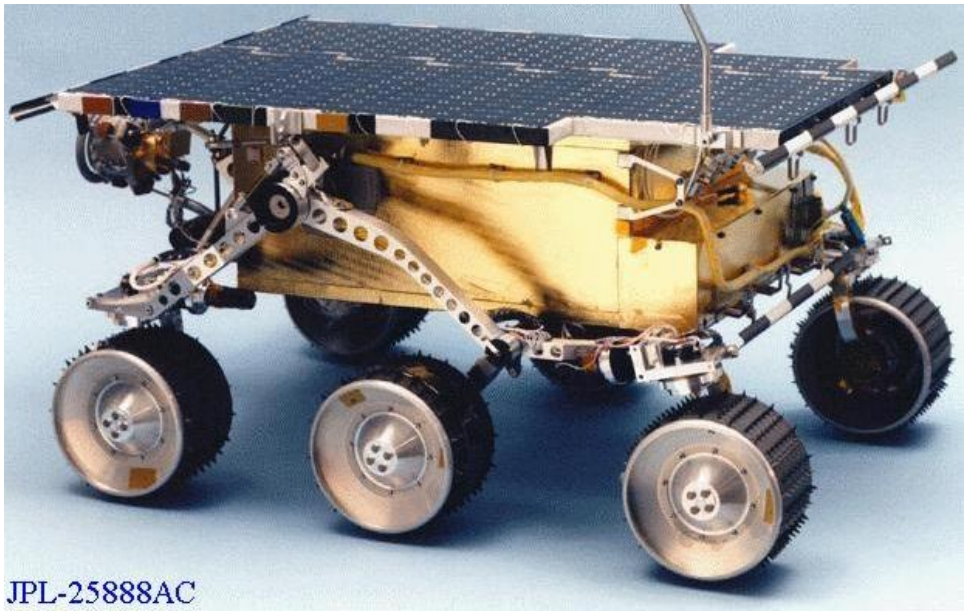

Figure 6: Rocker-bogie suspension system of the Mars Pathfinder rover, Sojourner

Many different variations on the rocker-bogie system have been built with various materials, but they typically contain tubular elements for the rocker and bogie links as well as sensors for determining the various joint orientations (Lindemann, 1999). Rovers that use a geared differential frequently have a large-diameter torque tube to transfer the forces inherent in the rocker system. The primary benefit to a rocker-bogie suspension is that a rover is able to climb an obstacle up to twice the diameter of its wheels while keeping all 6 wheels in contact with the surface. Because the front and rear wheels can help to push or pull the free-floating bogie link, it

is able to go over relatively large obstacles compare to its wheel size (Bickler, 1989). As a suspension system, the rocker-bogie contains no spring elements, and this helps provide stability while going over large obstacles (Miller and Lee, 2002).

Advanced rover mobility systems such as rocker bogie, rocker differencing, and novel wheel designs are key aspects of rovers capable of traversing extreme planetary terrain. These systems, in conjunction with advanced sensor capabilities, allow the rovers to operate without intervention in potentially hazardous situations. They also help improve stability and reduce the shock experienced by the rover chassis and scientific instruments.

2.2.2 Rover Hazard Avoidance

The other main aspect of rover mobility is hazard avoidance and autonomous planetary navigation relating to how the rovers are ultimately controlled. Unfortunately, it is not always feasible for the operator to maintain continuous manual control of the rover. Large distances and low bandwidth rates between Earth and where the rover is operating often lead to unacceptably high latencies for near-real-time teleoperation control. Furthermore, operators can damage the rover if they are not aware of near-by hazards. For these reasons, it is often necessary that some level of autonomy be introduced into such rovers. This autonomy can range anywhere from a reaction to a nearby obstacle to full-blown path planning and autonomous navigation.

The Mars Rovers Spirit and Opportunity utilize basic autonomous navigation to safely travel to operator-specified waypoints (Viotti, 2011). By taking pictures of the surrounding environment, the Mars rovers determine which location they can and cannot travel through, and then choose the "shortest, safest path towards the programmed geographical goal." Furthermore, an advanced visual odometry system helped to address wheel slip problems commonly associated with driving through sandy or rocky terrains and on steep slopes. The visual odometry system works by "comparing pictures taken before and after a short drive, automatically finding dozens of features in the terrain" (Viotti, 2011). In doing so, the rover is able to make a more accurate estimate of its actual location than would be possible through traditional odometry.

Before any autonomous hazard avoidance or path planning can be conducted, however, the robot must first be able to sense its surroundings and determine which parts of the terrain are passable and which should be labeled as obstacles. While there are numerous methods of identifying obstacles, there are two in particular that see promise in space-based robotics.

One of these techniques is stereo vision, which is arguably one of the most common tools used on rovers to observe and understand their environment. By positioning two cameras a fixed distance from each other and comparing their respective images, a stereo vision system can generate a 3-dimensional point cloud of the surrounding landscape (Andersen, 2004). Unfortunately, stereo vision requires large amounts of processing power to return accurate

results. However, even with significant amounts of computing power available to process the stereo image data, a rover may still need to travel at low speeds if it is to detect and avoid obstacles. Figure 7 shows a point cloud of terrain that was obtained with a stereo camera.

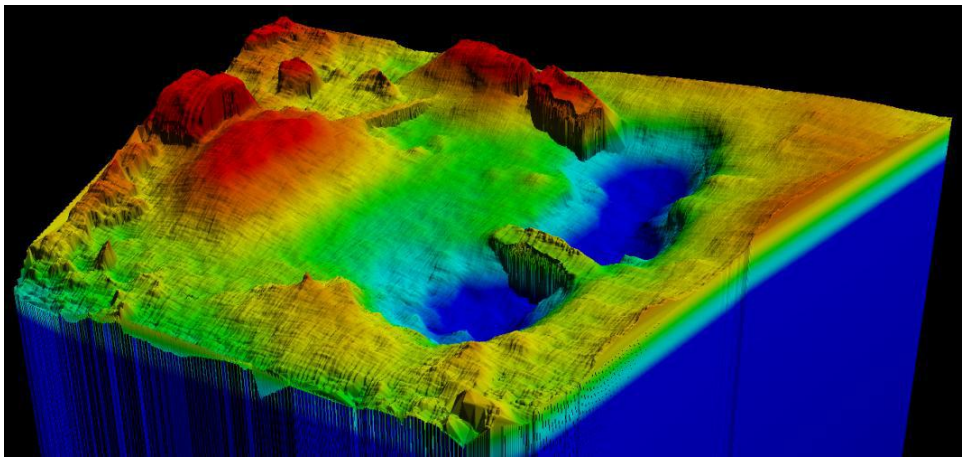

Figure 7: Stereo Camera Point Cloud with Color Depth Mapping of Terrain (Short, 2004)

One alternative to a stereo camera and its large computational needs is a 3D time of flight camera. 3D time of flight cameras operate by flashing a light pulse and measuring the amount of time it takes for the light pulse to hit a surface and return to each pixel in the camera's CMOS (Oggier, 2006). As the speed of light is a constant, each pixel can be given a distance value by finding the product of the speed of light and half the time it took for the light pulse to reach each individual pixel. Because finding the distance of objects requires only some basic multiplication, 3D time of flight cameras require relatively little processing power, and can often operate at high frame-rates (Ringbeck, 2007). Such cameras are not without their drawbacks, however. Most 3D time of flight cameras in production have lower resolutions, often as low as 64x48 pixels. While this is enough to generate a ground plane, the low resolution may make it difficult to distinguish between small obstacles. Furthermore, because they work by detecting a flash of light, historically, many 3D time of flight cameras have not performed well outdoors where the sunlight over-saturates the camera's flash (ProViScout, 2010). Recent improvements have reduced this limitation, making these sensors a viable option for rover navigation. Figure 8 is an example of the types of depth images that can be generated using this technology.

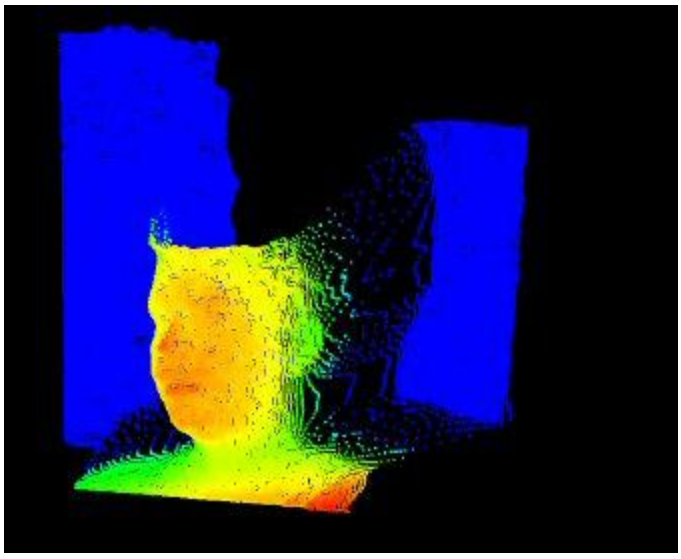

Figure 8: Depth Map Generated from a 3D Time-of-Flight Camera

The output of both types of 3D imaging systems is a data container known as a point cloud. A point cloud stores many samples of the sensor's surroundings in 3D space. The point cloud can be processed and used for obstacle detection and path planning. Ground plane detection entails using the 3-dimensional data, in conjunction with colored image data, to determine which parts of the image can be classified as traversable ground (Goldberg, 2002). If an object lies above the ground plane, and is in the path of the robot, it can be viewed as an obstacle (Zhou, 2006). Furthermore, by generating a ground plane, it is possible to search for negative obstacles, such as cliffs (Broggi, 2005).

2.3 Analog Testing in Harsh Earth Environments

Despite the many technological advances and increased interest in planetary exploration the cost of launch is still very high. With $2.3 billion invested in a mission likes NASA's Mars Science Laboratory, Earth-based testing is crucial to ensure each system will operate correctly (Chang, 2008). One of the common testing procedures in space technology development is extensive analog mission testing. Analog mission testing exposes potential space systems to harsh earth environments that closely represent the environment of the proposed mission (Lind, 2011). Veterans of space exploration, like NASA, have determined locations on Earth that make for appropriate analog testing sites. With current rover missions focused on Mars and the moon, such as those discussed above, a majority of NASA's current analog sites are well representative of the terrain seen on these two planetary bodies. Current analog mission testing sites are a combination of man-made facilities and naturally occurring earth landscapes such as deserts.

Numerous missions to our moon, both manned and unmanned, have been used to develop a reasonable understanding of environmental conditions on the surface of the moon. The moon is home to a variety of different geographic topography. As lunar exploration resumes, rovers will need to overcome a variety of difficult terrain types and withstand the extreme conditions on the

lunar surface. Craters, mountains, ridges, valleys, and rocks ranging from large to small make up the surface of the moon (Wilhelms, 1987). While many of these features are much like those on Earth, on the moon they are much more abundant and extreme. Another aspect making lunar exploration difficult is lunar regolith, which is made up of tiny particles created by the bombardment the moon's rocky surface (Meyer, 2003). The typical shape and size of the regolith particles makes it very abrasive and cohesive which is often very damaging to rover hardware. Not only is the moon home to hazardous geographic features, its lack of atmosphere presents a number of other challenges. Some of these challenges include extreme temperature swings or exposure to, cosmic rays, solar flares, and micrometeorite bombardment (Seybold, 1995). Surface temperatures on the moon typically range between -153° C to 107° C. Testing for the Apollo hardware in lunar analog environments was crucial to the program's success, as will be the same for upcoming lunar rover missions. Figure 9 is a picture of the lunar surface that was taken on the Apollo 15 Mission.

Figure 9: Photograph of Lunar Terrain from Apollo 15 Mission

With one of current NASA's primary interests being Mars exploration, much has been learned about Mars' geography through numerous probe and rover missions. With proper mobility to

navigate Mars' rocky plains, valleys, mountains, and craters new discoveries can be made and a more complete understanding of planet will be developed. In addition to the terrain features of Mars, dust is also a problem, which is often seen in the form of dust storms ranging in size and intensity (Cornell University, 2005). Mars is also relatively cold ranging between -113° C to 0° C, often being described as a "cold desert". In order to continue with the success of the Mars rovers, testing of new hardware in analog environments will remain extremely important. Figure 10 is a picture taken on the Martian surface, and is well representative of the color and type of rocky terrain, which covers most of Mars.

Figure 10: Photograph of Martian Terrain from Viking Lander

Next, we will discuss several analog-testing facilities, both man-made and natural, which have been used to validate new technologies on past and present space exploration rovers. The types of terrain present at these different locations is discussed, as mobility is a primary interest of this project and one of the most important analog tests for current rovers. Standards of ruggedness will also be presented as a measure to test rover hardware against extreme environments. The chapter concludes with discussion on how NASA has developed a series of competitions around analog testing of new technologies. All of this information together will be used to influence the ruggedness design aspects of our rover.

2.3.1 NASA's Rock Yard and Mars Yard Facilities

Both NASA's Johnson Space Center (JSC) and Jet Propulsion Laboratory (JPL) have on-site facilities designed for analog mission testing of new planetary technologies. Both of these facilities have different terrain that resembles what would be encountered on Mars or the moon.

The Mars Yard at NASA's Jet Propulsion Laboratory was specifically designed, under the Mars Technology Program, for testing rover prototypes in a simulated Martian landscape. This 2,500 square meter outdoor testing facility employs a variety of soils and rocks similar to what has been observed during Mars missions. These closely matched materials and colors make for an ideal facility to test both Mars rover mobility and vision technologies (Volpe, 2011). Growing demand for this facility, since the Viking landers, has resulted in numerous growths and improvements for this facility throughout the Mars Technology Program. Figure 11 is mobility testing with NASA's newest Mars Rover Curiosity, at JPL's Mars Yard.

Figure 11: MSL Mobility Prototype on JPL's Mars Yard

Similar to the Mars Yard is NASA's Johnson Space Center Rock Yard. The Rock Yard is a larger facility and serves as both a Martian and lunar analog test site. Some of the terrain includes lunar craters, a sand pit, and a Martian landscape, all of which can be seen in Figure 12. The lunar craters are made of gray crushed gravel, a similar color to what would be found on the moon. The Martian landscape contains both a rocky hill and boulder field, which well represents some geographical features of Mars (Hurlbert, 2010). This larger facility lends itself nicely to testing some of NASA's larger vehicle prototypes including the Centaur and Space Exploration

Vehicle. The Rock Yard also is situated at JSC such that it can be expanded in the future to support additional analog test facilities.

Figure 12: Bird-eye View of JSC's Rock Yard

Although both of these testing facilities are extremely important in NASA's development of future planetary rovers, they are often too small to conduct larger and more complicated analog mission tests. For these more involved tests, various natural environments are employed.

2.3.2 NASA's Analog Field Tests

In recent years, NASA analog field tests involving rovers and other vehicle systems have been held at three primary locations: the desert of Arizona, sand dunes of Washington, and an impact crater in Northern Canada. All of these sites were selected because of their harsh environments and terrain that is very similar to what exists on Mars and the moon.

NASA's annual Desert Research and Technology Studies (Desert RATS), held near the Black Point Lava Flow in Arizona, is one of the largest analog testing events of the year (Lind, 2011). NASA uses this event as a means to simulate and perform feasibility studies on proposed human and robotic missions, and the associated hardware. Conducting these analog tests in the harsh environment and terrain of the Northern Arizona desert provides insight to how various technologies may perform on the moon or Mars. The large area and variety of rocky terrain provides an analog playground for mobility systems of numerous shapes and sizes. The Arizona desert also simulates the dusty conditions and temperature swings similar to what exists on planetary surfaces. In recent years, NASA has performed extended tests on the ATHLETE, Space Exploration Vehicle (SEV), and Centaur mobility systems at Desert RATS. Desert RATS

provides invaluable information to NASA engineers on how new technologies might enhance upcoming planetary missions. Figure 13 shows NASA testing their SEV at Desert RATS 2011.

Figure 13: NASA Testing their SEV at Desert RATS

In 2008, NASA and Carnegie Mellon University held the Exploration Technology Development Program field tests at Moses Lake Sand Dunes in Washington. The primary goal of this analog testing event was to develop a better understanding of robotic missions for lunar surface exploration, while testing hardware in lunar like terrain. Moses Lake Sand Dunes are known for their extreme temperature swings, as well as frequent sandstorms. A variety of different soil types are present at the site, which is very beneficial from a mobility testing standpoint. Several of the rovers hosted at this field test included two of NASA's Ames Research Center K10 mapping rovers, NASA's JPL ATHLETE cargo-mover, an early prototype of NASA's JSC SEV Vehicle, and CMU's Scarab lunar drilling rover (Korsmeyer, 2008; Dean et al., 2008). CMU's Scarab rover is shown at this testing facility in Figure 14. Testing these various lunar rover technologies at Moses Lake Sand Dunes provided insight and vision into what future lunar missions may look like.

Figure 14: CMU's Scarab Rover at Moses Lake Sand Dunes

The Haughton-Mars Project is a meteorite impact crater site on Devon Island, Nunavut, that has been used for Mars analog testing by NASA and the Canadian Space Agency since 1997. Located in the arctic, Devon Island's climate and desert-like terrain makes for a perfect Mars analog test site. The site also contains many biologic and geologic features that are believed to be similar to Mars, making it appropriate for scientific analog testing as well. This analog site has hosted numerous rovers including NASA's Ames Reach Center K10 mapping rover in 2010, shown in Figure 15. Like the other discussed analog sites, Haughton crater is extremely useful for testing new technologies in an environment similar to Mars (Mars Institute, 2010).

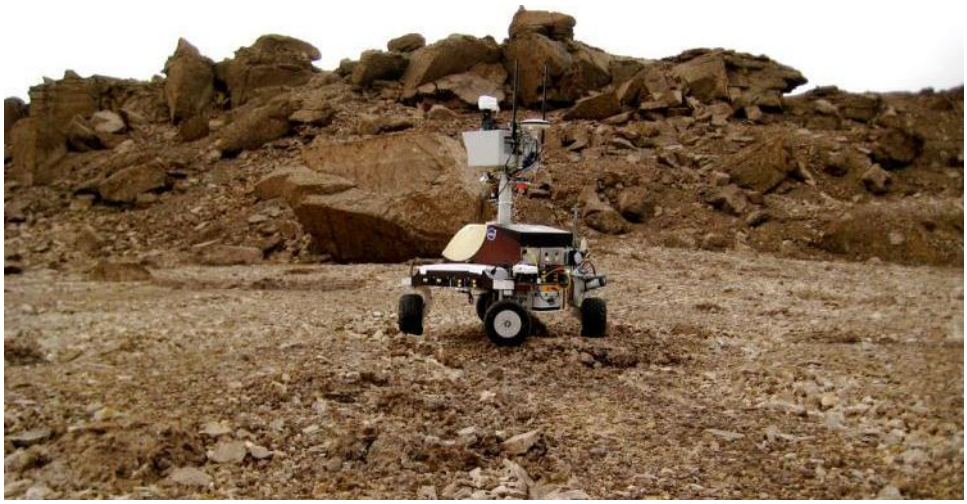

Figure 15: ARC's K10 Rover at Haughton Crater

To withstand analog testing in harsh earth environments, rovers, and other equipment must be properly ruggedized. The next section discusses considerations to be made when developing a system to operate in environments like those seen in analog testing.

2.3.3 Ruggedness Requirements for Harsh Earth Environments

As previously discussed, analog testing sites seek to accurately recreate conditions seen in planetary environments. Space vehicles such as planetary rovers already have a unique set of design requirements to cope with the harsh environment in space. However, coping with the Earth-based environment of an analog testing site also requires explicit design intent, because no Earth location exactly recreates extraterrestrial conditions.

Environmental conditions such as dust, shock, vibration, and extremes of temperature are common to both Earth-based and planetary rovers. However, Earth-based rover research platforms used for analog testing also need to have protection from water ingress and extended temperature ranges, particularly for electronic components. Many analog testing sites are in arid regions where air temperatures can exceed 50° C. Sudden inclement weather, as well as atmospheric humidity and wind-driven dust and water infiltration, can present serious danger to sensitive rover electronics and mobility systems if not adequately protected. One of the most difficult problems with direct analog testing of flight hardware is dealing with environmental temperature conditions in concert with internal heat-generating hardware such as computer processors. Environmental conditions on other planets typically require the use of an insulated electronics compartment with heaters to keep electronics warm, while the same rover driven on Earth would quickly overheat and likely requires additional cooling.

Engineering protections designed to safeguard rover systems from environmental hazards should also be tested to verify their performance. Standardized testing procedures for dust and water infiltration, shock, vibration, and temperature extremes have been written by several standards organizations, including the International Standards Organization (ISO) and the US Department of Defense. These testing standards can help engineers build and test rugged rover systems which are uniquely suited to planetary analog environments on Earth.

2.3.4 NASA's Competitions as Analog Tests for New Technologies

While NASA has funded the design of many rovers, they often utilize technologies that are privately developed. Many rover projects contain unique challenges that must be addressed through the development of new technology. One of the most common ways in which NASA solicits such improvements is through competitions that aim at tackling a particular scientific or engineering challenge that NASA faces (Comstock, 2007). These competitions take place in simulated lunar and extra-terrestrial landscapes and provide a venue for analog testing for the "citizen inventor" (Petro, 2010).

The most prevalent of these competitions are NASA's Centennial Challenges, which aim to "drive progress in aerospace technology" through "innovative solutions" to common technical challenges that NASA faces (NASA, 2011). While these competitions do not aim to completely change the way NASA designs rovers, they often focus on specific aspects of rover design that could benefit from innovative technological advancements (Petro, 2010). For instance, the NASA Regolith Excavation challenge challenged teams to design and build a robotic system to excavate lunar soil. The Night Rover challenge required that robots be able to collect enough solar energy during the day to be powered through the night. The Sample Return challenge requires teams to design a robot that can autonomously locate, identify, and collect a wide range of objects.

While it is not a Centennial Challenge, the National Institute for Aerospace, in partnership with NASA, has its own competition called Robo-Ops. In Robo-Ops, teams must design and construct a remotely operated robot that can navigate an obstacle-ridden terrain while searching for various colored rocks. While this competition may not seem as difficult as other NASA challenges, the team must address many of the common problems faced by NASA engineers, and the operators of such rovers. The chief among these concerns lies within the size and weight of the rover. Due to the high cost associated with sending materials into space, rovers must be as small and lightweight as possible if they are to make space-travel feasible. For the Robo-Ops challenge this specification requires that the rovers weigh no more that 45kg and fit within a 1m x 1m x 0.5m box. This sample return competition also requires rover to navigate over rough terrain in man-made analog environments that mimic surface conditions on the moon and Mars. Lastly, communication is another challenge teams must address, as a commercial broadband network will be used to communicate with the rovers. Given how closely these competition criteria will fit with our rover design we hope to enter the competition as a means of validating and testing our rover in NASA's analog testing facility at JSC.

3 DESIGN REQUIREMENTS & SPECIFICATIONS

Our main goal is to design, develop, and test a rover to serve as a mobility platform, suitable for testing planetary surface exploration technologies in harsh earth environments. The design will focus on incorporating features that are believed to be essential for most planetary exploration missions based on research of past and current rovers. Given what we have learned about existing rovers and the types of missions they aim to accomplish, our design goals for our rover have been made into three categories:

1. Mobility and navigation
2. Modularity and payload capabilities
3. Size and weight restrictions

While our rover will not be traveling to space, it is our goal to make a robust and ruggedized platform that will be suitable for testing in harsh earth environments, on terrain similar to that of our moon and Mars. Given sufficient mobility in planetary environments, the rover must also be able to accommodate payloads. Transporting sensitive scientific instruments across rough terrain is the main goal for nearly all exploration rovers, and thus one of our central requirements. Additionally, to be useful for other users both in academia or industry, the rover needs to easily integrate new hardware and software as part of its payloads. By providing a robust mobility platform that can accommodate a wide range of payloads, the rover should prove useful to anyone interested in testing rover related technologies or conducting research in the field of space exploration. Lastly, the rover will aim to recognize the size and weight constraints that all space bound vehicles face. While there are many resource constraints that prohibit us from designing a space-ready rover, the design will attempt to accommodate space considerations when possible.

As previously discussed, one of NASA's university level competitions, called RASC-AL Robo-Ops, is a design challenge that entails completing a sample return mission in lunar and Martian analog environments. Jointly sponsored with the National Institute of Aeronautics (NIA), this competition challenges students to design and build a rover that can operate in JSC's analog testing site, finding and collecting rock samples of interest. Given the similarities between this mission scenario and the goals of our rover, we have decided to design a rover that will be eligible for this competition. As a consequence, many of the design specifications for our rover have been derived from the rules and requirements of the RASC-AL Robo-Ops 2012 competition. Many design specifications, such as those related to mobility, largely overlap with what would otherwise be used given that the mobility challenge presented in Robo-Ops is nearly identical to the types of environments and terrains we would plan on using for testing. Conversely, some specifications such as size and mass are explicitly determined by Robo-Ops and have thus been adopted by our design in order to meet the basic criteria that make us eligible to compete.

In formulating the design specifications relating to mobility we wanted to ensure that the rover could traverse a wide variety of harsh Earth environments, similar to the landscapes reviewed in section 2.3. Such terrain includes deserts, rock fields, gravel pits, sand dunes, and mountainous areas in many different climates. Conveniently, the mobility requirements for Robo-Ops are similar, as they require the rovers to operate in man-made environments that simulate the moon and Mars. The simulated Mars environment is a rock field with varying densities of small rocks, while the simulated lunar surface is made from small gray gravel and has many craters. In examining these terrains we made design criteria relating to the size of obstacles, inclines, and speeds that the rover must achieve, in order to ensure that it could maneuver in many different environments.

According to the Robo-Ops design specifications, rovers must be able to overcome obstacles up to 10cm high. While this is largely sufficient in most scenarios the ability to go over larger obstacles always increases mobility potential. For our rover we set the goal of being able to traverse obstacles, both positive and negative to the ground plane, of up to 15cm high or deep. We believe this will allow for easy mobility in many environments, and is within the limits of what we are able to accomplish within the size constraints. Similarly, Robo-Ops specifies that rovers should be able to safely traverse slopes of 33% grade (19 degrees). Again we set our design requirements higher, as we believe that being able to navigate upslopes and downslopes of 30 degrees will increase the versatility of the rover. In terms of maximum speeds, Robo-Ops does not have any requirements. Based on speed capabilities of previous space exploration rovers, considerations regarding Earth-based testing, and issues related to ground compliance, a maximum speed of 1.2 m/sec was chosen. This is well above the 3-5cm/sec that most planetary rovers can achieve, and should increase mobility in some situations where high speeds are required.

The other aspect in terms of our rover's mobility requirements is how it will be controlled and manipulated. User controls will have other built-in autonomy to make driving and navigation easier. While some autonomy is crucial for planetary navigation much of the rover's mobility and decision making will come from user control. To facilitate efficient teleoperated control the rover will be equipped with many sensors that will relay feedback to the user. For example, a main camera will be used to facilitate driving, and data about the rover's orientation should help the user make decisions in some cases. Additionally, health monitoring sensors will convey important information back to the user, such as the temperature of motors and electronics as well as the amount of battery life remaining.

Another important category of design requirements has to do with the payload capabilities, and modularity considerations involving the types of things the rover will be used for. As a mobility platform for testing in harsh Earth environments our rover could potentially be used to transport

any number of payloads across different terrains. To accomplish this, the rover will not only need a modular mechanical interface to allow for easy installation of custom hardware, but will also need to supply the power and data ports for communications to electronics that may be part of an added payload. To satisfy the mechanical aspects, the rover will be equipped with a standard way mounting of attaching payloads. To power potential payloads, users will have access to power ports that will supply 5V, 12V, and Battery voltage (~24V). Additionally, available data connections will make it easy to connect to the rover's main computer through Ethernet or USB. Overall, our rover will be able to support up to 15kg of payloads, while still meeting all mobility specifications. Another requirement related to the rover's use in field testing is battery life. While Robo-Ops requires the rovers to operate for 1 hour without charging or replacing the battery we have made a requirement for a 3 hour battery life, so that more testing can be done between charges.

The last requirements of our rover relate to size and mass constraints. Given the large costs of launches, which can exceed $10,000 per kg, the size and mass of rovers is of large importance. In order to be eligible to compete in the Robo-Ops competition we inherited their requirements for mass and size: 45kg, and a maximum starting configuration of 1m x 1m x 0.5m. Below in Table 1, is a summary of the key design requirements that were discussed in this chapter. For a more detailed and comprehensive overview of design specifications, see the Design Specification sheet in Appendix A.

Table 1: Summary of Key Design Requirements

Design Requirements	Value
Maximum speed	1.2 m/sec
Maximum inclines	30 degrees
Maximum obstacle size	15 cm
Feedback	Video, Orientation, Temperatures, Battery life
Payload	15kg
Available power	5V, 12V, 24V
Available I/O ports	USB 2.0 (8), IEEE 802.3 Gigabit (2)
Battery life	3 hours
Maximum total mass	45kg
Maximum size	1m x 1m x 0.5m

4 DESIGN and ANALYSIS

This chapter will review our complete rover design and discuss how our key design decisions were made in order to meet the requirements and goals presented in the previous chapter. Our design and related analysis is divided into five main sections; mobility, electronics and communications, diagnostic systems, software design, and payload capabilities. Each one of these main categories is related to meeting fundamental requirements, and combined they provide a comprehensive overview of the software and hardware design.

4.1 Mobility

Mobility relates to the rover's capacity to traverse varying terrains, slopes, and obstacles. In beginning the process of formulating the drive architecture we reviewed current and past rovers in consideration of chassis design, suspension methods, wheel design, and power requirements. Since nearly all rover hardware is related to mobility, this section will review most of the mechanical design including the chassis, suspension, and wheel components. It will also review how the drive motors were selected, the expected capabilities of the drive system, and the selected power source.

4.1.1 Chassis Design and Rocker Differencing Suspension

In our review of existing rover drive architectures and suspension systems, covered in Section 2.2, we found that there are several popular approaches that are commonly used. For example, NASA has employed the rocker-bogie design in rovers that date back 15 years, and is continuing to use the same basic design on their most current rovers. This six wheel differencing suspension has four steerable wheels, allowing the rover to turn in place and avoid skid-steering. Additionally, the complex linkage suspension system gives the rover the ability to traverse obstacles much greater than the diameter of its wheels. Other rovers also use a differencing suspension, but only with four wheels and two rocker arms. This configuration can be done with four steerable wheels, or alternatively use a skid steering approach. This method boasts some benefits of the rocker-bogie system by providing a level of ground compliance; however, its main advantage is in its comparatively simple design, as it requires fewer wheels, axles, linkages, and motors.

Given the prevalence of these two suspension drive systems in current rovers it was logical to select a derivative of one of these designs. In selecting a design we weighed the mobility potential of each method against the complexity and costs that would be needed in terms of design and manufacturing. With the time and budget constraints of the project we selected the four wheel skid steer design with rocker differencing suspension. Providing one of the most economical solutions in many respects, this method also provides sufficient mobility to meet all design goals. In fact, the exact advantages of the six wheeled rocker-bogie design remains unclear. Previous NASA missions have not utilized the full potential of the system, and some analysis suggests that four wheel rovers can achieve similar capabilities by avoiding head on

paths with larger obstacles (Roman, 2005). In summary, the four wheel rocker differencing configuration was selected for its simplicity, and its ability to meet all mobility requirements.

To further simplify the design we choose to use one motor to directly drive each wheel. Since it is a skid steering rover an alternative solution could be to have one motor drive two wheels on either side, resulting in fewer motors and less mass. However, having one motor for each wheel reduces the need for a complex power transfer system, which is often done with belts, gears, or drive shafts. The selected design, which has four motors, also increases redundancy so that the rover can remain operational without one motor working, or can even individually control the velocities of each wheel to optimize trajectories over rough terrain.

As previously discussed in Chapter 3, the main requirements pertaining to mobility are the slopes that can be traversed, the maximum size of obstacles, and speeds. These design criteria drove constraints for the wheel size, wheelbase, and suspension configuration, which led to the design shown in Figure 16.

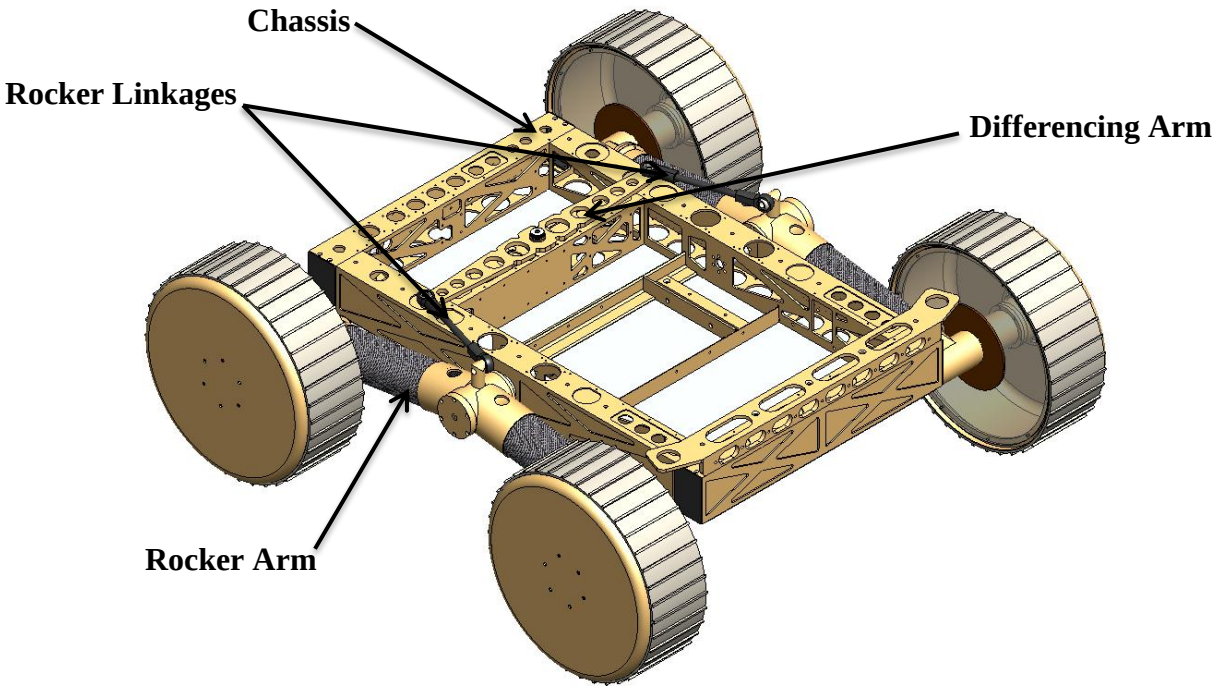

Figure 16: Chassis and Rocker Suspension Design

In considering slope traversal we looked at the location of the center of mass relative to the polygon on stability in order to estimate the tipping angles. Figure 17 shows the rover's polygon of stability to be a rectangle that is 86cm wide and 66cm long. To estimate the tipping angle the center of mass is approximated to be at the center of the rover, and the height of the center of

mass approximated to be 16.9cm high. Following these estimations we found the tipping angle to be 69.0° when tipping over the width and 63.2° over the length. Both of these figures are well above the 30° requirement, however, actual limitations on slope traversal will likely be traction limited.

With such high tipping angles it would be logical to raise the center of mass of the rover in order to increase its overall ground clearance. For example, increasing the length of the rocker arms or decreasing the distance between the front and rear wheels would allow the rover to traverse larger obstacles while still maintaining tipping slope limits above 30°. The primary reason for this design decision relates to the Robo-Ops challenge and the 1mx1mx0.5m size constraint. To stay within the limits of the 0.5m height restriction we needed to keep the top of the chassis well below 0.5m to ensure there would be height available to add the arm and sample storage payloads. If this size requirement was ignored the design would likely result in a higher rover, with much greater ground clearance. Figure 18 shows the resultant ground clearance of the Oryx 2.0 design.

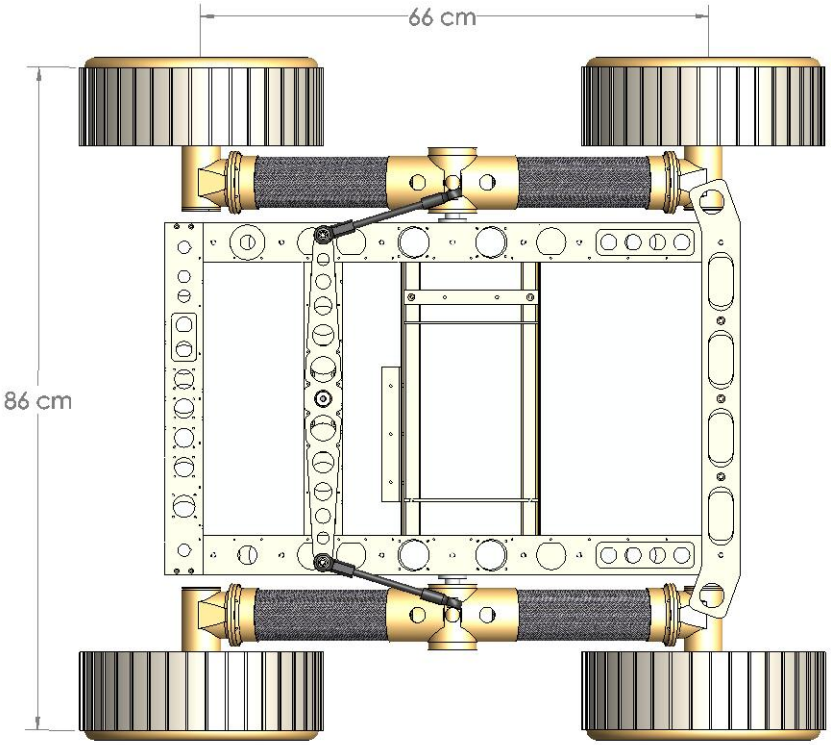

Figure 17: Polygon of Stability shown from Top View (dimensions in cm)

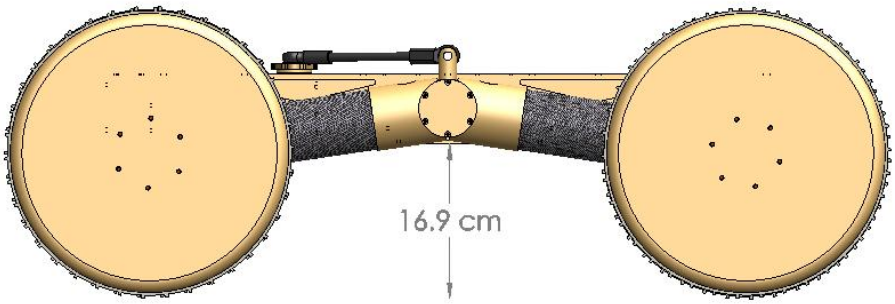

Figure 18: Ground Clearance shown from Side View (dimension in cm)

In addition to slope traversal, overcoming obstacles is an essential aspect of rovers. For our design criteria we set the goal of being able to traverse obstacles up to 15cm in height or depth from the ideal ground plane. This is mostly achieved by selecting a wheel diameter slightly greater than the maximum obstacle height. By selecting a wheel diameter of 31.1cm the rover should be able to easily surmount obstacles up to about 15.5cm. Additionally, the chassis has a ground clearance of about 16.5cm, which means the rover can easily go over obstacles that tall, if such obstacles are within the wheel base.

While this design suggests that 15cm obstacles can be traversed, the rocker differencing suspension provides the ability to traverse obstacles much larger, potentially up to one wheel diameter in height. One advantage of the rocker differencing suspension is its resulting ground compliance. This means that over rough terrain all four wheels can remain in contact with the ground, increasing stability and traction. Additionally, this type of suspension increases the maximum obstacle height that can be traversed above half the wheel diameter. This is due to a similar effect that is achieved with the rocker-bogie design, where the force required to lift a wheel vertically is reduced by the passive suspension. Figure 19 shows the rover with the maximum amount rocker differencing in affect, currently this is limited by hard stops that interfere with the motor cans as they are rocked to extreme angles. In the pictures below the differencing arm and rock linkages are highlighted in green in order to more easily observe their position.

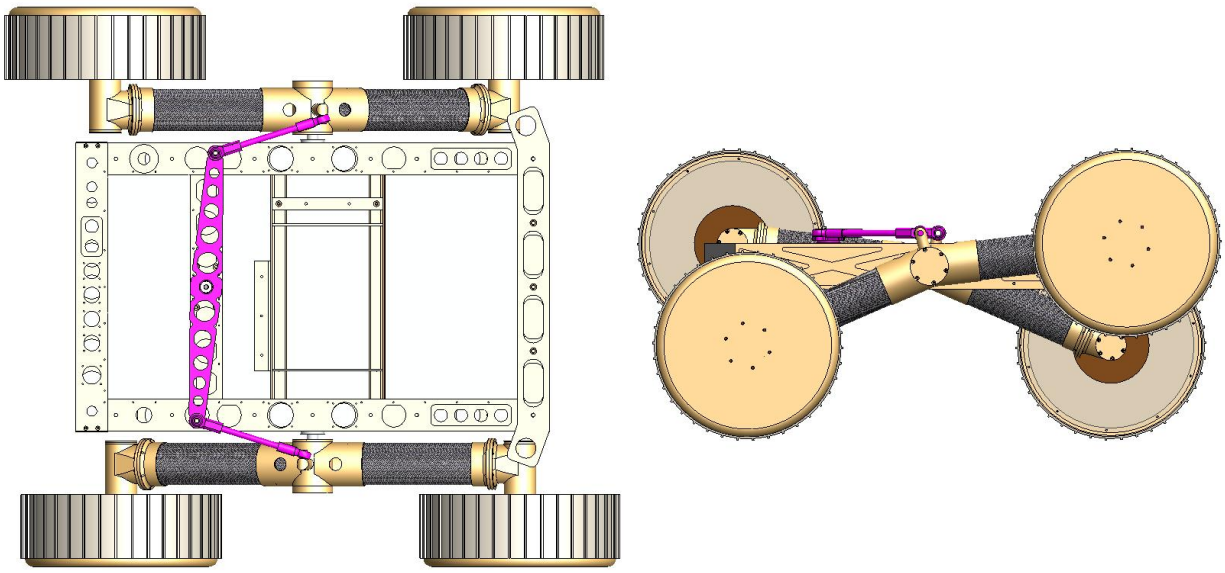

Figure 19: Maximum Amount of Rocker Position in Top View and Side View

Figure 20 highlights the rocker suspension in action. In this scenario the front right wheel has been raised by an obstacle resulting in the configuration shown. As seen in Figure 20, the chassis is tilted by half the difference between the sides of the rover as a result of the differencing effect of the suspension.

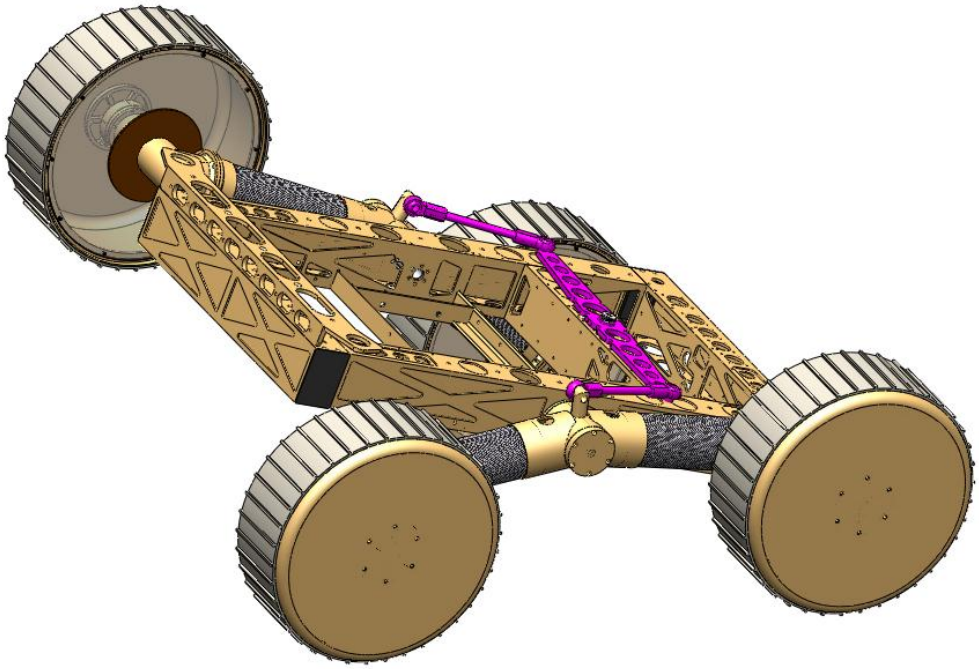

Figure 20: View of Rocker Suspension with the Front Right Wheel over an Obstacle

The linkage system chosen for the design consists on the main differencing arm in the middle connected to the two rocker arms though a tie rod with ball and socket joints. It should be noted that there are several different techniques for achieving the same style of passive differencing suspension. Common alternatives include a differential gear box between the two rocker arms, or a similar linkage system offset by 90°. Our specific implementation was selected mainly for its small form factor, and low mass.

The main body of the rover is made from five rails of 3x1in rectangular 6061 aluminum tubing with 1/8in wall, and is shown in Figure 21. Four of these rails are welded together to form a box, 74.9cm long by 45.7cm wide by 7.6cm high. The last chassis rail is welded across the width of the rectangular frame to add support, and is also used to secure a pivoting location for the differencing arm. In total, this one piece welded chassis has a mass of about 4.5kg.

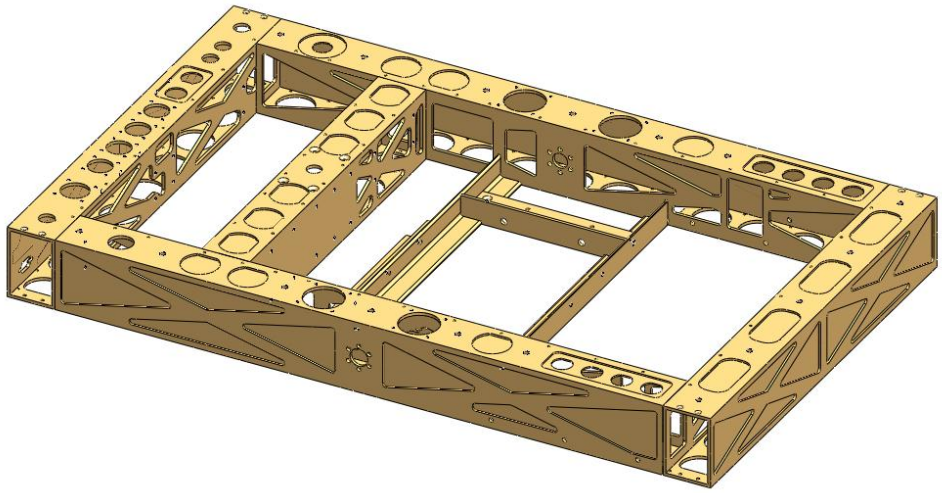

Figure 21: Chassis Design

To secure the rocker arms to the chassis a 3/4in hollow 7075 aluminum shaft is used to support two tapered roller bearings that are housed in the central welded assembly. The main shaft is secured to the chassis rail by a bolted flange in addition to an aluminum bolt at the end on the inside of the chassis. To securely rotate around the shaft the rocker arm is fitted with two tapered roller bearings, held in place by a bearing lock nut. Carbon fiber tubes are structurally bonded with Loctite 9430 to each side and are used to connect the wheel modules to the central pivoting assembly, forming the rocker arms. More detail on wheel design is provided in Section 4.1.2.
Lastly, to sense the position of the rocker arm a digital encoder is embedded inside the shaft and is connected to the rocker arm through a Fairloc hub. The design and layout of this assembly is shown in Figure 22.

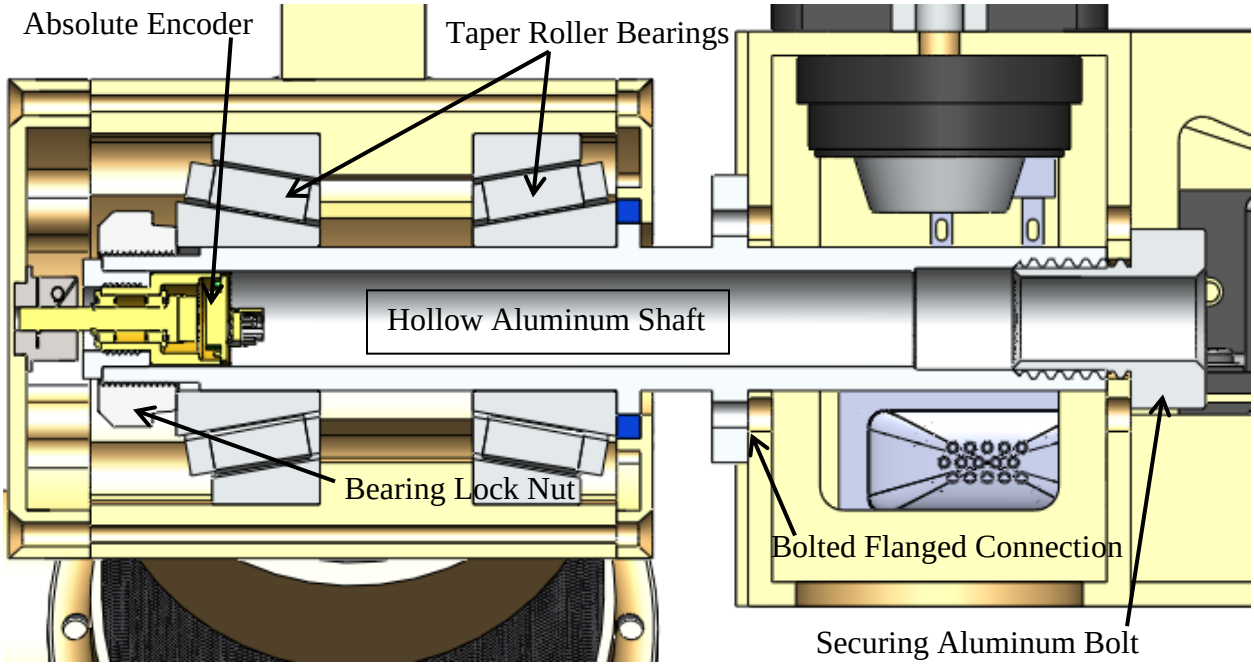

Figure 22: Section View of a Rocker Arm Bearing Assembly

Besides bearing all structural loads associated with driving and the rocker differencing suspension, the chassis must also be able to securely store all electrical components. Figure 23 shows the layout of the chassis in terms of where all electrical components are mounted. The small compartment in the rear of the chassis contains the four EPOS motor controllers which will control the drive motors. Moving towards the front, the other side of the internal chassis rail provides a place to mount the two DC voltage regulators and the liquid cooling pump. Aluminum angle welded across the center of the chassis secures the battery, in addition to the main contactor and battery management system (BMS). Lastly, an isolated electronics tray is mounted in the front; it holds the mini ITX board and other small electronics. To help remove the heat generated by the quad core i5 processor, a liquid cooling system is built into the chassis with the convector and fan attached to back.

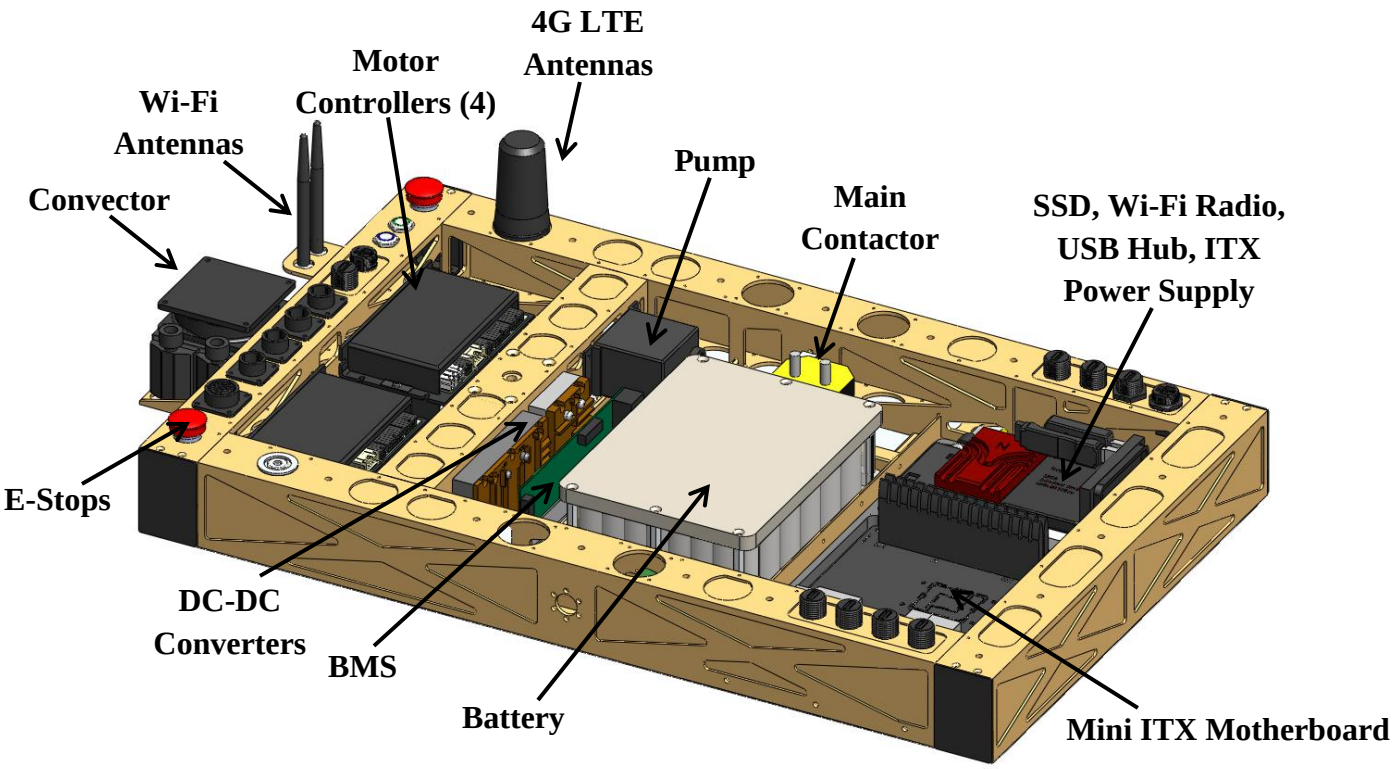

Figure 23: Chassis shown with Electronic Components

An important design goal is for the rover to be ruggedized and capable of operating in harsh environments. Consequently, the chassis must be relatively sealed and water resistant to prevent water and dust ingress. To accomplish this all pockets on external faces are not through pockets, and instead leave a 0.050in wall. The bottom of the chassis box is covered with .032in aluminum sheet and the top is covered by two pieces of thin Mylar sheet. Lastly, all external electrical connections use water resistant connectors that will have caps to seal them when not in use.

4.1.2 Wheel Design

As previously discussed, a wheel diameter of about 31.1cm was selected based on meeting mobility requirements. However, designing a lightweight wheel of that size that can sustain the loads of the rover posed some challenges. The main challenge in wheel design is distributing the load evenly around the wheel. Also, finding a way to secure suitable tread or machine the tread pattern into the wheel can be an issue.

In formulating the wheel design several options where considered. One option was to make billet wheels, and machine the wheel and tread from one piece of round aluminum stock. This method has the advantage of optimizing the wheel shape in order to efficiently spread load from the hub to the tread, through machined spokes. Machining the tread as part of the wheel is also beneficial, as it provides a light weight solution to achieving a custom tread design. The downside to this approach is the large costs in the amount of aluminum stock that is needed. Furthermore, the machining and manufacturing costs would be very high, and ultimately outside our budget.

In an effort to find a more economical solution, we explored wheel designs that used polycarbonate tube stock to form the main structure of the wheel. The hub and spokes would then be machined from thick aluminum plate, and then attached to the polycarbonate ring to form the wheel. Lastly, tread could be attached to the outside of the polycarbonate ring. This method greatly cuts down on machining time compared to billet wheels, however, with the polycarbonate ring and the aluminum required to make the spokes there is a substantial cost in the stock material.

In search of a more cost-effective option we investigated the process of metal spinning to form the wheels. A process that bends aluminum over a form to create bowl shaped aluminum parts, metal spinning can achieve strong and lightweight shell structures. Additionally, metal spinning companies have stock parts and often have the option of customizable products. Ultimately, finding a company (Toledo Metal Spinning) that sold a 12in tube cap spun from 1/16in aluminum sheet provided us with the option of buying the wheels as an off-the-shelf product.

This approach to wheel design and manufacturing was selected because the off-the-shelf product provided a cost effective way to make wheels that would require minimal machining to complete. In this wheel design the core wheel structure is the metal spun part, which is a 12in diameter 4in long end cap, made from 1/16in aluminum sheet. This stock part weighs 780 grams, and is shown in Figure 24 in the displacement plot generated by the finite element analysis (FEA). Forming nearly the entire structure of the wheel, the only required machining was the six holes needed to interface to the wheel hub. However, one issue uncovered by the FEA is that this wheel lacked the strength and stiffness to support the weight of the rover. To perform the FEA, fixture surfaces were defined as the location of the hub interface, and a force of 110N was applied to the bottom of the wheel simulating the normal force of the ground. In a static case this scenario approximates loading that would be seen by a 45kg rover on level ground, and as seen in Figure 24 the wheel undergoes substantial displacement. Specifically, the open end of the wheel sees a maximum displacement of about 3.7mm.

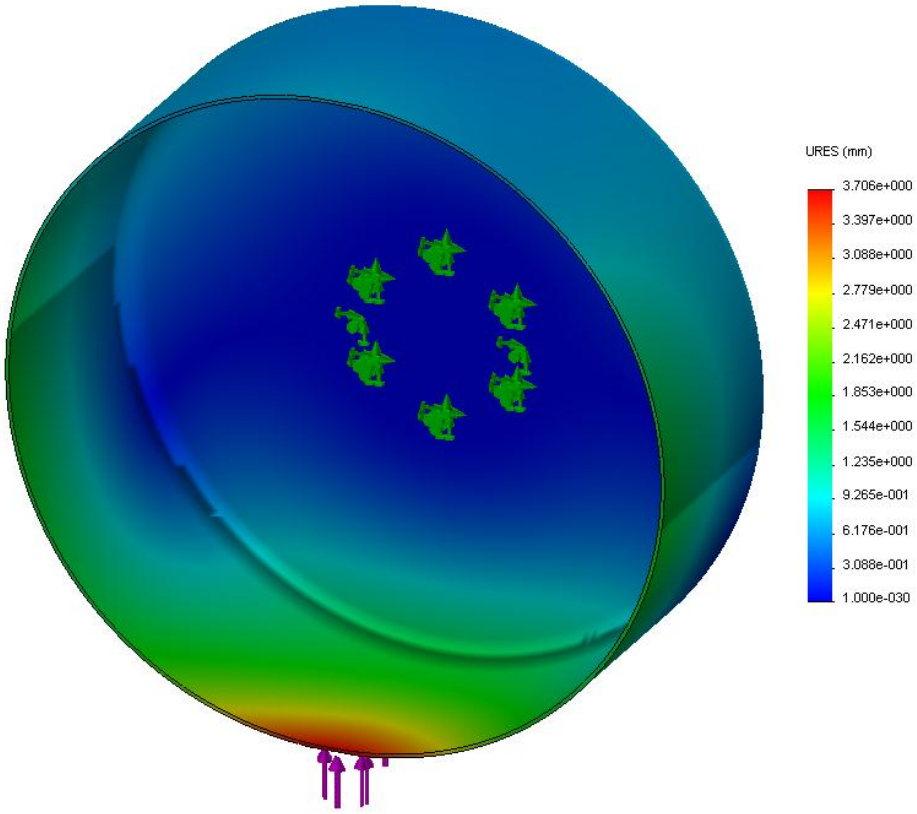

Figure 24: FEA of Stock Wheel

To stiffen the wheel a structural element was designed to be bonded to the open side of the wheel. Machined from 1/2in aluminum plate, this stiffener ring has a right angle profile and is structurally bonded to the inside of the wheel. Additionally, the face of this part contains a pattern of tapped holes that are used to attach a debris shield. The FEA was run again, with the addition of this stiffener ring, and the resulting displacement plot is shown in Figure 25. As seen in this figure the stiffener ring provides added support, and also helps to transfer the load more equally around the wheel. The result is significantly less displacement, with a maximum of only 1.4mm compared to the 3.7mm displacements that were likely to occur without the added support. Weighing only 170grams, this stiffener ring greatly increases strength while adding only a small amount of weight to the wheel.

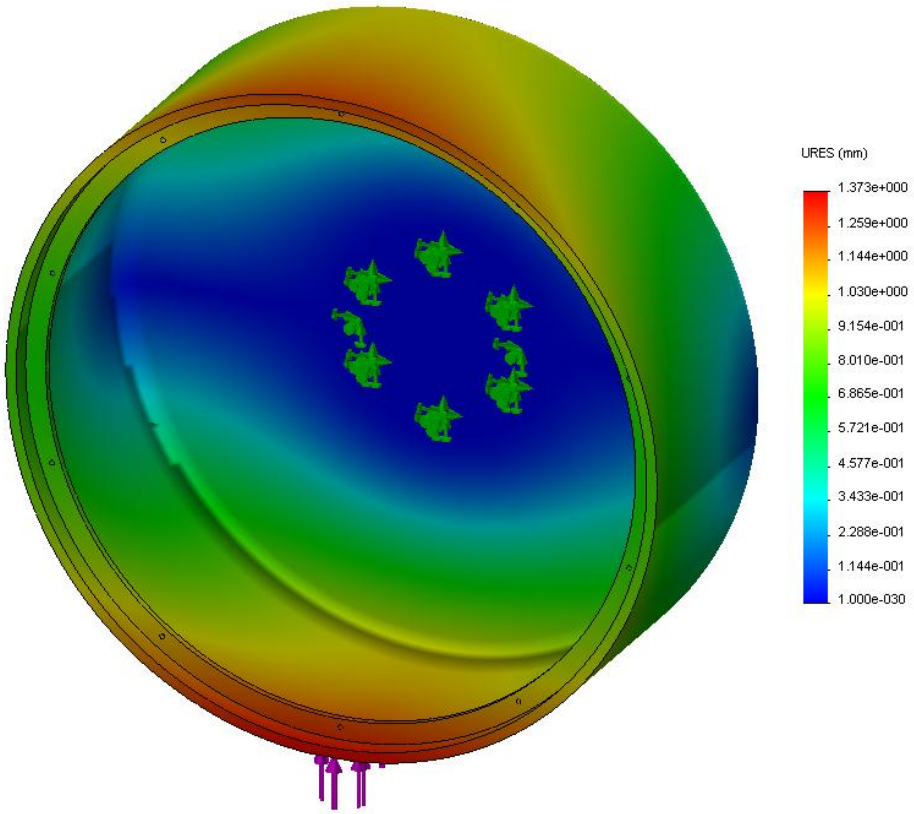

Figure 25: FEA of Wheel with Added Support Ring

While the stock end cap and addition of the stiffener ring make up the entire structure of the wheel there was still a need for tread and a debris shield. Unfortunately, the smooth finish of the spun aluminum caps would not provide good traction that is typically achieved through small cleats. In reviewing wheels from past rovers we found that small cleats across the width of the wheel, often in a 'Z' shape, are commonly used for rover missions to mars or the moon. To achieve a similar effect on our wheel design we needed to find something that could be attached to the outside of the wheel. After considering aluminum cleats and other options we found 4in wide conveyor belts that had desirable tread patterns. The conveyor belts are attached to the wheels using 3M VHB high-strength bonding tape, which secures it in place in a semi-permanent fashion.

The last component of the wheel is the debris shield. While many rover wheels have open spokes to allow rock and gravel to pass through the wheels, our wheel design relies on one solid flat spoke to support the load. In this case it is necessary also seal the open side of the wheel to prevent debris from accumulating inside the wheel during skid steering. To do this a debris shield is laser cut from 1/16in PETG. This shield bolts onto the stiffener ring and has a hole cut out in the center so that the wheel can fit over the wheel hub during assembly. Finally, to cover the gap between the motor can and debris shield, a piece is laser cut from 1/16in silicone foam. This orange foam will be glued to the PETG debris shield and will fit tightly over the motor can,

creating a dust and gravel resistant shield for the wheel. The resulting wheel design is shown in Figure 26, entirely assembled with the stiffener ring, tread, and debris shield.

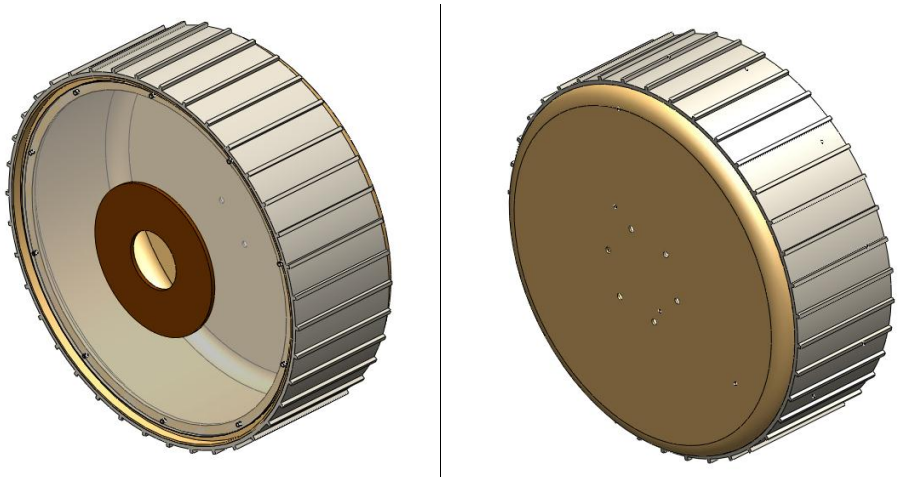

Figure 26: Wheel Assembly, back and front view

In total each wheel masses about 1500grams. One downside to this wheel design is that the tread adds a substantial amount of mass, approximately 350 grams, and yet provides no structural support for the wheel. Similarly, the debris shield adds mass and would not be required by some designs. Another non-optimal design aspect of this wheel is the spoke configuration. While being supported by a 1/16in think aluminum sheet flat spoke is sufficient for our rover, it is not ideal to distributing load in a mass efficient manner. Many rover wheels have multiple spokes in the shape of an arc between the wheel hub and the tread, which is a much more effective way of distributing load. Additionally, the wheel tread is often machined as the same part of the wheel, which can be another weight saving technique. While our wheel design may not be optimized in terms of strength and weight reduction, it resulted in a cost effective solution with minimal manufacturing time, and a wheel that should meet all design goals.

4.1.3 Drive Motor Selection

With sponsorship from Maxon Motors we were able to select ideal drive motors for the rover. The process of selecting motors began with reviewing power criteria of similar sized rovers and eventually considering the power requirements needed by our rover to meet mobility objectives. As previously discussed in Section 2.1.1 space bound rovers are slow, on the order of 3cm/sec, and generally do not allocate large amounts of power for driving. For example, NASA's most recent rover for Mars is designed with a top speed of 4cm/sec, although actual operation speeds will likely be closer to 2.2cm/sec. While such low speeds and low power consumption is required in space, our rover is not limited in the amount of power it can store or collect. Consequentially, design specifications for our drive motors are driven by requirements for successful operation in harsh earth environments, instead of strict power limitations that are required for space bound rovers.

To begin analyzing the power requirements we looked at how much power is required to drive up the maximum rated slope at the top speed. In this scenario, assuming a 45kg rover is driving up a 30° slope at 1.2m/sec, the rover would require 265W of drive power. This was done by calculating the change in potential energy over time as seen by the below equation.

$$265W = \frac{\left(45kg \times \frac{9.8m}{sec^2} \times 1.2m * \sin(30)\right)}{1\ sec} \quad (1)$$

Assuming a gear box efficiency of 60%, the rover would need about 442W of power by the motors to achieve about 265W of mechanical power at the wheels; divided by the four drive motors means that each motor should produce about 110W. Used as the basis for motor selection we began by investigating motors in the 100W to 200W range.

From the product line of Maxon motors, the EC-max and EC-4pole brushless motors were most attractive for their high power to weight ratio, efficiency, good heat dissipation, and excellent service life. After comparing motors between the two programs we decided to select a drive motor from the EC-4pole program, as they are some of the highest performance motors available especially in terms of power to mass ratio.

In the EC-4pole program there were three motors close to or within our desired power range; an Ø22 mm 120W motor, Ø30 mm 100W motor, and Ø30 mm 200W motor. Based on each motor's parameters we estimated the resulting performance that each motor would produce in terms of top speeds and slope climbing ability. Speed was calculated based on the motor's nominal speed and selected gear ratio. Slope climbing estimates were done using the motor's rated nominal torque, the gear ratio, and gearbox efficiency. Nominal, is nomenclature from Maxon Motor and simply refers to the maximum continuous torque that is allowed before overheating is an issue. While the motors can achieve speeds and torques far above the nominal values, operation outside of these values is not recommended for continuous operation.

In calculating drive speeds we assumed a nominal motor speed of 12,500rpm. Since this number is below the rated nominal value it ensures we are operating within safe limits. We assume a lower nominal speed for several reasons. Since the only power source on the rover is a 24V battery we are not able to achieve nominal speeds because the EPOS motor controller can only deliver up to 90% of the that voltage to drive the motor; meaning the motor will run slightly below its rated voltage and thus slightly below its nominal speed. Furthermore, performing the commutation from encoder feedback limits the top motor speed to 12,500rpm. While the controllers can be reconfigured to commutate from the hall sensors in order to increase controllable speeds, commutating from encoders provides better velocity control at very low speeds which is desirable in our application.

In calculating slope climbing abilities we assume no wheel slip, and simply observe the resulting force from gravity for a given slope, and the required wheel torques to counter that force. Since each gearbox is rated for maximum efficiency we subtracted each rating by 10% in order to approximate actual average efficiency. For each motor a gear ratio is selected to achieve the desired speeds and is based on available ratios. The equations used to calculate our estimated resulting speed and slope climbing ability are shown below. In these calculations we assume a wheel diameter of 31.1cm and a rover mass of 45kg.

$$v = \frac{\frac{\omega}{N} \times \pi \times D}{60\ sec} \tag{2}$$

where v is the rovers velocity (m/sec), ω is the motor velocity (rev/min), N is the gear ratio, D is the wheel diameter (meters)

$$Max\ Slope\ (degrees) = asin\left\{\frac{\frac{\rho}{g}}{M}\right\} \times \frac{180}{\pi} \tag{3}$$

where ρ is defined as the maximum continuous pushing force given by equation 4 (N) , g is gravitational acceleration (9.8 m/sec^2), M is the rover's mass (kg)

$$\rho = \frac{\frac{\tau}{1000}}{\frac{D}{2}} \times 4 \times N \times \eta \tag{4}$$

where τ is the motor torque (mNm), D is the wheel diameter (meters), N is the gear ratio, η is the gearbox efficiency.

As mentioned earlier, nominal ratings for speed and torque are used in the calculations so that we can assume the rover can operate continuously at the resulting speeds and slope. This makes these estimates conservative, because driving will rarely be a continuous operation and will actually by a highly intermittent task. As a result the rover will likely be able to exceed these torque and slope ratings, since intermittent use will keep the motors within their operating temperature range.

These calculations, and others such as the calculation of power to mass ratio, are done for each motor, and a detailed summary of the results can be seen in Appendix E. Ultimately, selecting a motor was straightforward because only the 200W motor could operate continuously up more than a 30degree slope. The other two, less powerful motors, could only continuously climb a slope of about 20 degrees, which is below our mobility specification. These motors could climb a 30 degree slope, however, it would be outside of their range for continuous operation, and would

likely be at a speed lower than 1.2m/sec. While this is probably sufficient for our use it is marginally below our desired requirements. Additionally, selecting the 200W motor was the easy choice because it far exceeds all requirements and only has the minimal tradeoff of a slight increase in mass. In summary, the EC-4pole 30mm 200W motor with a 156:1 reduction was the obvious choice. Based on our analysis we predict a top roving speed on 1.2m/sec and the ability to continuously sustain this speed up a slope of 44degrees; although slope traversal will likely be traction limited.

After the drive motor was selected we designed a wheel module, something that would encapsulate the drive motors to protect them from the environment, and also provide a means of supporting the drive shaft. A CAD rendering of the wheel module design is shown in Figure 27. It has a water resistant connector built into the mechanical interface, so that the wheel modules can easily be attached or removed from the rocker arms. It also has a hub, which provides a standard connection to the wheel so that new wheels can easily be added to the same wheel modules.

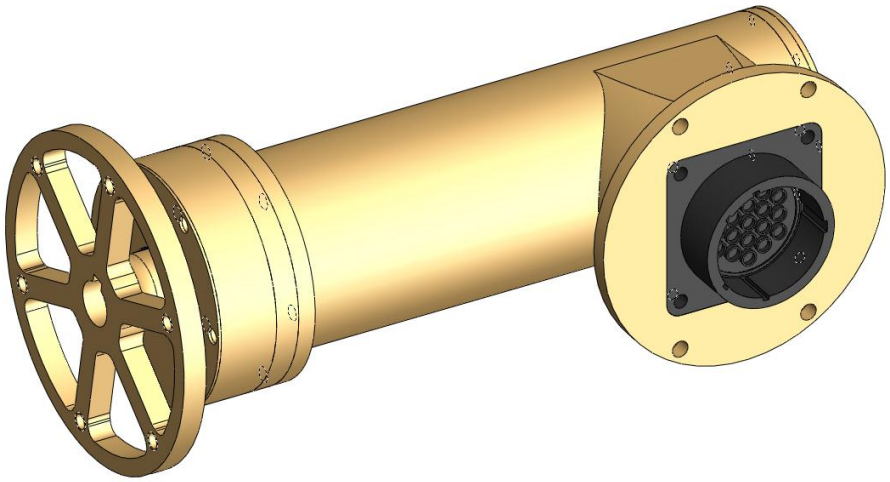

Figure 27: Design of Drive Module

To completely seal and protect the motor, the motor-gearbox combination is surrounded by the motor can. Flanges are welded to either side of the thin walled aluminum can to provide a pattern of tapped holes for attaching other parts. On the back, a thin cap is attached to seal the can on that end. On the front, there is a series of stacked plates that are used to attach the gearbox, secure the support bearing, and hold a lip seal. Figure 28 provides a section view of this assembly that reveals its configuration. The wheel hub fits around the drive shaft and through the lip-seal and bearing. At its end is a grove for a retaining ring which constrains the hub in place, and a keyed shaft is used to transfer torque between the gearbox shaft and the hub. Overall, the aluminum enclosure and assembly should provide a solid protective casing that will support the motor and wheel. It masses a total of 1260grams, 760grams of which is the motor and gearbox.

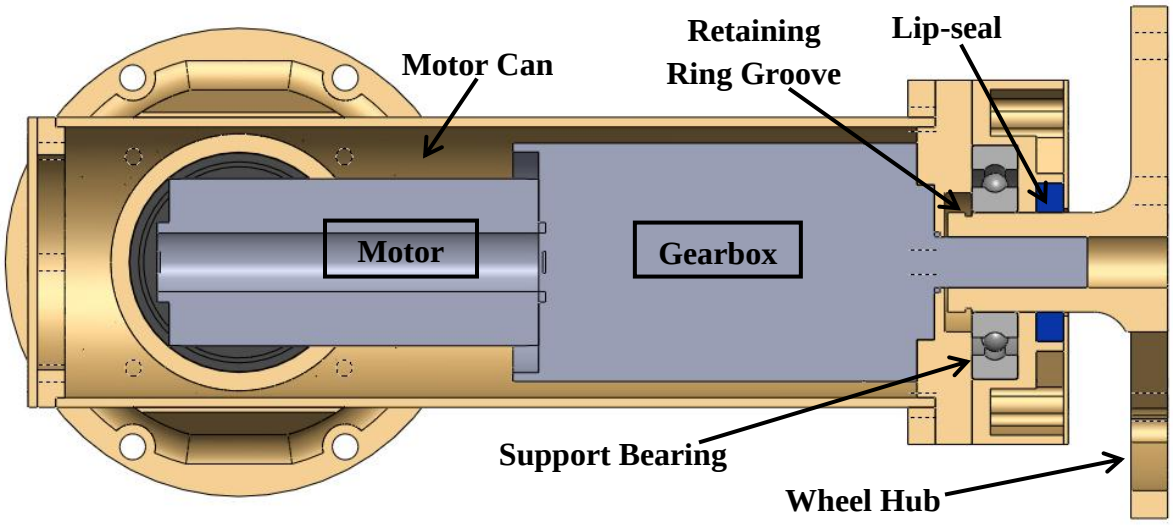

Figure 28: Section View of Wheel Module

4.2 Electronics and Communications

In addition to the mechanical design of the rover we designed and selected the electrical and communication systems for the rover. We selected a computer that was appropriate for the rover from both size and computing power standpoint; determined our system power need in order to design and build a custom lithium-ion battery pack; developed an simple elegant method of power distribution; and selected communications hardware for different ranges of teleoperation.

4.2.1 Selecting the Main Computer

While providing a means for physical connection is a key aspect of payload integration we also considered how software payloads may be added or integrated. In fact, there may be many scenarios where users will be primarily testing software on the rover, and so it was important to select a framework and software architecture that is widely used and expandable.

The two frameworks considered were the Microsoft .NET framework and ROS; however, as previously mentioned we selected ROS for its convenient communications framework and modular nature. Since ROS is not an operating system we needed to use a Linux OS to run it on top of and selected Ubuntu 11.04.

ROS is ideal for our application because it provides a communications framework that allows multiple programs across multiple computers to act as though it were a single program. This allows for intuitive compartmentalization of code; rather than having a single program controlling every aspect of our rover, we can instead write multiple programs and have them interact with each other without requiring potentially dangerous threading. Additionally, this

distributed programming coupled with the fact that ROS handles networking between computers on its own, leads ROS to be one of the most scalable software frameworks available. As a result, ROS makes it easy to add additional computers to the system or additional programs with little to no effect on the existing system as a whole. This aspect of ROS is well suited for use on a research platform because it makes it easy to build off of the existing system, add new programs, or add new computers.

While using the ROS framework has several advantages for a modular research platform we also wanted to ensure that users have access to the onboard computer and sufficient computing power. As previously mentioned, there will be eight USB connections and two Ethernet connections available on the chassis. In order to ensure there is enough processing power to handle most things that could be plugged in we evaluated and selected an appropriate computer.

In the early stages of selecting a computer we considered three main options, a PC104 stack, VIA Nano-ITX board, and a mini-ITX board. The advantage of the PC104 is that it is a modular system that is ruggedized to MIL standards. The size and costs of the PC104 proved to be prohibitive when we considered all the extra cards that would be required to meet minimal requirements. The Via Nano-ITX board had comparable processing power but in a smaller footprint, in addition to costing less than a comparable PC104 stack. The primary Via board that we considered was the EPIA-M900, which comes with a 1.6GHz dual core processor and all of the ports that we would need on our rover. While this computer would likely meet all our processing requirements preliminary tests found that we would use about half of its computing power to run our basic software and video compression algorithm. We determined that this would not leave the desired amount of reserved computer power for user payloads.

To guarantee that more processing power would be available to users we instead decided to use a more powerful quad core processor. Ultimately we decided on using a 2.5GHz Quad-Core Intel Core i5-2405S processor on the ASRock Z68M-ITX motherboard. While still maintaining a small footprint on a mini-ITX motherboard this configuration provides a great deal more processing power and more powerful integrated graphics. It also has a large number of available ports including 4 SATA, 8 USB 2.0, 2 USB 3.0, and a PCI Express 2.0 x16 slot. The selected mini-ITX computer is shown installed in the rover in Figure 29.

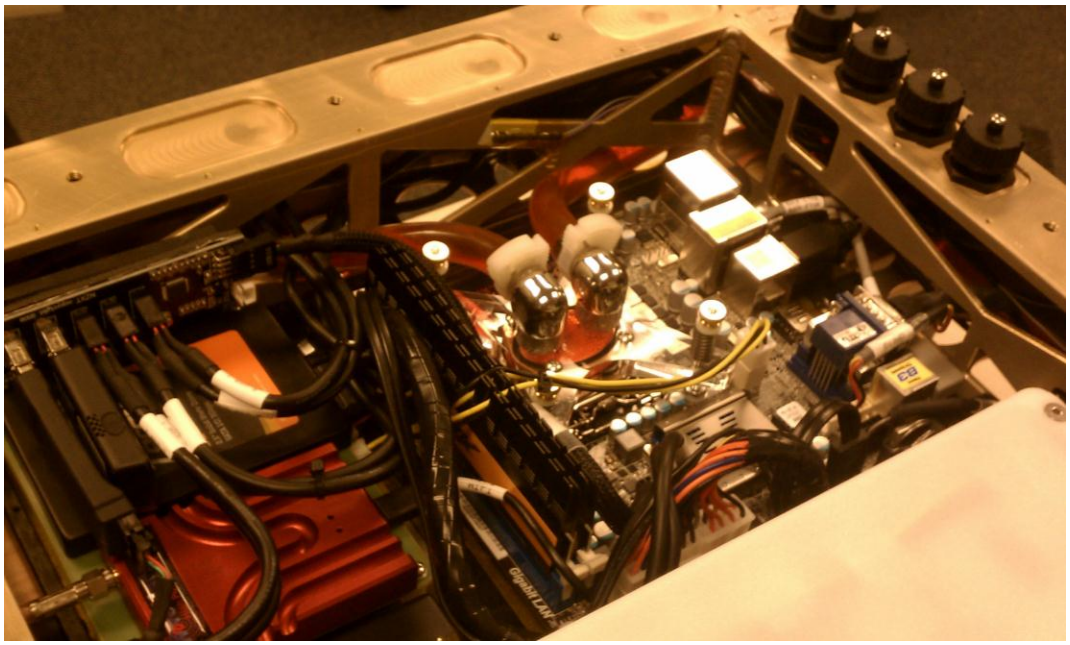

Figure 29: Mini-ITX Motherboard and Water-Cooling System in Rover

While this i5-2405S processor is the most power hungry option we considered, it is unlikely that all 65W will be used continuously for long durations. In some preliminary testing with this processor we found that running our basic software along with video compression resulted in about 10-20% of the processes capacity, resulting in power use of about 20W. However, while this is okay for our purposes we need to ensure that the system was capable of operating at full capacity in the event the some payloads required it to do so. Given the amount of heat created at 65W of power and the tight space constraints of environmentally sealed chassis this meant we needed a water-cooling system for the computer. Using an off-the-shelf water-cooling system, we routed the water lines through the chassis and a passive convector outside the chassis in the rear. Later sections of the report discuss the validation of this water-cooling system through various temperature tests.

4.2.2 Battery selection and the BMS

Driven by our drive motor selection and other electrical system requirements, we selected a 24 volt primary DC bus. Weight and volume considerations led to the use of Panasonic 18650 lithium ion cells in our main battery. These cells have an energy density of approximately 180 Wh/kg, which puts them near the peak of high-performance battery technology. They are common in many high-performance electric vehicles and other critical battery applications. The cells we used have a nominal voltage of 3.6V, a standard capacity of 2250 milliamp-hours, and a cycle life of over 2000 cycles. The mass of each cell is 45 grams.

Based on desired runtime, expected power usage, and mass constraints we selected a battery configuration that could provide 35Amp-hours at the nominal bus voltage. The completed battery system consists of 96 cells wired in 6 series strings of 16 parallel cells each. This system

has the potential to provide 810Watt-hours when fully charged. The total pack ranges from 25.2 volts to 18 volts depending on the state of charge.

To get the maximum output of the battery system over its lifecycle, we use a digital shunt-type battery management system onboard with full-time communications to our main computer. The Mk3x8 lithium battery regulator system from Manzanita Micro shunt-balances the pack on charge to help ensure the series strings stay balanced. It also provides high, low, and overvoltage monitoring as well as 6 channels of temperature monitoring. The battery management system communicates with the rover computer via a highly fault tolerant serial bus and a USB interface box. We can regularly poll the battery management system to give voltage and temperature telemetry and for data-logging purposes.

To estimate potential operation times, and ensure they are within requirements, we first assume that each drive motor is using 3Amps continuously. While each motor is rated to pull 9Amps continuously this is only in the worst case scenario, where the rover is driving 1.2m/sec up a 44degree slope. On level ground the loads and duty cycle will be significantly less, likely resulting in an average current draw of less than 1Amp. A current draw of 2Amps is assumed in order to produce a conservative estimate of operating time. Assuming this condition, at their nominal voltage of 22.5V the drive motors will use 202.5W of power. In estimating other energy consumptions we assume worst case scenario. For example, the processor normally uses about 20W of power, however, at full capacity it can run up to 45W, so that is the value used in creating our estimated battery life. Table 2 below is a summary of our estimated power requirements.

Components	**Power (Watts)**
Four drive motors	180
Quad-core i5 processor	65
Liquid cooling pump	12
Wi-Fi card	5
Contactor	1.1
Total	**263.1 W**

Table 2: Power Requirement Estimations

While this approximation does not account for all power drawing devices, it does provide conservative estimates for the five main power drawing components that will make up the majority of power consumption. Dividing this 263.1W by the 810W-hr battery capacity yields an estimated battery life of 3.08hours. This conservative estimate is in line with the 3 hour requirement and shows that our selected battery can provide sufficient power and operating times.

4.2.3 Power distribution

The power from the battery is distributed over a 24V nominal primary DC bus, which has an isolated ground. The battery is directly connected to a Gigavac GX-21 contactor, which will disconnect in the event of an electrical failure leading to uncontrolled current flow. Downstream circuit protection is provided by standard ATC fuses wired in with inline fuseholders for each 24V line. Our 12V and 5V secondary DC busses are supplied by a pair of Vicor DC-DC converters, with 150W available on the 12V bus and 50W available on the 5V bus. All three DC busses have isolated grounds. Other than internal requirements, all three DC busses are brought out to four TE circular connectors on the rear rail of the rover for use as the Payload/User Power connections. Specifics on these connectors and their pin out can be seen in the User Payload Development Guide (Appendix F).

4.2.4 Communications hardware

For teleoperation, the rover needs to have a robust communications link to the control station. Depending on the range and conditions under which testing or operation is occurring, the rover relies on multiple communication systems to accomplish this goal. The primary communications system for local teleoperation up to approximately 600 meter range is provided by 2.4 GHz 802.11N commercial WiFi system with a pair of 500mW diversity transmitters. The rover-side antenna array consists of two 5.5dB omnidirectional antennas on a 40 mm baseline. The control-side antenna array consists of two 8dB omnidirectional antennas on a 1.5 meter baseline. The same USB transmitter/receiver is used for both the rover-side and control-side links. The 802.11N link provides speeds up to 300MB/second.

For communications beyond the 600 meter range of our point to point 802.11N WiFi system, we rely on a Verizon 4G LTE broadband connection. This limits us to operation in areas with developed commercial broadband infrastructure. The Pantech UML-290 4G LTE broadband modem is connected to a CradlePoint broadband communications router. This allows us to seamlessly transition from the 802.11N WiFi to the 4G LTE broadband connections, with automatic failover to a 3G broadband connection. The broadband modem is connected to a Larsen 4dB quad-band commercial broadband antenna. This particular antenna also provides future expansion capability with coverage in the 800 MHz, 900 MHz, and 2.4 GHz bands.

4.3 Diagnostic Systems

Although the primary purpose is to develop a rover to be used as a modular research platform we also wanted to include basic autonomy into our software architecture aimed at monitoring system parameters to stay within safe levels. This will also be helpful to users who may operate the rover close to its limits and want a way monitor the rover's health. The two main safety systems we designed is an extensive temperature monitoring system and situational awareness, both of which are discussed in this chapter.

4.3.1 Temperature Monitoring

Running components for long durations in harsh climates where rovers are tested can result in high component temperatures. In addition, many components in the sealed chassis such as the battery, motor controllers, DC regulators, and i5 processor generate heat, making the system susceptible to overheating in some scenarios. Some components if run continuously at high temperature can be permanently damaged, have decreased performance, or even cease to function. Therefore, it is essential that we be able to monitor the temperatures of critical components at all times.

To monitor system temperatures we selected Maxim DS18B20 digital 1-Wire temperature sensors. Each sensor has a unique address and can measure temperatures between -55°C to 125°C with accuracy of ±2°C for the full range and better accuracy at less extreme temperatures.. To communicate to the sensors an Arduino microcontroller is used to request temperatures from all the sensors and publish them onto a ROS topic. Digital sensors with unique addresses like these can all be attached to the same communications bus, making it easy to connect many sensors to a single Arduino on a custom breakout board that accommodates up to 18 temperature sensors, Figure 30.

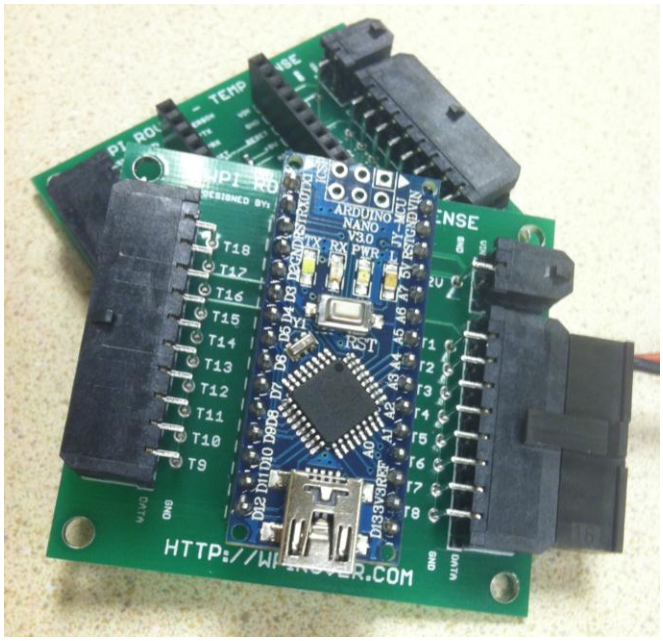

Figure 30: Custom Temperature Sensor Breakout Board

In total 9 of the 18 possible temperature sensors are used. One sensor is placed on each of the four drive motors to provide an estimate of the motor winding temperature. There is also one sensor on both the 5V and 12V Vicor DC voltage regulators since they have the potential to generate large amounts heat under load. A sensor was attached to the Northbridge chipset on the motherboard because generates a fair amount of heat under normal load and has no internal sensor. The two remaining sensors are distributed around the chassis compartments. One is

placed in the rear compartment where the four EPOS controllers are located. The last one is placed outside the chassis on the water-cooling convector, to monitor its effectiveness. All of these temperatures are relayed to the user through the GUI, and where applicable necessary action will be taken if critical components reach unsafe limits.

Four temperature sensor connections are connected to pins in the user payload ports, providing users with the ability to add temperature sensors to their custom payloads.

Other temperature sensors that are not part of the same system monitor the i5 processor and battery. Monitoring the temperature of the battery is built into the BMS. Six sensors are used to observe the temperature of each of the series packs and the computer will notify the user if temperatures are out of operational limits.

Given the high thermal dissipation of the Core i5 processor, as well as the fact that it is sealed from outside ventilation, it is necessary to constantly monitor its temperature. To do this, we are using an open-source library known as lm-sensors that provides access to low-level information of multiple computer components. If the CPU temperature is too high, the rover will alert the operator and begin taking steps necessary to cool the computer, including shutting down processor intensive applications. If the CPU temperature approaches dangerous levels, the rover will begin a shutdown sequence to prevent permanent damage. Figure 31 shows the locations all the temperature sensors distributed throughout the rover.

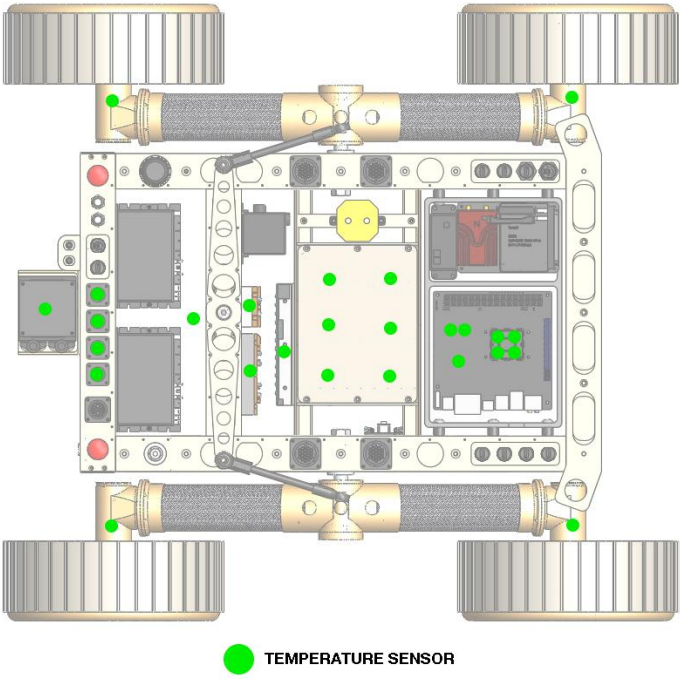

Figure 31: Distribution of Temperature Sensors in Rover

4.3.2 Slope Monitoring

One of the design goals of our project focuses on providing an adequate level of situational awareness to the operator of the rover. While a simple video feed may be enough to accomplish this goal, it is still possible for the operator to lose track of the position and orientation of the robot. Because Robo-Ops requires that the robot return safely to its starting position, such disorientation is unacceptable. Furthermore, the rocky and uneven terrain could pose a tipping hazard if the operator is not aware of the rover's orientation.

To address these issues, the rover will use an inertial measurement unit (IMU) to provide accurate orientation data to the operator. IMUs are able to measure acceleration and orientation through a series of accelerometers, gyroscopes, and, in many cases, compasses. They are further optimized by combining the data from all of the aforementioned sensors into a filter to return more accurate data than any of the sensors alone could provide. By using an IMU, the rover will be able to relay its orientation to the operator.

There are many factors to look at when deciding upon which IMU to use. Often, the most important specification to look at is the accuracy of the IMU. While IMUs are designed to significantly reduce error, they are still subject to inaccuracies caused by angular drift or noise, usually defined by a number of degrees per hour or in meters per second squared. While these errors may start out small, they will accumulate over time, and eventually lead to inaccurate and unusable data. As Robo-Ops requires that each rover be able to continuously operate for at least one hour, it will be imperative that we choose an IMU that minimizes error over this timeframe.
Maximum angular rate is also a key specification to analyze when choosing an IMU. The maximum angular rate describes how fast the IMU can rotate while still providing accurate data. If the rotational speed of the rover exceeds the specified value, there will often be errors in the resulting orientation data that the IMU provides. Therefore, it is crucial to ensure that the maximum angular rate of the IMU is faster than the maximum turning rate of the rover.

While there are other important characteristics to consider when choosing an IMU, the above two are the most important for our rover. These two specifications, along with cost and availability, were the determining factors in the selection of our IMU. Fortunately, the process of determining which IMU to use was not a difficult task, as InterSense, a major developer of inertial sensors donated one of their most accurate IMUs to our project.

The InertiaCube3, donated by InterSense, will provide the high accuracy angular data that we need to calculate the orientation of the rover. The reported error of the InertiaCube3 is less than 1° per hour in yaw, and just $.25^\circ$ per hour in pitch and roll. Furthermore, it has a maximum angular rate of approximately 1200° per second, which is more than enough for our rover.

While the IMU will provide accurate information on the yaw, pitch, and roll of the chassis it alone is inadequate to fully define the position of the rover. Since the rover has passive rocker differencing suspension the relative position between the wheels and chassis can change. To fully observe situational awareness it is necessary to combine the orientation data from the IMU with the known locations of the wheels. To provide this added feedback a 12-bit absolute encoder is used to measure the angle of one of the rocker arms. More specifically we selected the US Digital MA3 encoder which can read directly into ROS using a US Digital QSB.

4.3.3 Battery Management

As previously mentioned the BMS has a few functions, all of which monitor the health of our lithium-ion battery pack. One function is to charge the battery and balance the voltage of individual packs during charging. It also measures the temperatures of each of the 6 packs and sends that information to the main computer. Lastly, it monitors cell voltages during use which can then be used to estimate the remaining battery life. Most importantly this will also be used to shut shown the system if the battery voltage drops too low, as that indicates a fully discharged state.

4.4 Software Architecture

This chapter will briefly review ROS, as that was the software framework selected for use on Oryx 2.0. ROS is a commonly used communications framework in academia and industry, and has several advantages for our application that are discussed. A design diagram of the software architecture is presented in Figure 32. It describes how each software "node" integrates with Oryx 2.0. In this section, we will discuss what each of these nodes does, and explain why such software design decisions were made.

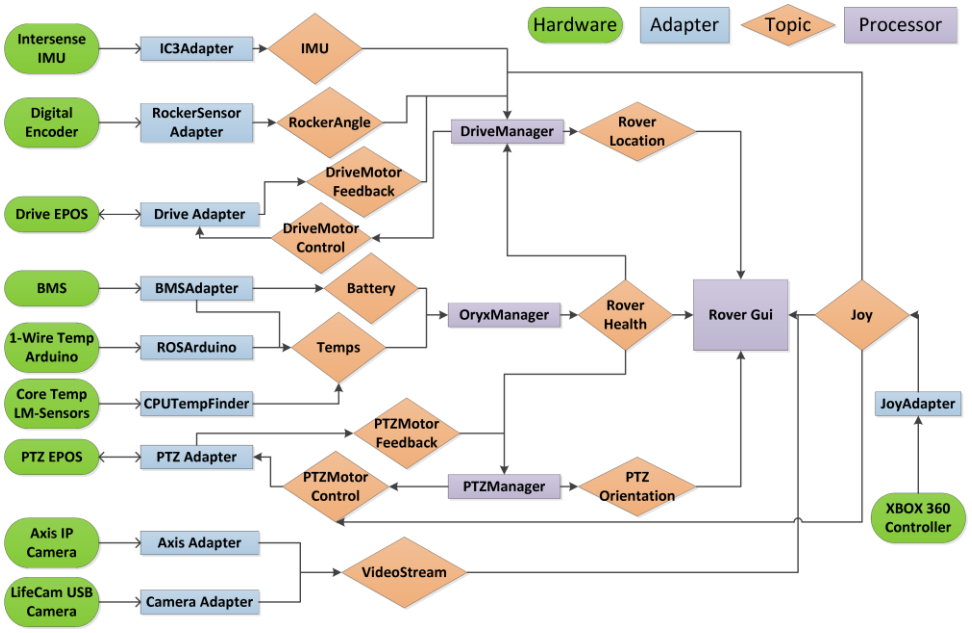

Figure 32: ROS Node Software Design Architecture

4.4.1 ROS Framework

The primary software and communications framework that our rover uses is Robot Operating System, commonly known as ROS(http://www.ros.org). Though its name may infer otherwise, ROS is not actually an operating system of its own. Instead, ROS is a communications framework that allows multiple programs across multiple computers to acts as though it were a single program. This allows for intuitive compartmentalization of code; rather than have a single program controlling every aspect of our rover, we can instead write multiple programs dedicated to a single task and have them seamlessly interact with each other.

The distributed programming that ROS allows for is used heavily in our rover. Each node is entirely separate from the others. For instance, the "BMSAdapter" is a not at all related to the "CPUTempFinder". Their only connection is through a communications bus known as a topic. Topics are the means by which nodes exchange information. Nodes can submit information to, and read information from, such topics, thereby allowing multiple programs to communicate with each other. Whenever new information is published to a topic, all subscribers to that topic will receive that information. The number of nodes subscribing and publishing to topics is dynamic, meaning there is no limit to how many nodes can communicate with others through an individual topic. The topics are also split up by what information they carry. If the user wants to listen to temperatures, they only need to listen to the "Temps" topic. This results in a more intuitive software architecture than could be achieved if only one main program was used.

4.4.2 Software Design and ROS Nodes

This section will review the software design for Oryx 2.0 by discussing all major ROS Nodes and their functions. While ROS provides a convenient communications framework it was still necessary to design our own organization of tasks to facilitate teleoperated driving, telemetry, controls, and some autonomous features.

EposManager

Arguably the most time consuming piece of software to write was the EposManager. Given that all of the motors used EPOS controllers, we decided to write a ROS wrapper for most of the EPOS functions. Currently, both the DriveAdapter and PTZAdapter nodes use EposManager.
One of the most useful aspects of EposManager is its dynamic reconfiguring and launch-time parameter inputs that allow the user to use EposManager for multiple motors without ever having to recompile the software. It does this by loading parameters from a YAML text file, and passing the name of that text file to EposManager as a launch argument. The user can then change motor parameters by editing the text file. Furthermore, multiple EPOS controllers in a chain can be accessed simply by passing in additional text files when launching an EposManager node. While a single EposManager can handle multiple nodes in a chain, it cannot control multiple separate chains of EPOS controllers. In these instances, the user needs to launch an additional EposManager with a different port parameter. Additionally, some, but not all, parameters can be

changed while the program is running through the built-in “dynamic_reconfigure” node, seen in Figure 33.

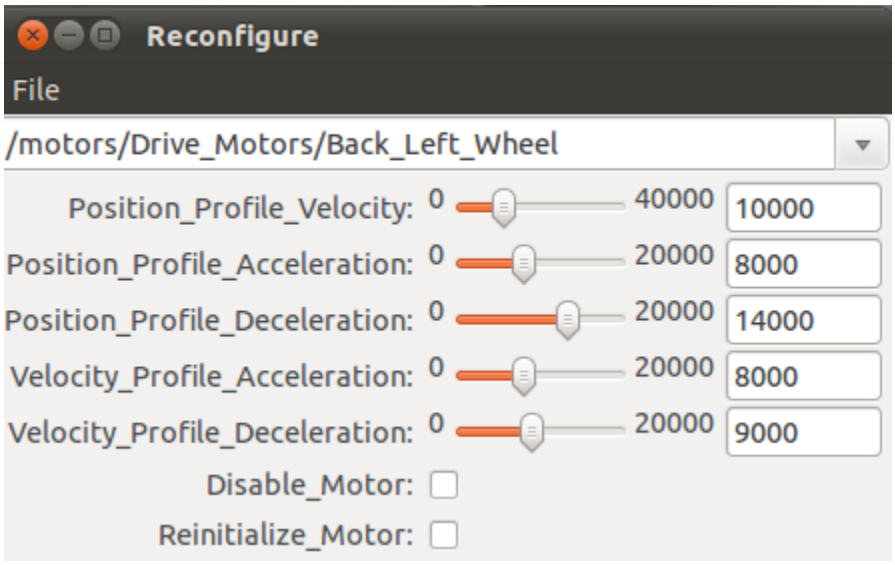

Figure 33: Dynamic Reconfigurable part of the GUI

While the EposManager is running, the user has multiple ways of controlling the motors, each with its own benefits. First, there is single motor control, in which the user, or their program, sends a single EPOSControl message to the EposManager. Doing so will result in only one motor moving, and is best if motor velocities need to be sent separately from each other, as would be the case if homing multiple axes. For simultaneous control, a GroupEPOSControl message is to be used. This allows the user to command all the motors to move at the same time with minimal delay. Furthermore, the user can choose to control the velocity, relative position, or absolute position of the motor, giving them a great deal of control over how they want their motor to move.

Similarly, the user has multiple ways of receiving information from an EposManager node. Each EposManager will publish to a “Motor_Info” topic that contains information on the state of the motor including its velocity, current, position, enable/disable state, and any errors detected by the EPOS. Just as with the EPOS control, there is a topic that sends single “Motor_Info” messages serially, and one that sends groups of them at once. The former is best if Each EposManager will publish to a “Motor_Info” topic that contains information on the state of the motor including its velocity, current, position, enable/disable state, and any errors detected by the EPOS. Just as with the EPOS control, there is a topic that sends single “Motor_Info” messages serially, and one that sends groups of them at once. Both return the same motor information; however the latter should be used if each motor’s information needs to be received at the same time, for instance, to calculate odometry from wheel velocities.

DriveManager

Though the EposManager allows for control of the motors, having the user directly setting motor speeds is an unintuitive method of controlling a rover. The DriveManager acts as an intermediate step between the operator and the motor control, transforming joystick and twist commands into motor speeds. By publishing joy messages to the "joy" topic, the user can control the drivetrain in an intuitive manner. In the current setup, the user can drive the rover through the left and right joysticks, mapped to the left and right wheels of the rover, or through the D-Pad. The D-Pad allows the user to drive forward, backward, or to turn sharply without having to worry about ensuring that each joystick is pressed exactly the same amount.

Additionally, the DriveManager node converts the velocities received from each of the drive motors into an estimated position and orientation, and publishes it as an odometry message. It is important to note that, due to the skid steering that the robot uses, wheel odometry alone is unlikely to be accurate when turning. This odometry message can then be used by nodes implementing a Kalman Filter, thereby producing a more accurate estimate of the position and orientation of the rover.

PTZManager

Like the DriveManager, the PTZManager allows for more intuitive control of the camera boom. The PTZManager takes in two types of user input for controlling the camera boom's motors. The first of these is through an XBOX 360 controller, where the left joystick controls the pan and tilt motors. In order to differentiate control between the pan and tilt motors and the drive motors, the operator must also hold the left bumper on the XBOX 360 controller when controlling the pan and tilt motors. A software limit is placed on these motions to ensure that the camera boom does not try to extend past any of the hard stops, potentially damaging the motor.

The second method of control is through a "dynamic reconfigure" node, where the user can specify the desired angle of the pan and tilt motors. If this method of control is to be used, however, the pan and tilt motors must first be homed. This can be done through the same "dynamic_reconfigure" node by checking the "Home_Pan" and "Home_Tilt" checkboxes. This will cause both the pan and tilt motors to begin driving until they see a current spike. They will then begin driving in the opposite direction until a second current spike is detected, after which they will drive to the position halfway between the two hard stops. After both motors are homed, the PTZManager will also begin publishing the orientation of the camera.

Besides the pan and tilt motors, there is also a boom motor that lifts the camera payload to its full height. The boom motor can be controlled through a joystick by pressing the select and start buttons at the same time, and then using the left joystick. This is done to reduce the chance of someone accidentally driving the boom motor during normal operation. The preferred way of controlling the motor is through the "dynamic_reconfigure" node by using the "Home_Boom"

checkbox. One of the challenges encountered was that, due to the weight of the camera and the extended lever arm caused by the boom, the boom motors see a high level of current when raising the boom. Unfortunately, the current seen while driving the boom up is close to the current seen when the boom motor hard stops. If the home current level is increased, the timing belt runs the risk of skipping before seeing the current spike. To counteract this, the boom motor is driven slowly when it is raised. Often times, this speed is undesirably slow. In these instances, the "Home_Safely" checkbox can be unselected prior to homing the boom motor. Doing so will cause the boom motor to drive at a high speed for a preset amount of time before slowing down and monitoring current. This works well, but should only be used if the camera boom is fully non-deployed.

OryxManager

The primary purpose of the OryxManager is to monitor the rover's health and alert the user when any system begins operating in dangerous levels. In particular, it monitors the battery voltage, temperatures, and communications link between the rover and the operator.

The first function of the OryxManager stems from its battery monitoring. The lithium ion cells used on our rover may become permanently damaged if their voltage drops too low. Therefore, we must constantly monitor the cells and ensure that they never drop too low. To do this, the OryxManager node subscribes to the Battery topic published by the BMS node and records the voltage of each cell. If it detects that a cell's voltage is below the specified threshold (in our case, 3.4 volts), it immediately tells all motors to halt and begins a safe shutdown sequence of the computer. Doing so dramatically reduces the power consumption of the rover, while guaranteeing that no data becomes corrupted, as could occur if the rover shuts down due to low power.

Additionally, the OryxManager node monitors temperatures from various sensors throughout the rover. Depending on the monitored temperature, and the corresponding location of that temperature sensor, OryxManager decides what the best action may be. For instance, if it detects that a motor's temperature is becoming too high, it will disable that motor until its temperature lowers to safe level. If it senses that the CPU core temperature is approaching dangerous levels, it will begin shutting down non-essential processes. If it continues to rise, OryxManager will shut down the computer. Additionally, all of these temperatures are recorded to a log file in a MATLAB friendly format so that users can graph the temperatures over time.

Finally, the OryxManager monitors the communications between the operator and the rover. By enabling the "Remote_Heartbeat" option in a "dynamic_reconfigure" node, the OryxManager will constantly listen for a heartbeat from the operator's computer. If it does not sense one for too long a time, it tells all motors to immediately halt until it receives another heartbeat message. This ensures that, if communications is lost while driving, Oryx 2.0 will not continue to drive

uncontrollably. This has the additional effect of guaranteeing that the rover will stop if the roscore crashes.

CameraAdapter

The CameraAdapter node is a simple, reusable node that publishes images from USB webcams. Regardless of the source, the CameraAdapter can publish the images in either raw, MJPEG, or Theora format. This allows it to easily transmit high quality images over wireless connections by significantly reducing the bandwidth consumed by the images.

While the CameraAdapter initially used OpenCV to grab images from the webcams, it was found that doing so resulted in approximately a quarter of a second delay on the image stream. Furthermore, even for low resolution image streams, OpenCV required far more USB bandwidth than was necessary. The result is that no more than one webcam could be used per USB bus. To address this issue, we rewrote the CameraAdapter to use the UVC driver, an open-source webcam driver. Using the UVC driver gave us fine control over how much bandwidth would be requested from each USB bus per video camera, allowing us to stream images from multiple cameras on the same bus. Additionally, the latency from grabbing the image was significantly reduced. The one downside posed by the switch to the UVC driver is that we are no longer easily able to change the resolution of the image on the fly. Given that the resolution can be changed by simply restarting the camera node, we determined that this was an acceptable solution.

BMSAdapter

The BMSAdapter node creates a serial connection between the BMS and the rover computer. From this connection, it monitors the voltages and temperatures of each battery cell, as well as the pack as a whole. One important aspect of the BMSAdapter is that the /dev/ttyUSB* port of the BMS needs to be passed into it as a parameter. Unfortunately, this port is not always clear to the user. To simplify this task, we created a udev rule that uses the serial number of the BMS to identify what port it is on. Thus, the user only needs to pass in /dev/BMS and the program will identify what port the BMS is on. It is also important to note that, in order for the BMS to work, it must be disconnected and reconnected to the USB port after boot. Fortunately, we have been able to mimic this action in software through a series of shell commands that run at boot, but it can inconvenience users who do not know about this problem.

ArduinoTemps

As the name suggests, the ArduinoTemps node uses an Arduino and multiple temperature sensors to monitor the temperatures of various systems throughout Oryx 2.0. This is accomplished through the “rosserial_arduino” package, which allows Arduinos to be treated as serial ports. Code is simply loaded onto an Arduino, and then run by launching the rosserial node with the USB port of the Arduino as an argument. As with the BMS adapter, a special udev rule was written to automatically determine which port the Arduino is on.

IC3Adapter

To determine the orientation of Oryx 2.0, we use an Intersense InertiaCube3. The IC3Adapter reads in the orientation and angular velocity data from the InertiaCube3 and publishes it as an IMU message. Linear acceleration is also published, however the accelerations returned by the IC3 are highly inaccurate, and using it to find the position of the rover would lead to erroneous results. For this reason, the covariance field in the IMU message corresponding to the linear acceleration is set at an extremely high value.

Rover GUI

As Oryx 2.0 is intended to be teleoperated, we decided to create a graphical user interface for user control of the rover. This GUI is written using RosJava, a java implementation of the ROS core. By using Java, we were able to develop a GUI in the powerful Swing environment, while making it easy to modify the GUI if need be. The final GUI can be seen in Figure 34.

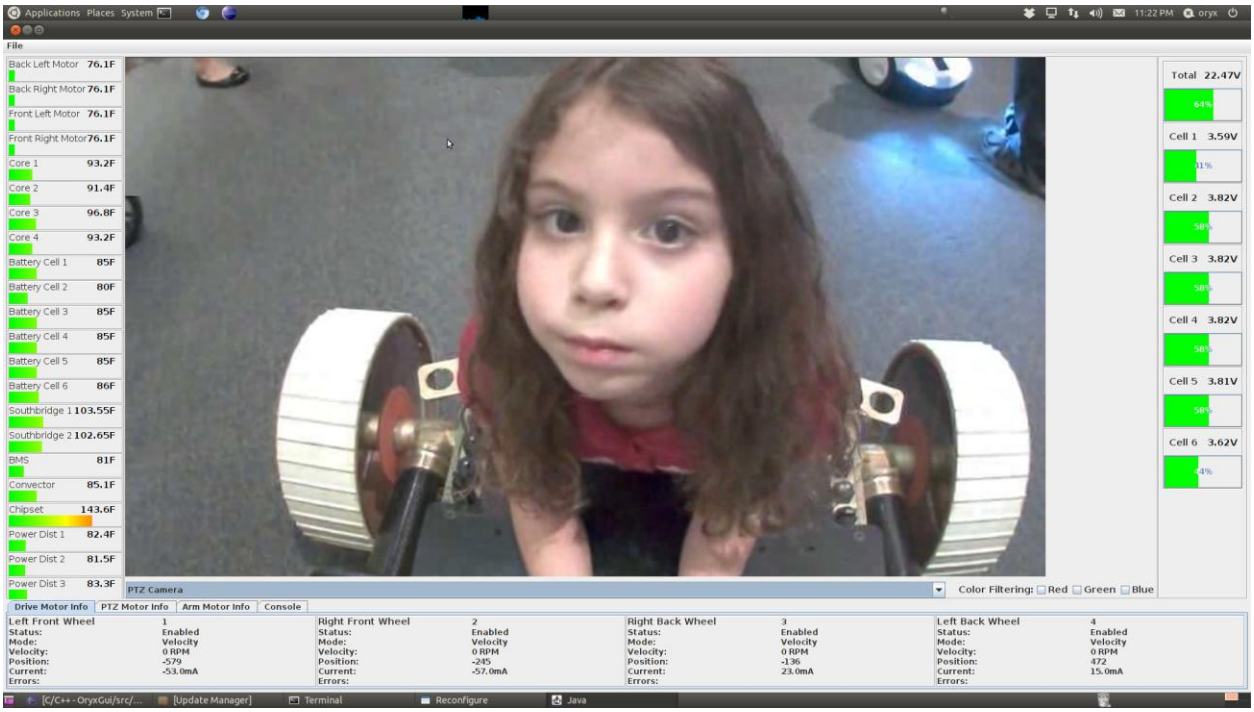

Figure 34: GUI for Teleoperation and Telemetry

As seen in Figure 34, most of the GUI is dedicated to displaying the video feed. Also of note is the selection box directly below the video feed. This allows the user to select which video stream they wish to receive if multiple video streams are being published. The GUI differentiates between which image belongs to which stream by looking at the header_id of each image message and cross checking it against the name in the selection box. If they are the same, it displays the image. Otherwise, it discards it. If an image is published with a header_id that is not

already listed in the selection box, the GUI will automatically add it to the list of possible video streams in the selection box, allowing for the dynamic adding of camera streams.

Temperatures are displayed on the left side of the GUI, and are updated as soon as a new temperature message is received. As can be seen in Figure 34, both the text value of the temperature, as well as a visual indicator, are displayed. This allows the user to quickly gauge the temperature of each system on Oryx 2.0. Additionally, the text field containing the number value of the temperature will turn red if high temperatures are detected, immediately alerting the user if any system is operating in dangerous levels.

Battery voltages are shown on the right side of the GUI. Just as with the temperatures, the battery meters are large enough so that the user can clearly see what battery is at what voltage, but small enough that they do not intrude upon the view of the video stream. Though it is not shown in Figure 34, the battery meter will turn red if it detects too low a cell voltage.

Finally, at the bottom of the screen, there are tabbed panes containing motor information for each motor chain. Within each pane are multiple panels corresponding to each of the motors in that chain. Each panel displays the motor's velocity, current, position, and state. By quickly cycling through the tabbed panes, the operator can easily see the status of each motor and react accordingly.

4.5 Payload Interface

A critical aspect of all rovers is their ability to carry payloads. In fact, the primary purpose of space exploration rovers is to safely transport scientific instruments between sites of interest. Payload integration is often done in parallel with rover design, resulting in highly specific configurations based on the payloads for a given mission. Since a primary goal of our rover is to test a wide variety of payloads, we needed to develop a standard payload interface that would allow the rover to be reconfigurable for a multitude of tasks.

To accomplish this goal we took a holistic approach to payload integration, by considering all related aspects such as the hardware interface, electrical connections for data and power, software, and available computing power. This section will discuss our design approach to each of these features, divided into two main sections, hardware and software interfaces. We will also review our design of a deployable camera payload. Relevant to the NASA Robo-Ops challenge, the deployable camera also aims to validate our payload interface by providing an example of a successful payload.

4.5.1 Payload Hardware Interface

In developing the standards for how payloads should be connected to the rover we considered both the mechanical attachment and how users would be able to connect to power and data ports.

Since the computer is inside the sealed chassis we needed a way to breakout commonly used data ports to the user, in a way that kept the chassis sealed and also provided water resistant connections.

For mechanical attachment we choose an optical table type of approach, where the top of the rover is a flat plate with a grid of tapped holes. The design of this top plate is shown in Figure 35. It is machined from one piece of 3/8in aluminum plate and is heavily pocketed to reduce mass. It also has a 2in square grid of #10-32 UNF tapped holes to secure user payloads. With the exception of antennas and connectors around the perimeter the top plate is entirely flat by design in order provide an open area that is easy to connect to. There is also a row of tapped holes on the front of the rover to provide an alternative place to attach components. To connect payloads to the computer several USB and Ethernet connections are made available on the chassis around the top plate.

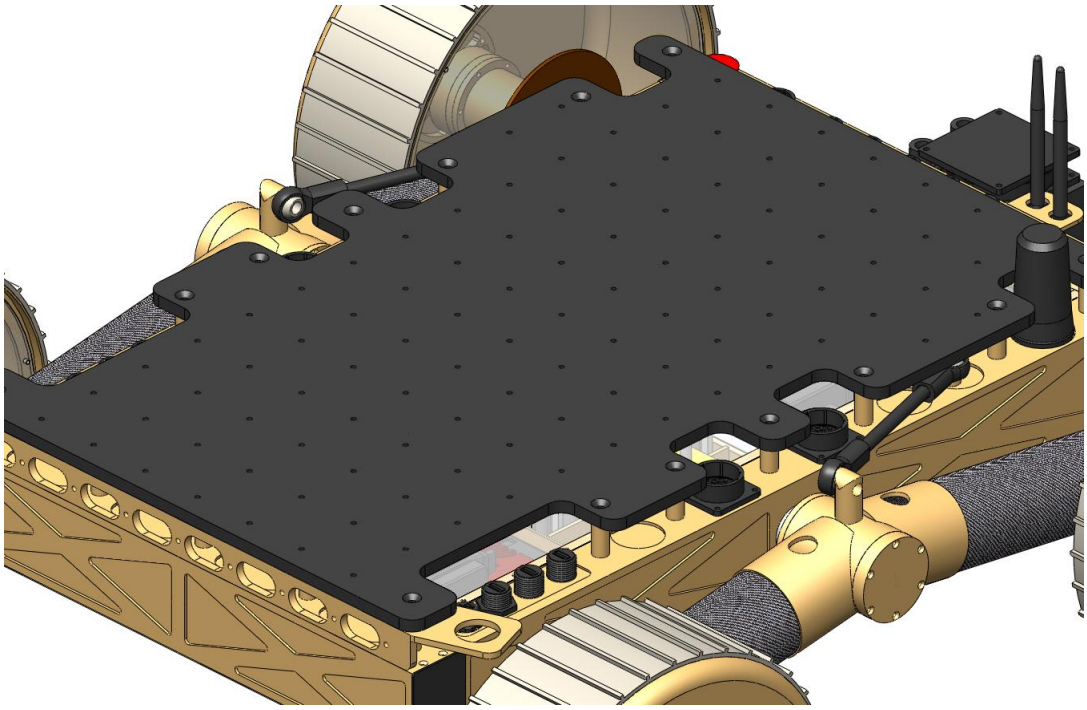

Figure 35: Design of Top Plate for Hardware Interface for Payloads

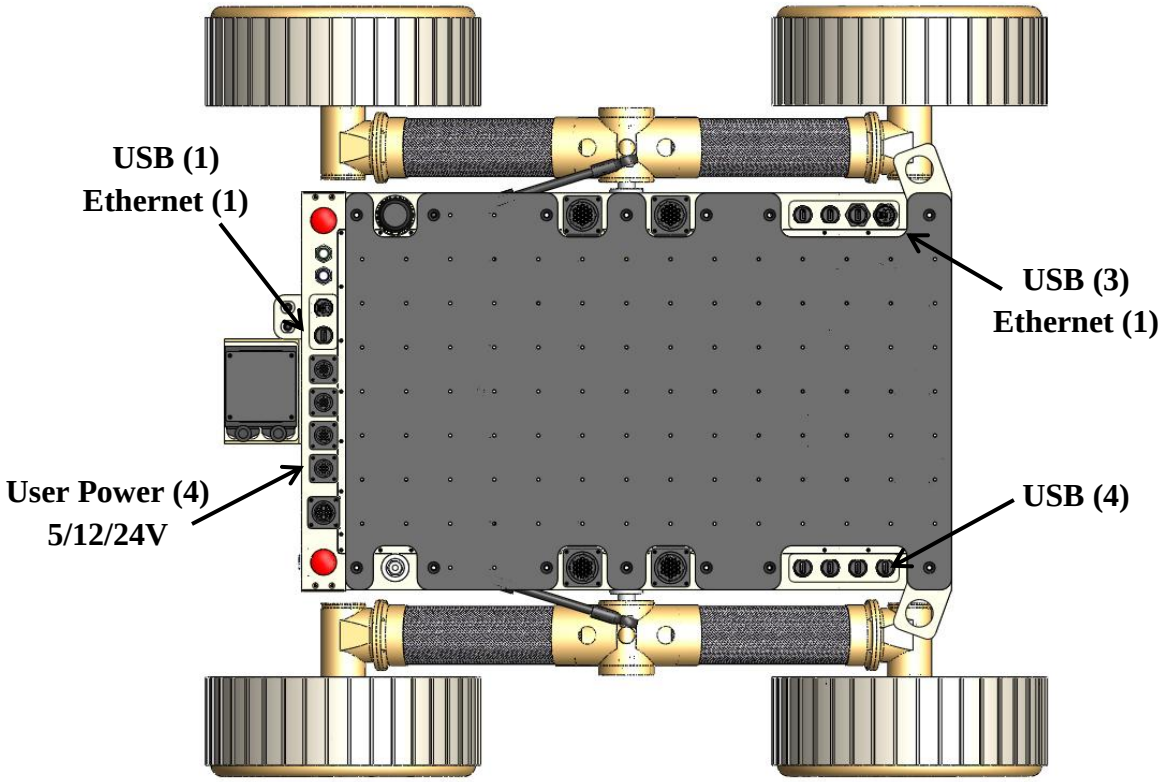

Figure 36: Top View of Top Plate and Available Connections

Figure 36 shows a top view of the rover, which shows the layout of USB, Ethernet, and power ports. On the front of the rover there are seven USB connections and 1 Ethernet, and on the back there is one USB, one Ethernet, and four power connections. Each of the four power plugs carries 5V, 12V and 24V. Also, all connectors are water resistant and have sealing caps for when they are not in use. The result is easy access to power and a convient way to connect to the computer through USB or Ethernent, which should accomdate a wide variety of payloads.

4.5.2 Deployable Vision Payload

A key aspect of the NASA Robo-Ops competition will be our ability to quickly locate colored rocks, something that should be made easier with a high resolution pan-tilt camera. To provide the operators with a good view for surveying the landscape we designed a deployable camera boom as a payload for the rover. By following our payload specifications outlined above we also hope to demonstrate the efficacy of the payload integration features.

Figure 37 shows the overall design of this payload. The carbon fiber boom lays flat in the storage configuration and is raised into place in order to secure the camera about 76cm above the top of the rover. The camera is an Axis M1114 enclosed in a weather proof case. It has selectable resolutions up to 720p, an auto DC iris, and a varifocal lens. In total this payload has three degrees of freedom, all powered by EC-max 22mm 12W brushless Maxon motors.

Figure 37: Design of Deployable Camera Payload

The deploying and panning actuation joints are located at the base of the camera boom, shown in Figure 38. To lift the camera boom in place the motor has a 1526:1 gear reduction through a Maxon planetary reduction. It then goes through a 4.5:1 reduction through a timing belt that transfers torque directly to the panning gear box, which forms the base of the camera boom. After factoring in gearbox efficiencies we expect to achieve about 29.6Nm of torque at a speed of 1.16rpm at the output shaft. Based on the length of the boom and camera mass this is three times the required torque needed to lift the boom in the horizontal configuration, providing a large factor of safety. While the output speed is slow at just over 1rpm it will travel the desired angle of 90degrees in about 15seconds, which is sufficient for a one time deployment.

Similar to the deploying stage, the panning degree of freedom uses a Maxon motor with an 84:1 planetary reduction to a 5:1 reduction in the timing belt stage. This results in an estimated output toque of 2.8Nm at a speed of 19rpm. An Igus slew ring is driven by the timing belt and acts both as the basis of the revolute joint and to reduce the friction of normal forces. Given the low inertial loads of the deployed camera boom the motor will mainly be loaded by frictional forces of the Igus slew ring. Since these forces are difficult to estimate we assume that 2.8Nm will be sufficient. Also at a speed of 19rpm it will be able to rotate its full range of 300 degrees in about 2.6seconds.

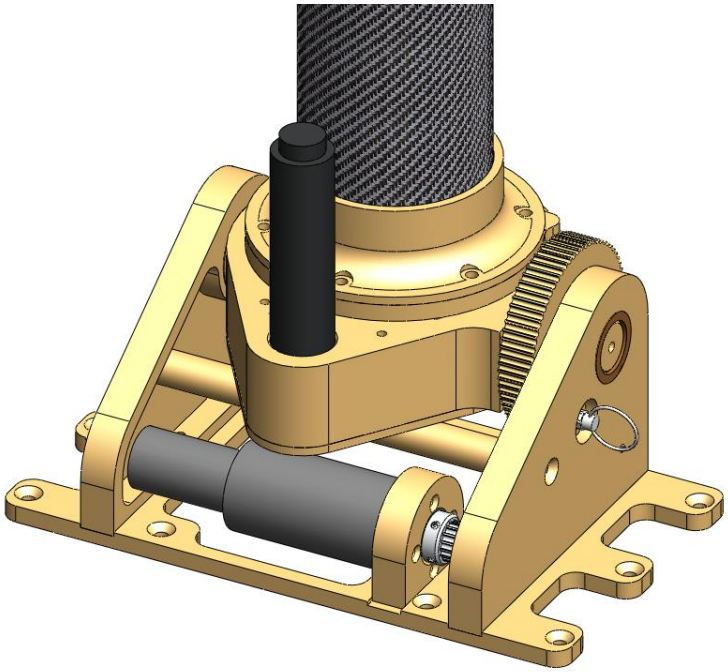

Figure 38: Deploying and Panning Actuation of Camera Payload (belts not shown)

To control the tilting actuation of the camera a Maxon motor with a 690:1 planetary reduction directly drives the camera platform. Shown in Figure 39, this motor is enclosed in a can and connects to the camera by a Fairloc hub. Resulting in 3Nm at 11.6rpm, this should be enough torque to hold the camera and enough speed to traverse the 90degree range of motion in about 1.3seconds.

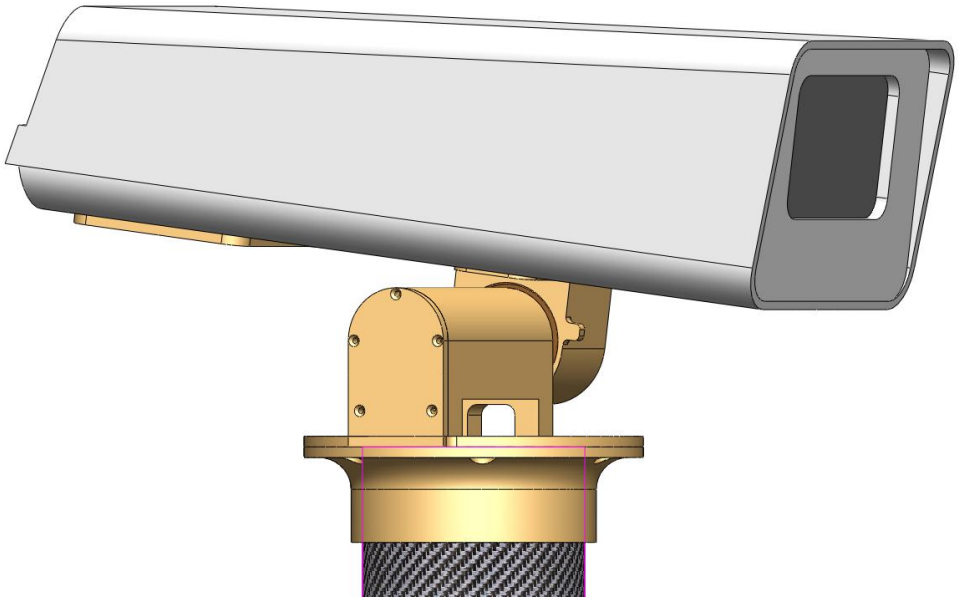

Figure 39: Tilt Actuation of Camera Boom

To control the camera payload we use EPOS 24/2 motor controllers, and feedback from the built-in motor encoders that provide information on the speed and location of the motor shaft. While no absolute position sensors are used, the motor will perform a homing sequence upon deployment. For every joint there will be hard stops located at the range limits. By observing current spikes when each joint hits these hard stops the software will record encoder values at each end of the range. Using this information absolute position control is done in software, which allows the user to command viewing angles with respect to the rover.

Overall this deployable camera boom should provide an excellent tool for surveying the landscape in search of colored rocks. All motors are powered by the battery voltage, about 22.5V, and require one USB connection to communicate to the computer. The Axis camera can be powered by either 12V or 24V and requires one Ethernet connection. Lastly, the entire base of the payload uses the 2in square grid of tapped holes to bolt onto the top plate. As a result this payload should easily integrate to the rover by using available USB and Ethernet ports, and standard voltages that are made available.

4.6 Matlab Simulation and Velocity Controller

One challenge with rovers that use passive suspension is added complexity to the controls problem. Furthermore, straight line trajectories are complicated by rough terrain, which can result in different distances traveled by multiple wheels. With the rover's driving kinematic model, it is trivial to follow a straight line trajectory simply by commanding identical speeds of all four wheels. However, in practice this fails over uneven terrain; for example if the rover traverses a rock that is only on the right side of the rover the right wheels will traverse a greater distance over the same time period, which results in wheel slipping and undesirable yawing. The aim of this controller is to adjust each wheel velocity individual, based on estimations of the terrain profile, to improve straight line trajectory over uneven terrain.

With knowledge of the 3D orientation of the rover chassis and position of the averaging suspension, a 3D kinematic model can be made to locate the wheel positions relative to the rover's chassis. This information is then used to find pseudo-global wheel heights, providing an estimation of the terrain profile. The ultimate goal of the controller is to minimize deviations in yaw and wheel slip, which would otherwise result from constant wheel speeds over uneven terrain.

While this approach should yield similar results to more complex methods, it has several limitations. Mainly, it assumes no wheel slip and cannot verify forward progress though feedback. It also relies on the assumption that an ideal ground plane exists, and that at least one wheel is on this ground plane. The controller is more effective when more wheels are on the ground plane. Given the relative and localized nature of this approach such factors do not

significantly adversely affect the controller. A Matlab simulation is first performed to verify the usefulness of the controller. Finally, the controller is implemented and tested on Oryx 2.0.

4.6.1 3D Kinematic Model

Rovers with passive suspension can be implemented in several ways; however, they generally have similar kinematics where one degree of freedom can define the locations of the wheels relative to the chassis; as is the case with Oryx 2.0. Figure 40 shows the kinematic model of Oryx 2.0, parameterized as follows.

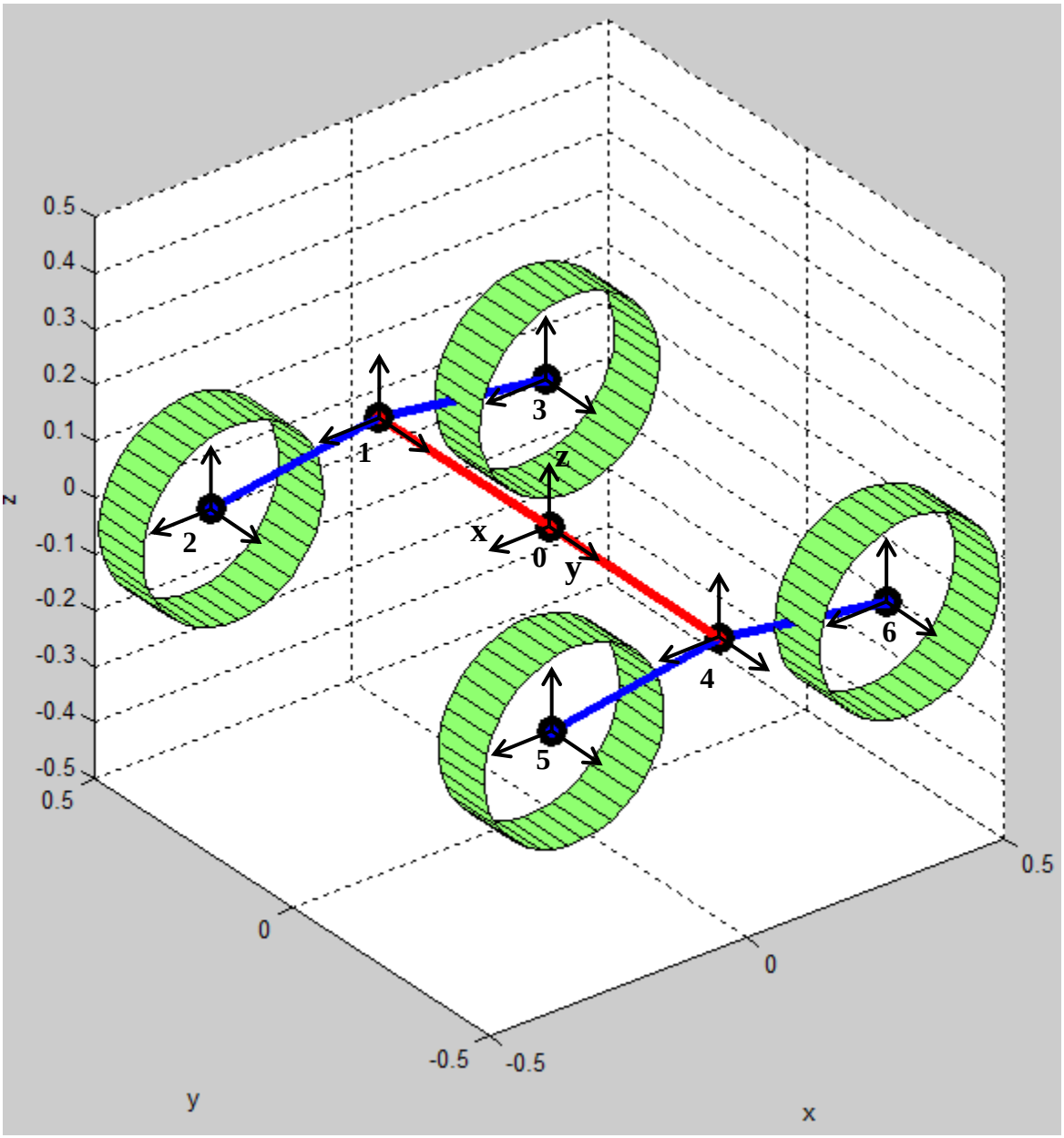

Figure 40: Kinematic Model of Passive Averaging Suspension

In characterizing the rover, three kinematic parameters are needed. One is the wheel base (b), defined as the distance between the left and right sides of the rover, illustrated by the red line in Figure 40. The second is the length of the rocker arm (l), defined as the distance between the rocker pivot and center of the wheel; illustrated by the distance between coordinate frames one and two. The third parameter is the acute angle between the wheels on one rocker arm pair (a), defined as the angle between the rocker arm and the horizontal axis. For Oryx 2.0 these parameters are constant and have the following values; b = 0.86147m, l = 0.3302m, a = 0.14835 radians.

The four inputs to the kinematic model consist of the rocker arm angle (Θ) and the yaw(γ), pitch(β) and roll(α) of the chassis, as measured by the absolute encoder and orientation sensor. The rocker arm angle defines the position of the passive degree of freedom, locating the two suspension members. The yaw, pitch, and roll, are rotations around the z-axis, y-axis, and x-axis respectively, of coordinate frame zero. Using this information it is trivial to locate each wheel's pose relative to coordinate frame zero, which is the basis of the kinematic model.

4.6.2 Feed Forward Velocity Control

The concept of the feed forward velocity controller is to estimate terrain slopes for each wheel at discrete time steps, and adjust velocities accordingly. Terrain slopes are estimated based on the 3D kinematic model and an ideal ground plane estimator algorithm, which is deterministically dependent on the yaw, pitch, roll, and rocker angle. The proposed controller relies on the following core assumptions:

1. An ideal ground plane exists
2. At least one wheel is on or near the ideal ground plane
3. The rover's forward velocity is constant and equal to the desired forward velocity

The presented kinematic model provides the locations of each wheel relative to the rover, making it insufficient at providing useful feedback on the terrain profile. In order to successfully adjust wheel velocities, an accurate estimate of terrain slopes are required. To achieve this, pseudo-global wheel heights are calculated using a combination of the 3D kinematic model and a ground plane estimator algorithm. These wheel heights are pseudo-global because they are with respect to the ideal ground plane, which inherently is relative to the rover. The algorithm for estimated the ideal ground plane is as follows:

Algorithm 1: Estimating the ideal ground plane and adjusting wheel heights to form pseudo-global values

---

1. Determine largest magnitude wheel height based on kinematic model
2. If this is a positive value
    a. Determine the smallest wheel height

b. Subtract this value from all wheel heights
c. Repeat at next time step

3. If this is a negative value
    a. Determine the largest wheel height
    b. Subtract this value from all wheel heights
    c. Repeat at next time step

This proposed algorithm takes in four wheel heights has outputted by the 3D kinematic model. It then converts these local values into pseudo-global wheel heights as described, and repeats at each time step when new sensory data updates the kinematic model. While highly trivial, this algorithm proves to be effective in a variety of simulated scenarios, and can handle both positive and negative obstacles. It does, however, perform much better when the ideal ground plane exists and can fail in cases were all four wheels are on obstacles.

While pseudo-global terrain heights are calculated at each time step, an estimation of the forward progress is needed to calculate terrain slopes. This is typically done with odometry, visual odometry, or inertial measurement units. While odometry was available to provide feedback on wheel velocities a simplifying assumption of a constant rover velocity was made. This avoids problems that can occur with wheel slippage and the need to develop more complex dynamic models.

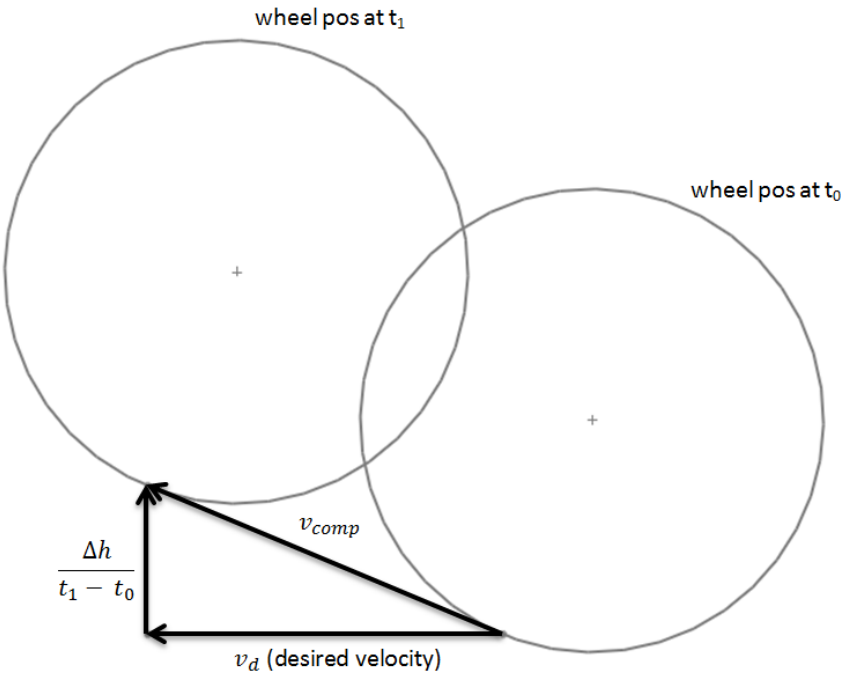

Figure 41: Method for Calculating Adjusted Wheel Velocities

Under this assumption the controller takes a single input, the desired forward velocity, and then adjusts each wheel's velocity based on the desired forward velocity and the controller's

estimation of the terrain slopes. Figure 41 illustrates how this estimation is made. The change in height is the difference between two pseudo-global heights calculated across one time step. Knowing the time between the measurements, this is then converted to an estimation of the wheels vertical velocity. The resulting compensated velocity (v_{comp}) is simply the magnitude of the estimated vertical velocity and assumed forward velocity, as seen in equation 5.

$$v_{comp} = \sqrt{\left[\frac{\Delta h}{t_1 - t_2}\right]^2 + {v_d}^2} \tag{5}$$

This is repeated for each of the four wheels, and at each discrete time step new velocities are calculated and fed forward to the each wheel. In all simulations and experiments the discrete time step used is 0.05second, or an operation of 20Hz.

4.6.3 Matlab Simulation Results

Initial Matlab simulations inputted a desired forward velocity and terrain, in the form of ground heights on either side of the rover. This data was then used to calculate the expected roll, pitch, and rocker angle that the rover would experience over the course of traversing the given terrain. The described controller is then simulated in Matlab, and the calculated desired wheel velocities are observed to visually confirm the success of the controller. Given the idealized nature of this simulation it could only confirm that wheel velocities were being adjusted correctly.

To gain a better understanding of the usefulness of the controller, Matlab simulations were performed again with data logged from Oryx 2.0. In the experimental setup shown in Figure 42, Oryx 2.0 is driven on flat ground over an obstacle while logging data. The obstacle is a trapezoid with known dimensions and slopes of 45degrees. While traversing the trapezoid the roll, pitch, and rocker angle data are logged so that they can be used as the inputs for the Matlab simulation. Using this data the simulation uses the 3D kinematic model and ground plane estimation algorithm to calculate the pseudo-global heights of each wheel. This information is then used to calculate the resulting wheel velocities that the controller would generate as a result of the obstacle. The simulation results of the pseudo-global wheel heights and wheel velocities are shown in Figure 43 and Figure 44 respectively.

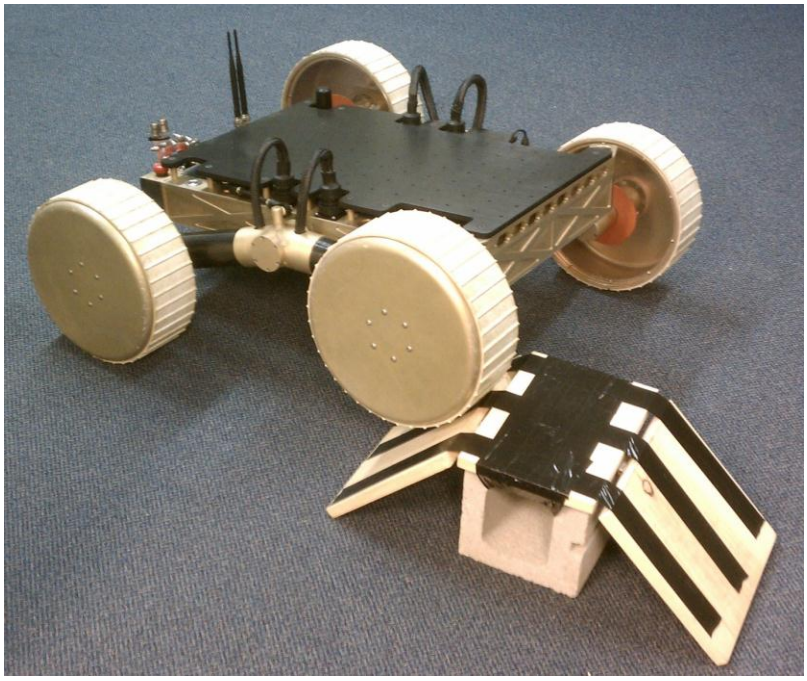

Figure 42: Experimental Setup for Testing Velocity Controller

All tests, including data logged for simulation purposes had a desired forward trajectory of 0.13m/sec, and an update rate of 20Hz.

The pseudo-global wheel heights were as expected, and clearly show the profile of the trapezoid; first under the front right wheel and then under the back right wheel, with a short duration of overlap. The two left wheels remain mostly flat (on the ground). It is notable that the front left wheel is observed slightly above the ground; however, since the controller is only affected by slopes in the wheel heights this constant offset should have no adverse effects.

Resulting wheel velocities were also within reason. Since the slope of the trapezoid is 45degrees the desired wheel velocity should be ~41% faster than the desired speed (0.13m/sec), which would result in a wheel ground speed of 0.183m/sec. As observed between t=20 and t=50 the desired velocity of the front right wheel (the wheel on the incline of the trapezoid), fluctuates between 0.14m/sec and 0.18m/sec, with an average of ~.16cm/sec. This shows that the controller is effective in this scenario and only slightly underestimates the true slope of the terrain. A similar outcome is observed between t=200 and t=240. This is expected given the symmetry of the trapezoid.

During the two instances where the front right and the back right wheel are on the flat of the trapezoid respectively, there are almost no changes to the velocity. This is correct since none of the wheels are on sloping terrain. Between t=100 and t=150 there is a transition period where the front wheel is progressing down the end of the trapezoid while the rear wheel is beginning to climb the front. During this period each wheel is on a slope of 45 degrees, meaning the ideal

compensated velocity is again ~41% faster than the desired speed. In this case, however, the controller calculates moderately high values, about .21m/sec which could have a negative effect on the results.

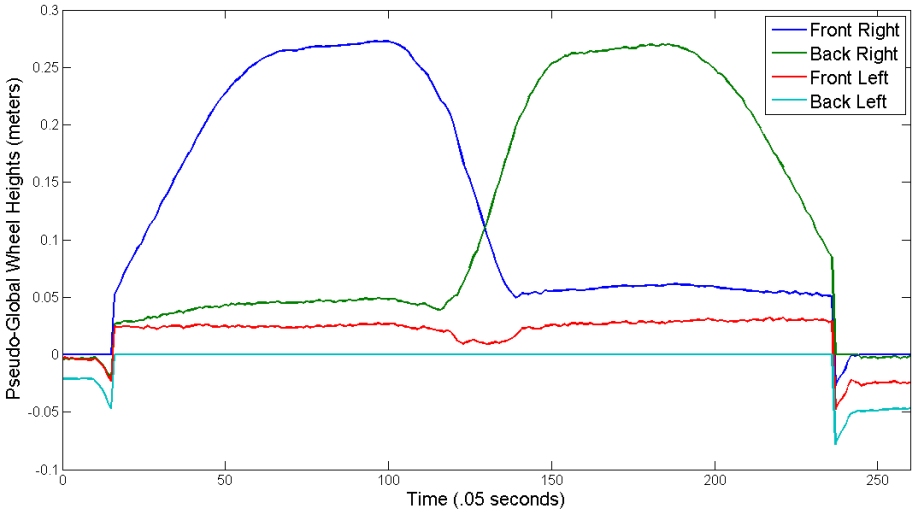

Figure 43: Rover's Estimate of Terrain Profile for Each Wheel in Controller Simulation

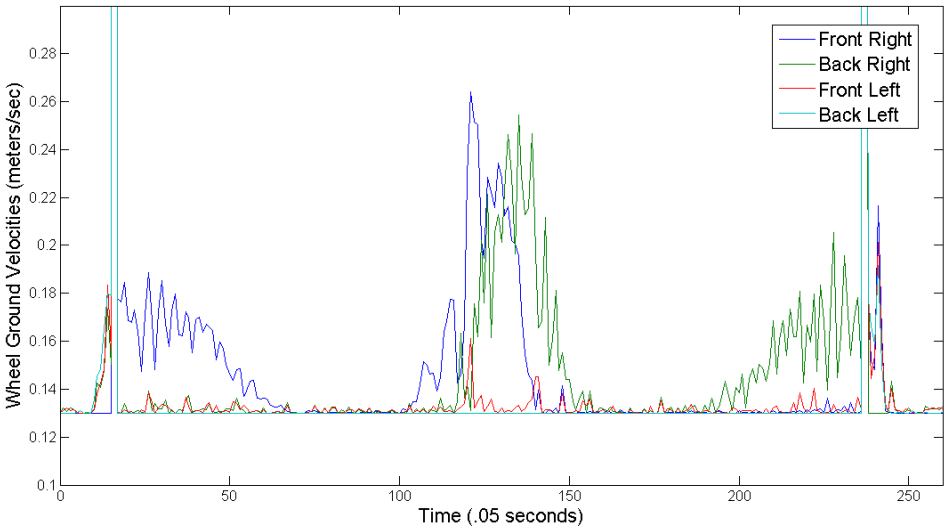

Figure 44: Desired Wheel Velocities from Controller Based on Simulation

Overall these simulation results showed that the controller is operating correctly, although with some limitations. While no direct metrics can be evaluated the calculated wheel velocities were close to the desired values based on the know profile of the trapezoid. In order to get a better understanding of the practicality of this controller it is implemented in the ROS environment on Oryx 2.0. This test and the results are discussed in Section 6.3

5 SUBSYSTEM TESTING AND VALIDATION

In addition to planned field testing to validate the rover system as a whole, several tests are conducted at various stages in the manufacturing process in order to better understand the performance of specific subsystems and to ensure each system can operate within planned limits. Of primary concern are the temperatures from electronics operating in sealed compartments. Temperature tests are done for both the drive motors and Core i5 processor, since these components are most likely to overheat.

5.1 Temperature Testing

Since the rover is designed to operate in extreme environments it must be able to withstand high and low temperatures. The main concern is overheating of electronics while operating in hot desert like environments, since all components are in sealed compartments. One key concern is maintaining safe operating temperatures of the quad Core i5 processor. Another potential problem is overheating of the drive motors. In addition to system wide temperature testing, these two components underwent specific experiments designed to quantify resulting temperatures under different conditions. This section will review these experiments, related results, and our conclusions regarding the performance and safe operating limits.

5.1.1 Motor Module Reliability and Temperature Tests

After the drive motor modules were assembled we wanted to perform reliability testing to ensure they could be operated continuously while maintaining safe temperatures. Since each motor is sealed inside the motor cans, and can operator at up to 200W of power continuously, overheating is a potential problem. Furthermore, the motors are not thermally coupled to the motor can, so cooling of the motors is only done by free convection, with limited conduction through the gearbox. For these reasons we wanted to measure the motor's temperature at different conditions for extended periods to time to gain a better understanding of potential limits, or see if additional cooling methods were required.

The first temperature test was done at full speed with no load. As previously mentioned the maximum speed of the motors is 12500rpm, as limited by the EPOS motor controllers when performing sinusoidal commutation. This scenario approximates conditions where the rover is driving about 1.3m/sec on level ground. For this experiment the motor was run continuously for about one hour, and the temperature of the motor and ambient air was recorded at 1Hz. The ambient temperature simply monitored the temperature of the room which remained constant at 22°C, and the temperature sensor for the motor was attached to the motor casing. This means the measured motor temperature is somewhere between the winding temperature and the temperature of the air directly surrounding the motor. The results of this experiment are shown in Figure 45.

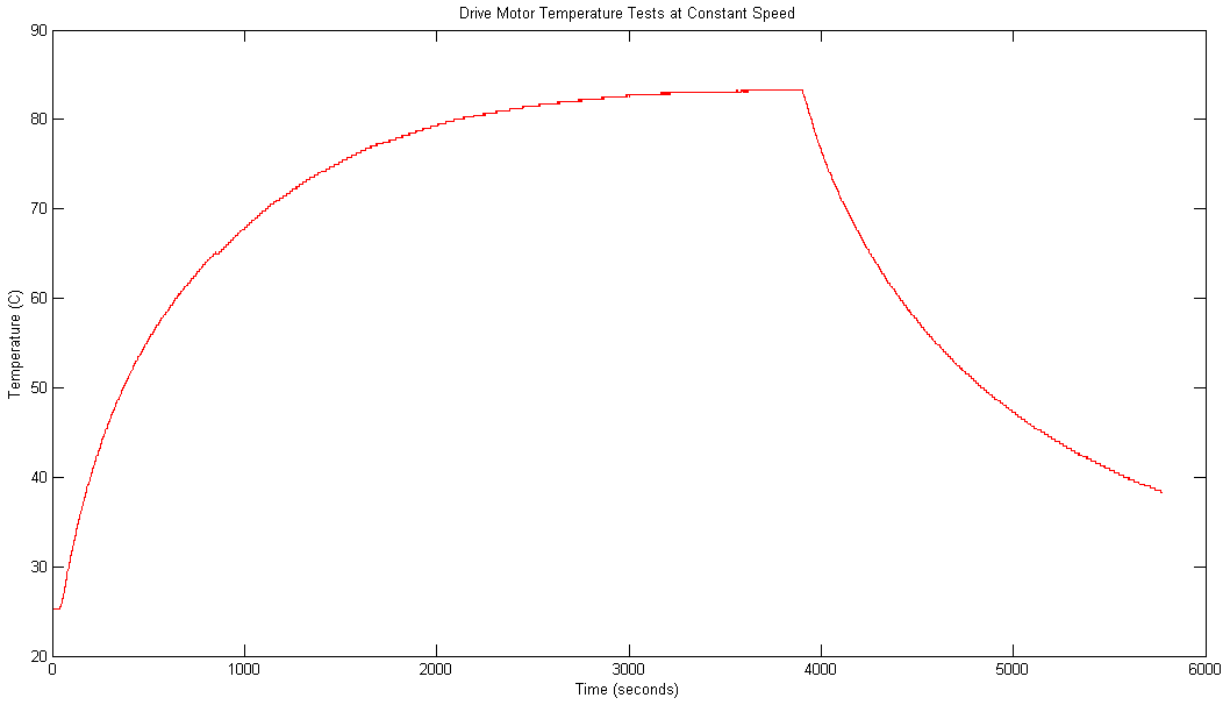

Figure 45: Drive Motor Temperature Tests at 12500rpm and No Load

As evident in Figure 45 the motor is run continuously for about 4000 seconds before it is turned off. During this time of continuous operation the temperature increases logarithmically from 25°C to about 83°C where it seems to reach a plateau. After the motor is stopped it immediately begins cooling, as expected the heat decay also approximates a logarithmic curve. As provided by Maxon Motor's specifications, our drive motors are rated for operation at up to 100°C ambient, or 155°C for the winding temperature. While our temperature sensor does not directly monitor either of these temperatures it can be used to approximate the winding temperature. When measuring the motor's casing Maxon Motor recommends adding 20°C to that temperature in order to estimate the temperature of the motor winding. Using this approximation our maximum observed winding temperature after about one hour of continuous use was about 103°C. This is well below the 155°C limit, suggesting that the motor will be able to operate continuously under these conditions.

While this test shows safe temperatures resulting from continuous no load use, roving on rough terrain or on slopes will result in dynamic loading on the drive motors. To approximate this type of loading a 2.5kg mass was suspended from the drive module hub by a cable attached to one of the tapped mounting holes. In this setup the mass exerts a constant downward force that creates a torque on the motor based on the angle of the hub and relative position of the mass. As a result, constantly rotating the hub creates sinusoidal loading on the motor. This is verified by Figure 46 below which shows the current draw of the motor in this condition.

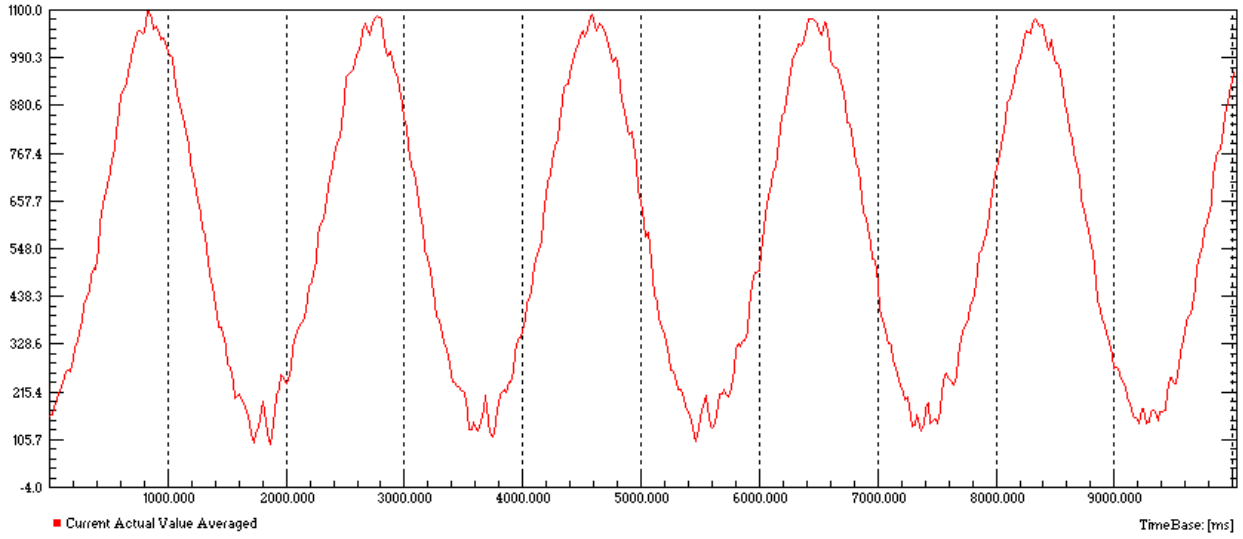

Figure 46: Current Draw during Sinusoidal Loading Temperature Test

Due to mechanical limitations of this experimental setup the motor speed selected was 4000rpm. While higher speeds could be achieved they resulted in unpredictable shock loading when tension was lost in the cable supporting the suspended mass. Running at 4000rpm for about two hours under these loading conditions resulted in a similar logarithmic function, with the maximum temperature leveling off at about 38°C. Figure 47 shows the results from the test. As 38°C is well below all safe limits this experiment also suggests that the drive motors will remain within operating temperatures in most operating conditions.

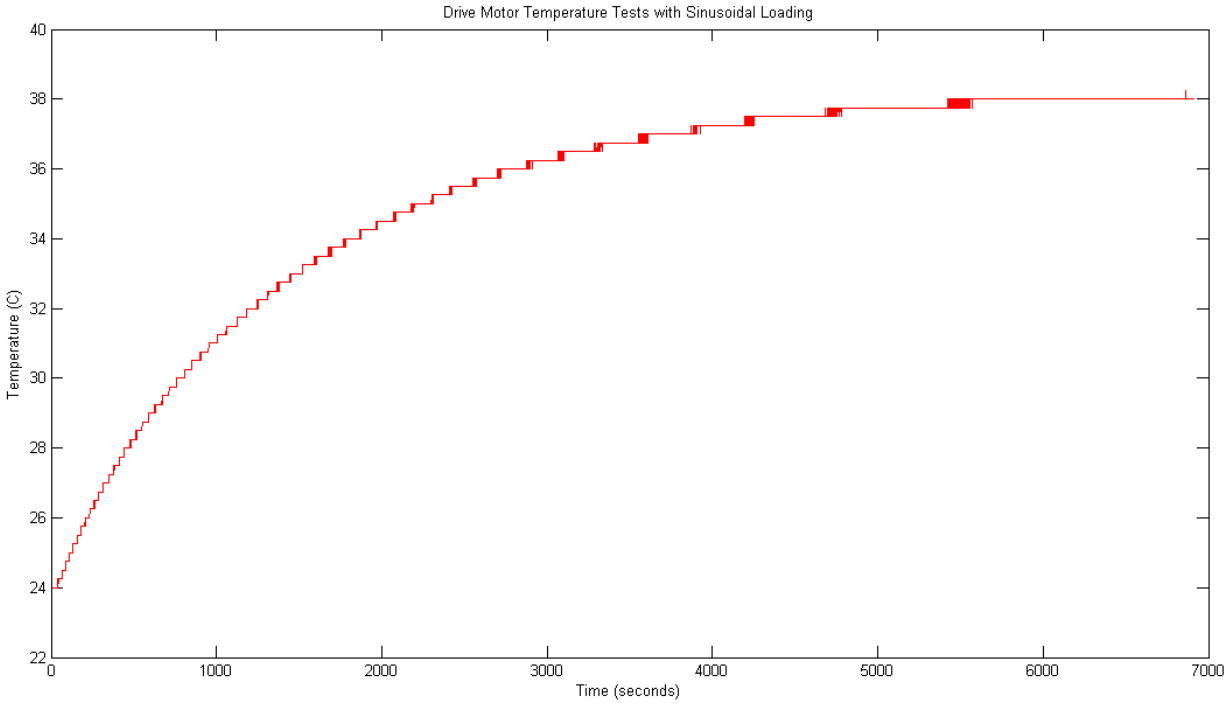

Figure 47: Drive Motor Temperature Tests at 4000rpm and Sinusoidal Loading

While these brief experiments to do not exhaustively test drive motor temperatures across all conditions they do provide evidence that suggests the motors dissipate heat fast enough for most scenarios. One factor that will affect the cooling rate is the ambient temperature. While these tests were done at room temperatures of about 20°C, it is not uncommon to see temperatures of about 35°C in desert environments. Another factor that greatly affects the amount of heat created is the loading on the drive motors. The second experiment simulates a specific loading pattern, however, the drive motors may experience much greater loading in the field for short periods of time. To compensate for these factors and to provide a conservative estimate we ran both temperature tests at continuous operation. In real operating scenarios continuous roving would be unlikely, as most tasks require large portions of time where the rover is not moving. With a more realistic driving duty cycle of 25-50% there will be significantly less time where the motor is creating heat and more time for heat to dissipate. Overall, these tests suggest that the drive motors can handle a variety of operating conditions while maintaining safe temperatures, and do not require further heat sinking.

5.1.2 Stress Testing CPU and Liquid Cooling System

Anther primary concern is the temperature of the i5 processor, which is capable of operating at 65W of power inside the sealed chassis. To test the effectiveness of the liquid cooling system we ran each of the four cores at full load, creating the maximum amount of heat while the liquid cooling system was running. During a period of about one hour the temperature of the cores was recorded and the results are shown in Figure 48. While each core has its own temperature the data below is the temperature of the hottest core, to provide the most conservative analysis.

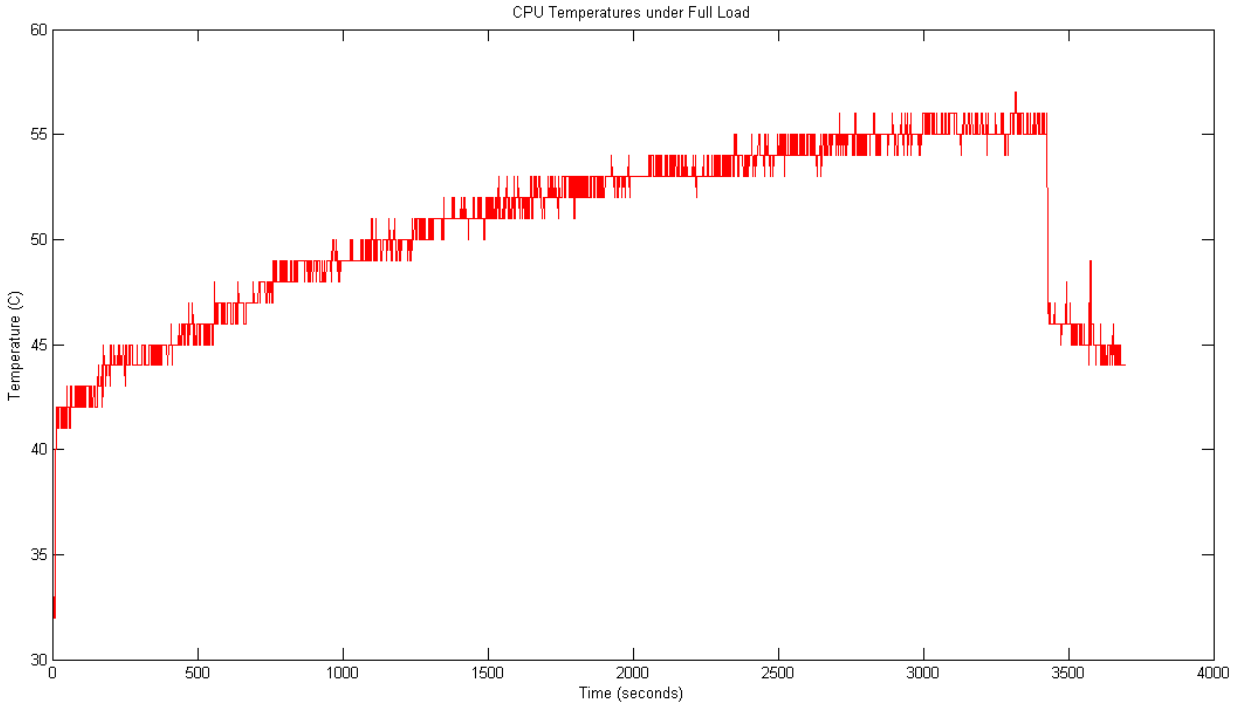

Figure 48: CPU Temperatures under Full Load

Reaching a temperature of about 56°C in 3400 seconds shows that the cooling system was effective. With a warning temperature of 80°C and a danger temperature at 85°C, 56°C is well within the limits. The tests were also done without the use of a fan to create forced air convection through the radiator, creating a worst case scenario. This combined with a full processing load and 100% duty cycle on the processor suggests that the cooling system will be adequate for almost all operating conditions. More realistic CPU loading was found to be about 20-30% with varying duty cycles that resulted in significantly less heat than when the processor is at maximum capacity. General system temperature tests, discussed in the next section, attempt to analyze the temperatures of the entire rover when running under maximum load.

5.1.3 General System Temperature

In addition to running extensive temperature tests on specific systems we also ran a more general test on the entire rover. For this test data was collected from a FLIR A320 Thermal IR Camera. A picture of the experimental setup can be seen in Figure 49.

Figure 49: Experimental Setup for System Level Thermal Monitoring Testing

The test was started with the rover and all its sub-systems at room temperature near 75°F. After the rover was powered on, all four cores of the processor were subject to the Ubuntu stress test and the drive motors were run at full speed for approximately 1 hour. This test was primarily focused on the temperatures inside the chassis so running the motors with little load is acceptable. Figure 50 shows the image captured by the thermal IR camera at the end of the test.

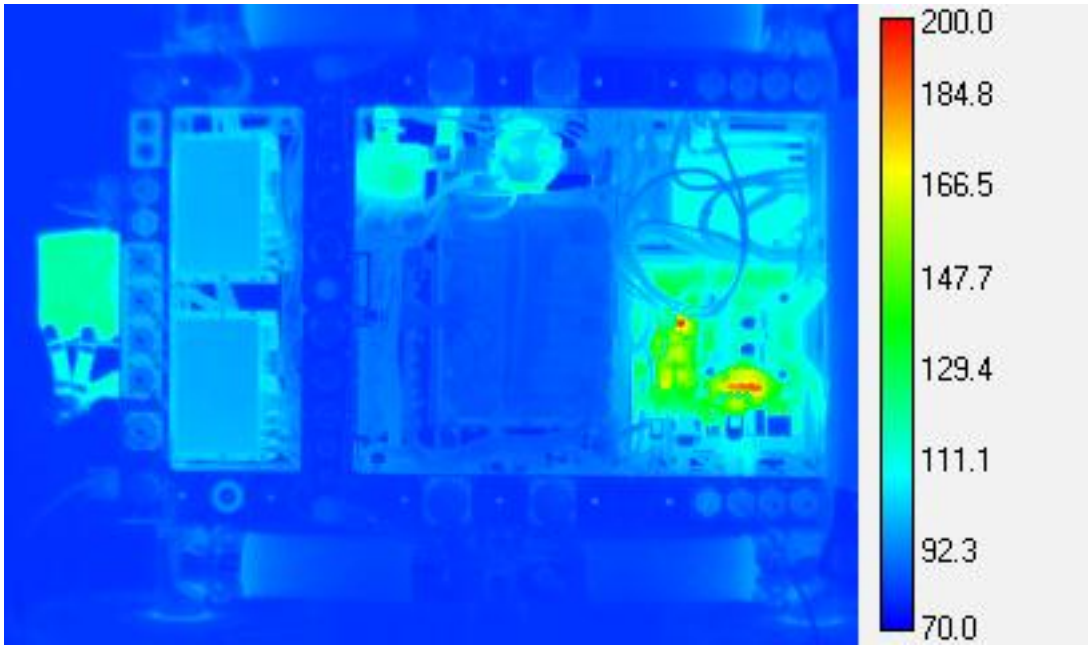

Figure 50: Final Temperatures Observed After Stress Testing

The hottest components revealed by the thermal IR imaging are on the Mini-ITX motherboard and are rated to temperatures higher than what they reached during testing. Based off the data collected running the computer and motors at their extremes we determined that the system will operate as desired under normal conditions without any temperature related problems.

5.1.4 Battery Discharge Testing

In the course of our system qualification and testing, we conducted a set of full-capacity battery system discharge tests to evaluate the overall battery system. An example of these tests is shown in Figure 51, with the voltage information gathered by the battery management system and logged by the rover computer.

In this bench top test, all four wheels of the rover are run continuously at full speed, resulting in a relatively constant draw of current of about four amps, in addition to power being drawn from the computer, pump, and other electronics. As seen in Figure 51 the battery lasted for ~3.7hours in this condition. However, what is notable about this test is the non-linear rapid discharge in cell packs 1 and 6. While all 6 cell packs start fully charged, cells 1 and 6 discharge more quickly until cell 1 reaches the battery cutoff voltage of 3V. This is highly undesirable because it shows

that there is a substantial amount of charge left in cells 2-6, even though the battery can no longer be used since cell 1 hit the cutoff voltage.

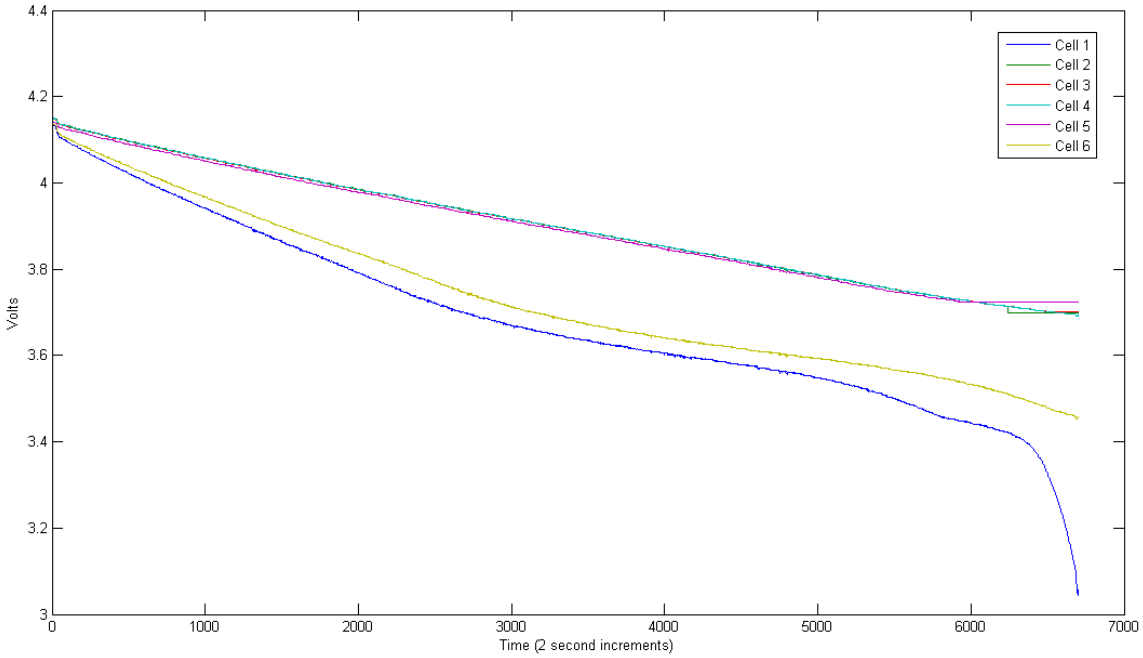

Figure 51: Battery Cell Voltages during a Full Discharge Cycle

The exact cause of this issue is unknown. It could be small variances in manufacturing or manufacturing defects in one of the cells, in cell 1 and cell 6 that lead to more rapid and uneven discharge. It could also have been a factor in our assembly process such has overheating certain cells in the heat-shrinking or soldering process. In either case determining the exact cause of this problem is a very challenging task. Given the results from this experiment we determined that run times during actual field testing would be between 2 and 3 hours. While marginally below design specifications we decided to use the battery in its current state, since constant battery monitoring and auto shutdown would prevent any permanent damage; and the battery could still operate for several hours.

5.2 Video Compression Processor Testing

Given the restricted bandwidth available through wireless communications, relaying high-quality video from the rover to the operator is one of the more challenging aspects of this rover. Significant compression is required even if low-resolution images are to be sent over a wireless network. However, the more compressed an image becomes, the more the quality of the image suffers. Furthermore, compressing a video stream enough to make it transmittable is a highly processor intensive task. Unless a powerful processor or dedicated compression hardware is used, the amount of time it takes to compress and decompress an image may result in a video stream just as delayed and stuttered as an uncompressed video.

In order to address this challenge, we will use an image transport package that has already been integrated into ROS. This package, aptly named *image_transport*, allows the rover to transmit video data through three different transportation schemes: raw, MJPEG, and Theora.

Raw, as its name implies, is the untouched image data taken directly from the camera. As there is no compression involved, this is the simplest and least processor-intensive method of transmitting video. Furthermore, raw images do not suffer from any compression artifacts. This is most useful when processing stereo images where even minor compression artifacts can result in erroneous data. Unfortunately, the lack of compression also makes it unfeasible to transmit it wirelessly; a single 960x544 stream running at ten frames per second consumes more than twelve megabytes per second in bandwidth. Therefore, a raw video stream would never be viewed by the operator. Instead, raw video streams are useful when onboard vision processing is required, where the bottleneck is not bandwidth, but processing power. If one wishes to transmit video wirelessly, as we do, compression must be used.

The most widely used compression scheme is MJPEG, or Motion JPEG. An MJPEG stream works by performing JPEG compression on each individual image before transmitting it. Depending upon the compression ratio used, the stream can be of similar quality to a raw stream, while requiring only a fraction of the bandwidth. MJPEG compresses each image by removing information that the human vision system cannot detect (such as small changes in hue and saturation), and reducing high frequency information of the images. Because each image is processed separately from every other image, MJPEG compression does not require a great deal of computing power. It is not uncommon for low-power single-board computers to handle the encoding and decoding of MJPEG streams without issue. Unfortunately, while MJPEG streams can be easily transmitted over wired and Wi-Fi connections, the bandwidth required is still more than a cellular network can provide. In these instances, one must use a video compression algorithm.

The primary video compression codec used by our rover will be Theora, a free and open source video format. Theora is very similar to MJPEG in that it removes high frequency information from the image to reduce its size. In fact, they use almost the same algorithm to do so. The difference between the two lies in how they handle sequential images. As stated before, MJPEG considers each image in a stream to be separate from every other. Theora, however, compares each newly captured frame to the previous one. If it finds that portions of the image are similar between the two frames, it does not send them. The result is an image of similar quality to MJPEG with a near 20-fold reduction in bandwidth. Indeed, in instances where the image is more or less the same from frame to frame (as would be the case if the rover is not moving), the bandwidth required to stream a 720P video at 10 frames per second drops below 15 kilobytes per second. Even in worst case scenarios, the video bandwidth for such a stream peaks at 150 kilobytes per second. Given the 4G connection available to our rover, this is more than

acceptable. The primary drawback with Theora stems from the processing power required to encode and decode high definition, high frame rate video streams. Unlike MJPEG and raw, encoding a Theora video stream is not feasible with a low power CPU.

To test the network load of our video feed, we streamed high definition video at 10fps with no compression, MJPEG compression, and Theora compression, and monitored the bandwidth of each stream over 30 minutes. As seen in the Figure 52, the bandwidth required by the raw stream was about 11MB/sec, far more than is available over a 3G or 4G network. Using MJPEG compression, we are able to reduce this to just 500KB/sec, which is pushing the network bandwidth to the limit. The bandwidth on the Theora stream, however, averages only 22KB/sec, well within our bandwidth requirements. The resulting video stream is still of high enough quality to drive and operate the rover without demanding a high-speed internet connection.

Figure 52 show the results of bandwidth testing that led us to selecting the Theora compression algorithm. Since we selected a quad-core i5 processor the increased computing load due the Theora algorithm is not significant in comparison to overall processing power that is available. Ultimately, the significant savings in bandwidth reduction far outweighs the small cost in computing resources.

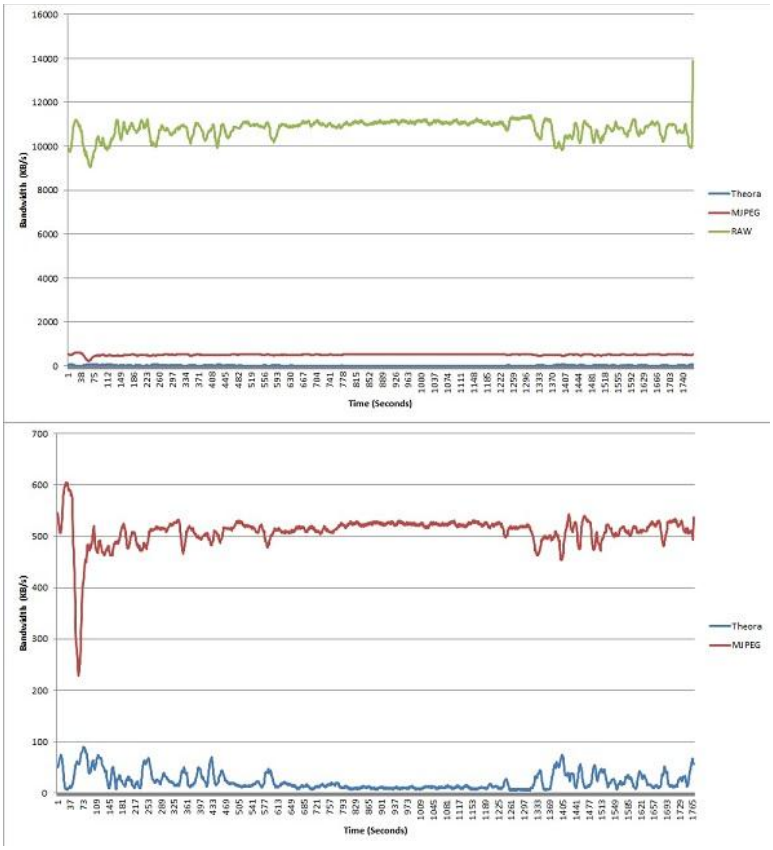

Figure 52: Results from Video Compression Bandwidth Testing

6 FIELD TESTING AND RESULTS

With the completion of our rover extensive field testing was conducted to validate the ruggedness of the design and key performance metrics related to initial design goals. Most interest was related to the rover's mobility, in terms of slopes, speeds, stability, operating time, traction, and ability to traverse obstacles. We also evaluated the ease of payload integration by installing and testing our sample vision payload. Lastly, data logged during many testing trials were examined to show that temperatures and battery voltages maintained in safe limits.

6.1 Mobility Performance

To test mobility we roved around rough terrain in the Worcester area. During these tests we made qualitative notes on general stability and traction, and also quantitatively evaluated slopes and obstacles that were traversed. In general, stability and traction were very good in all terrains tested; grassy fields, rocky terrain, small gravel, dirt and sand. The tread selected performed very well, easily gripping rocks and traversing vertical obstacles (ex. cinder block) with little to no slipping. The passive averaging suspension performed as planned, with the ground compliance guaranteeing that all four wheels remained in contact with the ground. In some rare occurrences the rocker suspension reached its mechanical limit, in which case one wheel is lifted off the ground; however, this only occurred with obstacles >50cm in height.

Rated to traverse positive and negative obstacles up to 15cm high or deep, Oryx 2.0 never encountered a scenario where it could not traverse obstacles of this size. Overall, the rover could easily traverse obstacles up to 20cm high and in some cases navigate over rocks ~50cm tall. This exceeded mobility expectations in many ways. In some scenarios obstacles larger than 20cm resulted in high-centering, when a front wheel traverse the obstacle but then has the obstacle stuck under the chassis or rocker arm. In all of these occurrences the rover was able to traverse off of the obstacle.

Additionally, the rover's ability to traverse steep slopes was examined. Testing showed that it could traverse grassy slopes of ~37degrees. Traction on rocky terrain or gravel should be similar although slopes with these materials were not available for testing. Also, the rover's low center of gravity makes it theoretically possible to traverse even steeper slopes, about 50degrees, although these scenarios will likely be traction limited depending on the soil/terrain type. The maximum speed of 1.2 m/sec was also achieved on this slope. Overall, original design specifications for obstacle traversal sizes, slopes, and speeds were successfully met and verified through field testing.

While largely dependent on driving frequency and the slope of the terrain, battery performance typically resulted in ~2.5hours of operating time during field testing. This is slightly below our original design goal of 3hour operating times. As previously discussed, this is due to a discharge

imbalance between the series cells of the battery pack. If this issue is fixed we would expect operating times between 4 and 5 hours.

Figure 53, Figure 54, and Figure 55 show some of the types of terrain used throughout the field testing process. It is important to note that no mechanical or electrical issues were encountered in any of the testing; a testament to the ruggedness of the mechanical design.

Figure 53: Field Testing over Rocky Terrain

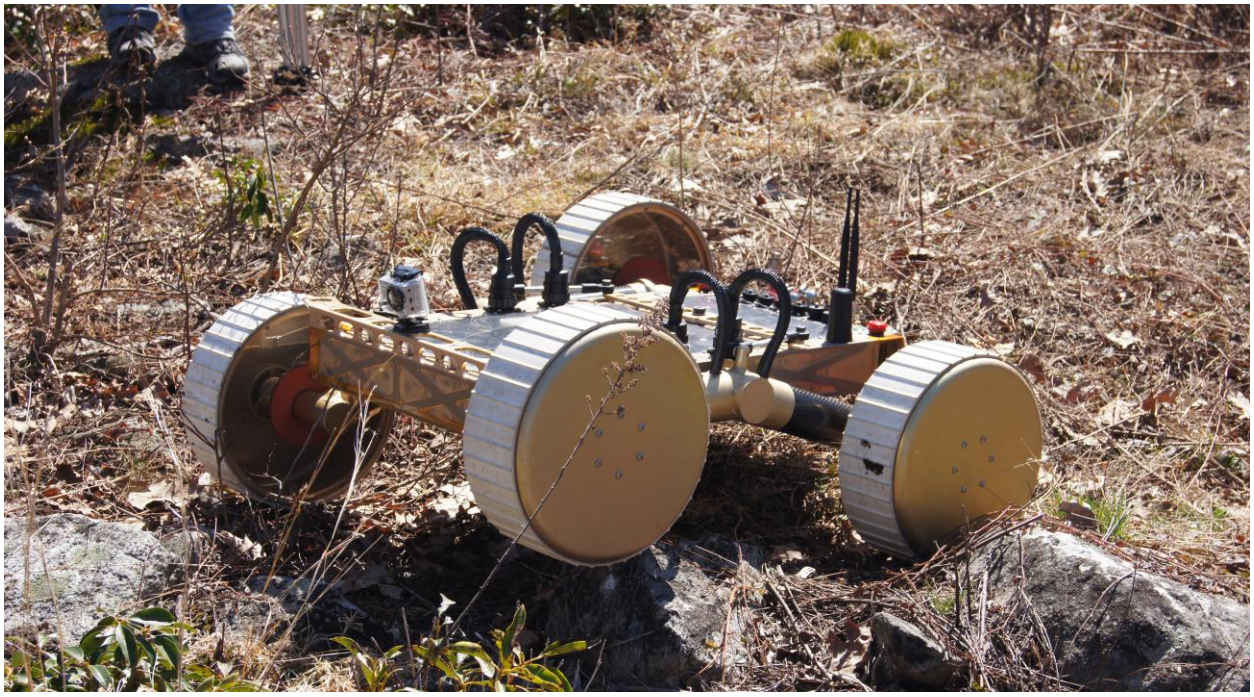

Figure 54: Field Testing over Rocky Terrain and Small Shrubbery

Figure 55: MQP Team with ORYX 2.0 for the First Field Testing Trial

6.2 Payload Integration Results

To evaluate the effectiveness of our payload integration features we designed a deployable pan-tilt camera payload to serve as an example. All design goals for this camera payload were met. It autonomously deploys from the stored position and then homes the pan and tilt DOFs based only on monitored current spikes. Once homed, it is then controlled via an X-Box gaming controller joystick, and HD video is relayed back to the GUI. This payload is shown in the storage configuration and deployed in Figure 56 and Figure 57 respectively.

Equally important as the functionally of the camera payload, is how easy it is to integrate to the rover. Mechanically it was trivial to attach this payload. It is bolted to the top plate with ten 10-32 machine screws, and it connects to data and power through the USB port, Ethernet port, and user power port, which are all provided around the perimeter of the top plate. This process takes ~5min to complete. A time-lapse example can be viewed here (http://www.youtube.com/watch?v=fYZwzTGBkQs), actual time in this field test was 7min, which included the time to reboot so that the rover could initialize with the payload attached.

Using the ROS framework provided it was also easy to develop the needed software to deploy and control the panning and tilting of the camera. Most of the software was developed without the hardware to test with, and yet little trouble was encountered when hardware was integrated. Overall, software development took about ~20hours, which is reasonably low for this type of application. In general the easy-to-use mechanical interface combined with the use of ROS should make for a modular mobility platform that can accept a variety of payloads.

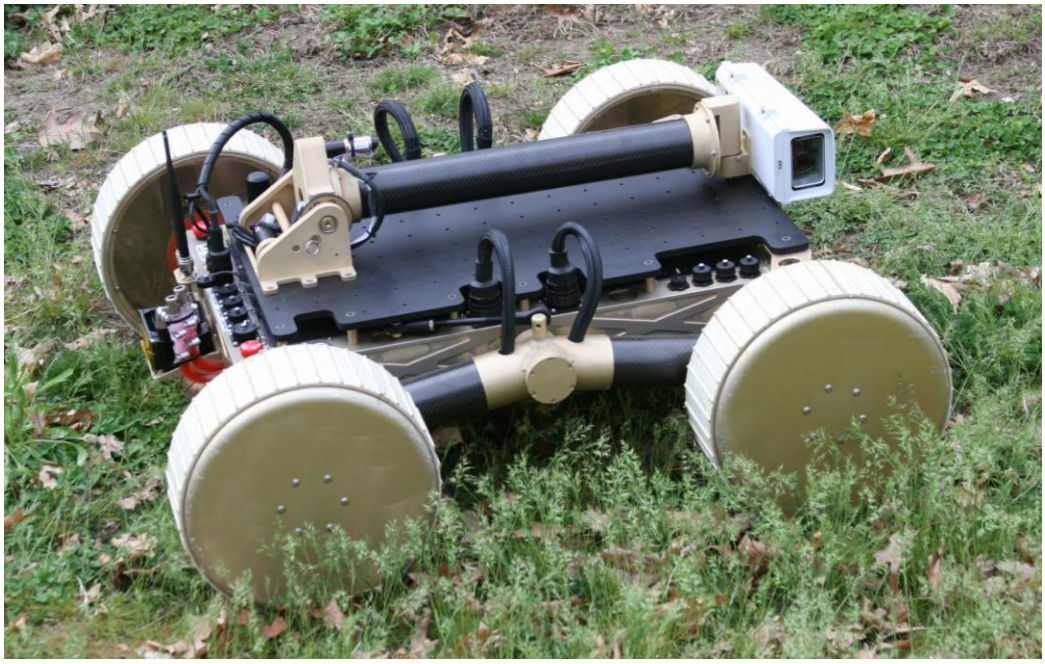

Figure 56: Camera Payload in the Storage Configuration

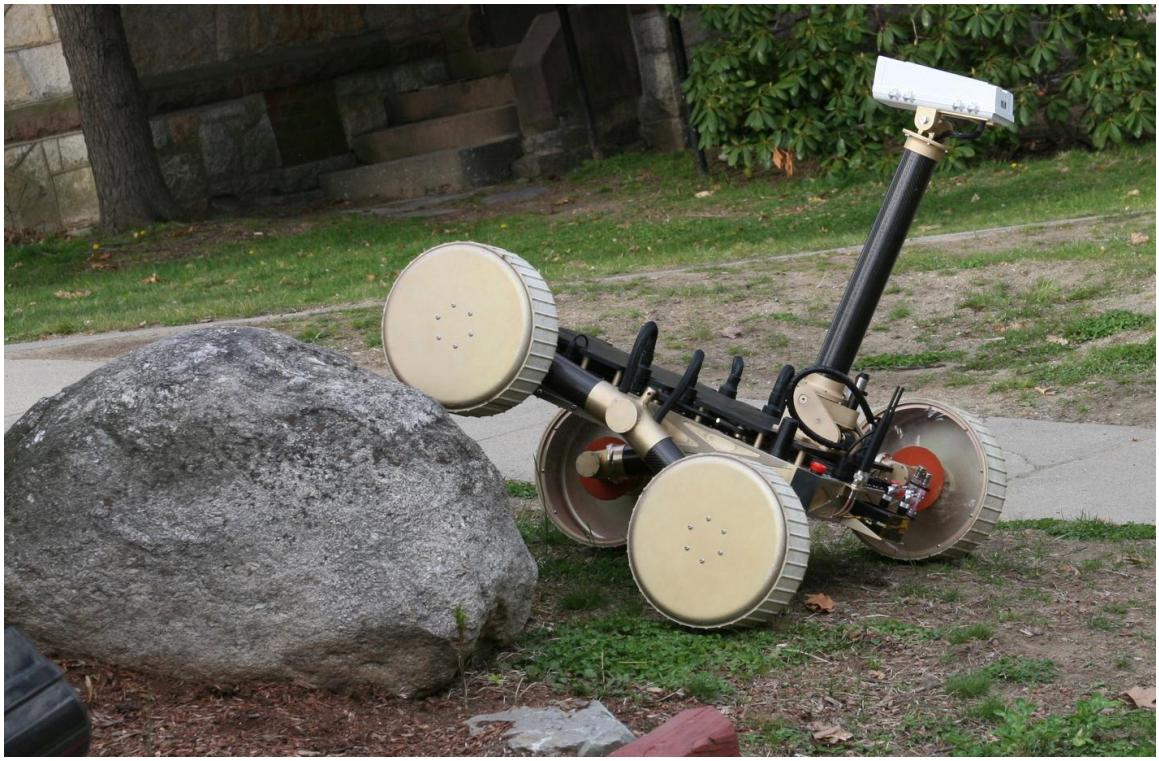

Figure 57: Camera Payload Deployed while Traversing Large Rock

6.3 Testing the Feedforward Velocity Controller

With the apparent success of the controller through the Matlab simulation, identical experiments were repeated with and without the controller in effect. As mentioned, the controller was implemented on Oryx 2.0, and ran at 20Hz. The main metric used to evaluate the success of the controller were changes in yaw (measured by the orientation sensor), since these are deviations from the straight line trajectory. An ideal controller would keep the yaw at 0degrees, while operating without any controller produces increasing yaw inherent to traversing rough terrain.

Figure 58 represents the results from two trials, one with the controller on, and one with no controller. The experiment was repeated multiple times and similar results were found in each case, with end yaw error between 7 degrees and 9 degrees for no controller, and between 1 degree and 3 degrees with the controller in use.

Overall, this large reduction in yaw achieved shows that the implemented controller was successful. In line with expectations from the simulation, the controller fails to compensate fully for the slope in the cases where the front wheel and rear wheel are on the slope at separate times. Occurring at the beginning and end of the traversal, the yaw is observed increasing at these times as a result. Similarly, the over compensation during the transition period resulted in a change in yaw in the negative direction. While ultimately an error in the controller, this change improved overall performance by balancing out the other two main sources of yaw error, and was

repeatable in multiple trials. While these preliminary results show that is simple controller may be useful, more testing is required to evaluate the controller in outdoor field settings.

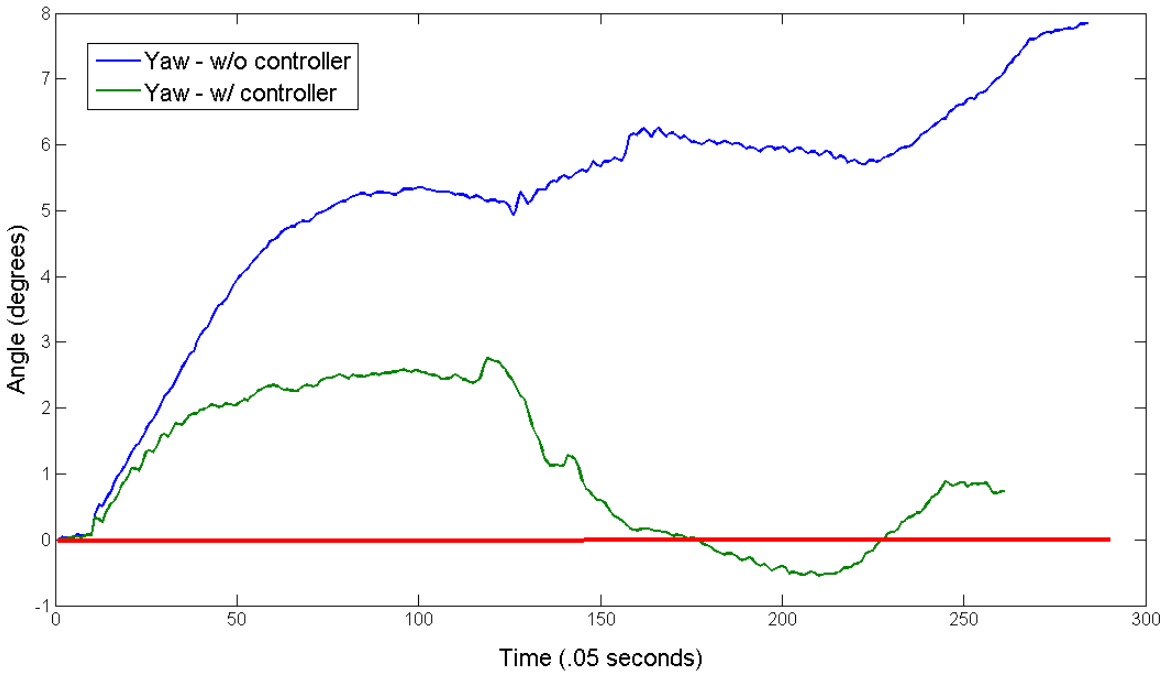

Figure 58: Yaw Results from Experiment to Validate Velocity Controller

6.4 System Reliability Through Diagnostics Evaluations

As previously mentioned, no mechanical or electrical problems were encountered in any testing. In addition to this metric for ruggedness all field testing logged data, on the yaw, pitch, roll, rocker angle, battery cell voltages, battery cell temperatures, and 22 temperatures of various rover components. This data was then analyzed to see if components were reaching unsafe operating conditions.

Through all the data analyzed no components ever reached unsafe operating conditions. Of most concern were drive motor temperatures, CPU temperatures, and battery voltages. Drive motor temperatures remained cool, and well below their limits. Similarly, the water cooling system proved more than adequate at cooling the processor. Battery voltages did reach critically low limits, although that is expected when using the maximum amount of charge from the battery. To prevent dangerously low voltages (less than 3V), the computer would disable the drive motors when any of the cells reached this low limit. This happened on several occasions and proved to be a reliable feature for notifying the operator that the battery is low.

6.5 Robo-Ops Challenge and Testing at JSC

The RASC-AL Exploration Robo-Ops competition, sponsored by NASA and NIA, is scheduled for May 30, 2012. It involves the long range teleoperated control of our rover in a sample return

mission at NASA's analog testing facility, the Rock Yard at Johnson Space Center (JSC). The competition involves roving around analog Martian and lunar terrain in search of colored rocks that are then collected.

Our rover will be Worcester Polytechnic Institute's entry for the 2012 RASC-AL challenge. Our field testing has proved the mobility of Oryx 2.0 is more than capable of operating in the Rock Yard at JSC, and meets all of a NASA's recommendations for doing so; traversing sand, obstacles up to 10cm high, and slopes of 33% grade. It also meets all requirements such as size and mass constraints. The camera payload developed will also be applicable for this competition. It will provide the drive team with the ability to survey the landscape in search of rocks and will also have color detection software that will help to identify specific color rocks even at far distances. Also, the installed 4G broadband card with CradlePoint gives Oryx 2.0 a reliable 4G connection which will be required for the competition.

The remaining components for the competition include the sample acquisition system and sample storage. This will likely be an arm and small storage bin, which will be developed outside of this project. The ability to quickly and easily integrate these payloads will attest to our success in developing a modular configurable research platform.

7 SOCIAL IMPLICATIONS

This chapter will discuss the non-technical aspects of the project. This includes the broader societal impacts that such a modular mobility platform has, in addition to the potential ethical and environmental considerations that future applications may have. We also briefly review aesthetic and safety considerations.

7.1 Broad Societal Impacts

While Oryx 2.0 is not designed to operate in space it is intended to serve as a model for a low-cost reconfigurable rover that may one day be used in space applications. As space exploration trends towards private enterprise there is the potential to have an entirely new sector emerge from space exploration and harvesting resources from space. If this trend continues there will be a growing need for rovers like Oryx 2.0 that can easily integrate payloads for testing different mission scenarios. Similarly, a space-ready rover modeled after Oryx 2.0 could also be useful since its reconfigurable nature means it can be quickly adapted for a variety of missions.

While applications in space could have profound impacts on society and economics they are likely to be many years in the future. More pertinent to the near future are Earth based applications for ruggedized modular mobility platforms, like Oryx 2.0. Currently, mobile robots are moving out of laboratories and into real-world outdoor environments working autonomously or alongside people in useful ways. For example, mobile robots are being used to autonomously transport goods and organize warehouse supply chains, in addition to many exploration applications in the military. They are also used in tasks that are deemed unsafe for people, such as exploring mines or collecting data near volcanoes. Agricultural applications continue to have growing uses for robotics. Because Oryx 2.0 is ruggedized and capable of operating in harsh environments over rough terrain it potentially has many uses in these categories. With specific payloads Oryx 2.0 could be useful for operating in mines or near volcanoes to collect samples or data. With the addition of more capable autonomy and vision systems Oryx 2.0 could also be used to collect things in unstructured outdoor environments. Similar to how it was designed to locate and collect colored rock samples on planetary terrain, Oryx 2.0 could be reconfigured to collect things like strawberries or trash in agricultural and environmental applications respectively.

7.2 Ethical, Safety, and Aesthetic Considerations

Related to the previously discussed applications there are a few ethical and safety considerations. One obvious one is that Oryx 2.0 could potentially be operating alongside a person, which always poses the possibility of causing an injury to a person through software or hardware malfunctions. The main safeguard against this are the two E-stop buttons located on either side of the rover. In the event that it makes unexpected or dangerous movements hitting either of these buttons will disable the drive motors. However, these events are highly unlikely because Oryx 2.0 is slow and generally not dangerous to be around.

Other potential ethical issues relate to the economics of robots used in the workplace. For something like space exploration Oryx 2.0 would potentially be creating a whole new sector of economic potential that would generally be viewed as a positive thing. Some arguments however, would claim that space exploration is overall a waste of human resources since there are many societal issues that require attention on Earth. However, Earth based applications in exploration or agricultural may have different effects. For example, it is unlikely that people will complain about sending Oryx 2.0 into dangerous situations, like mines, volcanoes, or disaster areas as a scout or means of collecting data. In these applications our rover would be keeping people out of harm's way. However, in applications involving the harvesting of strawberries, blueberries, or other low hanging fruit Oryx 2.0 could potentially take away jobs from human harvesters. The argument can be made that taking such low-level jobs is beneficial because it allows people to spend more time on other things. But taking any salary from a person with a robotic solution always brings up an ethical issue.

While mostly unrelated to ethical issues the rover's aesthetics were an important consideration in the development of Oryx 2.0. No visible component was left in the unfinished state. Chromate conversion was used to give most components a gold finish, and anodizing was used to finish some parts black. Combined with the glossy black carbon fiber, the gold and black color scheme provided a unique and professional quality appearance. Careful cable management also provided a clean put-together look, in addition to having reliability and ruggedness benefits. Overall Oryx 2.0 has a unique recognizable style, which will prove useful for public outreach and marketing purposes. A photograph of Oryx 2.0 in Figure 59 reveals the gold and black color scheme and professional quality appearance.

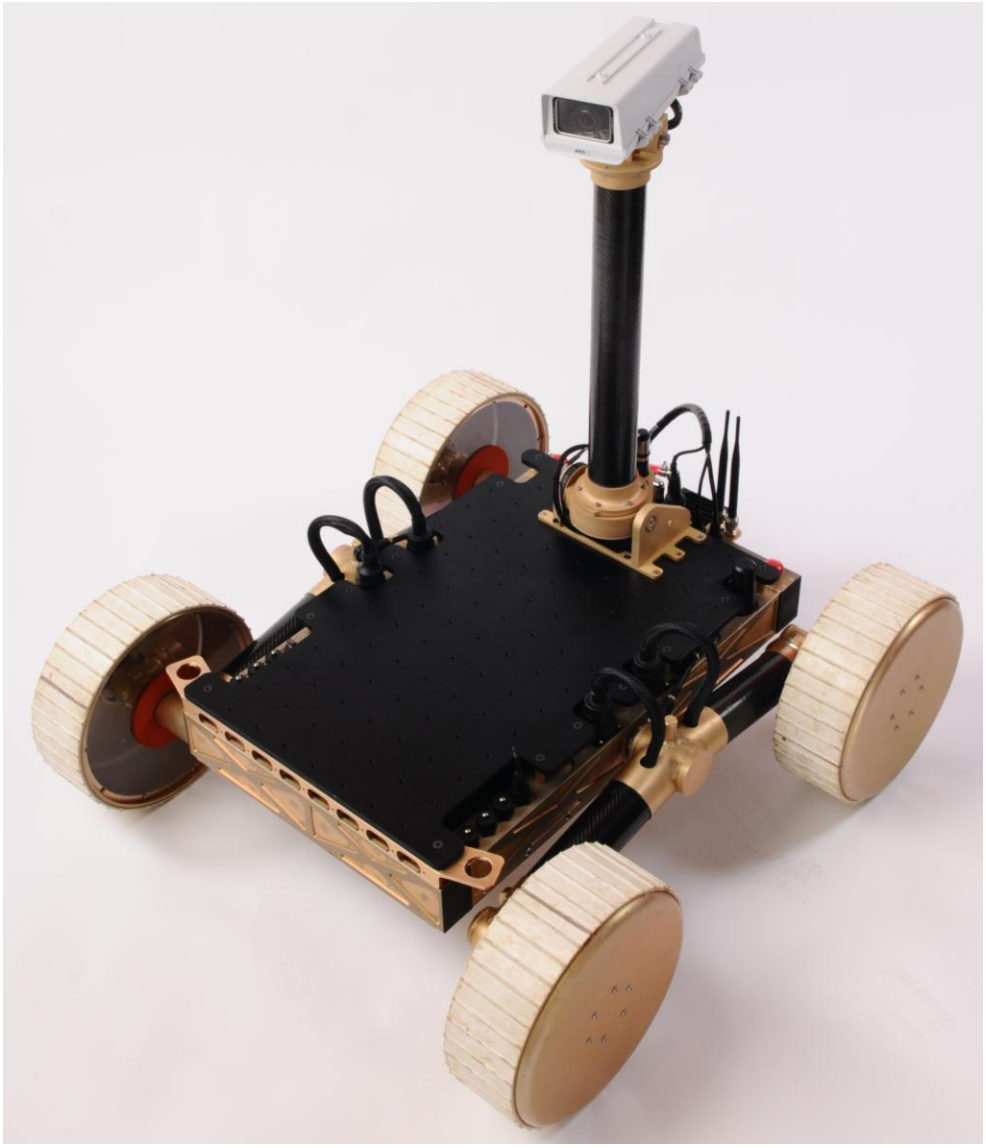

Figure 59: Photograph of Completed Rover to Highlight Product-like Aesthetics

8 CONCLUSIONS

This project was successful in reaching nearly all of our design requirements, and in many respects exceeding original design goals. Furthermore all components, mechanical and electrical, were thoroughly tested as a completed system in real-world field testing conditions to validate their success. Overall, preliminary estimates for the general scope, budget, and timeline, for the project were closely followed; with the exception of the project going moderately over budget, and with the project scope being reduced to make more realistic software goals within the timeframe.

8.1 Hardware

As previously mentioned no mechanical problems were encountered during any sub-system testing or field testing trial. However, this testament to the ruggedized mechanical design of Oryx 2.0 does not imply that there is no room for improvement. Mainly, field testing revealed a few potential weaknesses in the wheel design, rocker pivot joint, and rocker differencing linkage system. While all of these components are expected to continually operate as planned, mechanical improvements can be made to improve performance and longevity.

While the spun aluminum wheel design provided a quick commercially available component to use as the main structure of the wheel, it is not ideal in several ways. The single solid 1/16in aluminum spoke on one side of the wheel is not optimized for distributing load. As a consequence it underwent moderately high deflections, especially under the loads that occur during skid steering. In some cases this also resulted in plastic deformation of the spoke, although these deformations were very small and inconsequential to operational performance. The tread selected was also commercially available cleated conveyer belt and performed very well in providing traction in all tested terrain. With a total mass of 1.5kg this wheel design is significantly higher mass than is required.

The rocker pivot assembly, consisting of the 3/4in 7075 hollow aluminum shaft and tapered roller bearings, did not encounter any functional problems during testing but could be improved upon. During skid steering these shafts exhibit large moments; the exact load is difficult to quantify, however, small deflections were observed in some skid steering cases. While this joint continues to operate soundly there is small concern that bending fatigue may result in failure over very long periods of operation (1000-5000 hours). A larger shaft diameter would provide greater rigidly and alleviate any concerns about long term fatigue failures. Or an identical shaft can be made from titanium or steel.

Finally, the only other small mechanical issue was in the rocker linkage system. A combination of backlash in the ball and socket connections and compliance in the rocker differencing arm resulted in a slightly springy linkage system with small amounts of backlash. Backlash in the igus ball and socket connections means that one rocker arm can rock slightly with no effect to

the other rocker arm (backlash in the chassis). Also, compliance in the rocker differencing arm results in undeterminable wheel locations. In general these issues had little to no effect on the rover's mobility performance. The compliance in the rocker differencing arm was mainly caused by a stress concentration formed by the addition of screw access holes. A more rigid rocker differencing arm and better tie rod connections would reduce backlash and vibrations in the chassis.

Overall, the rover is mechanically sound and met or exceeded all design goals related to mobility. Improving the few minor issues mentioned would produce a small increase in performance and longevity. In total the rover massed 35kg, 5kg higher than the original design goal. However, this small increase in mass had no impact on performance.

8.2 Software

While we may have been able to accomplish many of our goals had we not used ROS, without it, the software would have been significantly less capable. The ROS framework has allowed us to split our code into individual components, each dedicated to a single task. Not only has this made the code far easier to understand, but it results in well-organized code. Additionally, the code is highly modular. Additional sensors can be added simply by running a new instance of their corresponding node. This allows us to easily add and remove software modules as easily as we can remove hardware modules.

Arguably the greatest benefit to use ROS, however, comes from how it handles communications between multiple computers. ROS not only masks the TCP/IP handling from the user, but also from the programmer. Even someone with no experience with network-to-network communications can have two computers transmitting data between each other in a matter of minutes. This allowed us to focus our limited time on other software issues, and was likely the key behind our rover's success.

While the Maxon motors driving our rover may have performed admirably, the EPOS controllers have proven to be problematic, particularly with their software. We have found that their software for Linux has been full of bugs, often causing segmentation faults for seemingly no reason. Unfortunately, the code they provided has almost no underlying documentation, so identifying the cause of the problem is challenging.

Additionally, the EPOS controllers in Linux require the use of a specific FTDI driver called ftd2xx. This driver works well in Windows, but has significant issues under Linux. Specifically, is almost completely incompatible with the standard ftdi_sio driver used by nearly every other FTDI device. This has the unfortunate result of disabling every other FTDI device on the rover, such as the IMU, Arduino, Rocker Sensor, and BMS, whenever any of the EposManagers are run. To address this, we needed to blacklist the ftdi_sio driver so it would not run at boot, run all

of the EposManagers, reload the ftdi_sio driver, and then run all of the FTDI devices. While this does work, there are a number of problems. First, is that the boot time of the rover increases by roughly 30 seconds. The second, and more important issue, is that if any EposManager is launched after the ftdi_sio driver is enabled, all other FTDI devices will become unusable until the computer reboots. This is not a problem in normal operation, but does make it difficult to debug and test code if the rover needs to be restarted after every trial.

Finally, while we are reliably able to connect to the EPOS controllers, there are occasions where we cannot do so. Unfortunately, we have not been able to find a cause behind such errors, but a restart is occasionally required. This can also be attributed to the instability of the ftd2xx driver in general.

In conclusion, the EPOS controllers have been at the root of almost all of our software issues. Most of these stem from the ftd2xx driver, and we would recommend not using any device that requires the use of that driver. Unfortunately, the ftd2xx driver is the only one supported by the EPOS controllers, so it must be used unless the controllers are switched out.

8.3 Project Logistics

This capstone project entailed the complete design, manufacturing, wiring, assembly, integration, software development, and field testing of a planetary exploration mobility platform and deployable pan-tilt camera payload. Being the work of four undergraduate students this project required careful management of key deadlines and progress in addition to budget considerations. A Gantt chart of the proposed project timeline is shown in Appendix C.

Overall, this project closely followed the proposed timeline and schedule of tasks. One change was in the reduction of software goals that occurred as the project progressed. Originally there were plans to implement stereo vision and more complex navigation autonomy. However, due to increased effort needed on motor control software and increased effort towards manufacturing, stereo vision was ultimately determined to be out of scope for the project. All other software goals were successfully met.

Against the planned project schedule, manufacturing was started much earlier than planned, since increasing complexity in overall design led us to anticipate that more time and effort would be required for manufacturing (machining, welding, chromate conversion, assembly). Starting the manufacturing process as early as possibly made it possible to complete the project on time. At the beginning of March 2012 we were about two weeks behind schedule, due to unforeseen delays in the manufacturing process. This led to slightly less time for field testing, however, the allotted seven weeks was only reduced to four weeks which left plenty of time to validate and thoroughly test the rover. Additionally, no mechanical or electrical issues were encountered

during testing, which meant that the time allocated to repair any problems could be used instead for more field testing and documentation.

While this project closely followed the planned schedule, it did go over budget and required additional fundraising from corporate sponsors as the project progressed. Originally, the project budget was $10,000, the amount award by NASA and NIA as part of the RASC-AL Robo-Ops competition. Neglecting the stereo camera reduced the budget slightly, however, large costs related to manufacturing quickly exceeded original estimates, which ultimately increased the project costs to ~$15,000. Including the estimated value of non-monetary donations from sponsors (services and components), the total project cost was ~$28,000. A large factor in this increased cost was in money spent on machining parts for the camera payload. This was not planned but became necessary in order to save time. Other large costs accrued through miscellaneous hardware, wires, pins, and connectors. Ultimately it was the support of many generous sponsors that made this project financially possible.

8.4 Future Work

As modular research platform the rover developed by this project is designed specifically to facilitate future work. Related to rover hardware and software, future work should consider addressing the minor issues previously discussed. Mechanically, new wheel designs, stiffer rocker shafts, and a stiffer differencing arm have the potential for small increases in performance. Wheel designs should consider a billet or composite approach, as these methods have been proved by other rovers to makes wheels stronger than our current design in under half the mass. Replacing the battery may also be beneficial, since the current battery is unbalanced making it inefficient.

Future software developers should investigate alternatives to using Maxon Motors EPOS2 controllers. This was the main software challenge encountered in this project, and while many issues were fixed (including Maxon's source code) there is still the rare occurrence of segmentation faults inside of Maxon's source code that take down the system. While this is rare, and solved by a reboot more robust methods of motor control would be preferred.

Aside from fixing minor issues related to the rover, we believe there are a host of research topics and other features that can be added to the rover. More autonomy, in terms of a vision and path planning system can be implemented on Oryx 2.0. Integration with a stereo camera, LIDAR, or flash LIDAR can provide the rover with 3D data about its environment, which open up many more potential applications. In addition to many software oriented applications other payloads such as an arm, drill, soil collection system, or other scientific instruments can easily be tested on Oryx 2.0. For example, there is interest in using robotic vehicles to explore volcanoes to collect data and samples. Oryx 2.0 could be fitted with a suite of payloads designed to operate in and

collect data around volcanos. Similarly, there are other Earth based applications that could be served well by our ruggedized mobility platform.

Finally, Oryx 2.0 can be used for future rover competitions. It was designed specifically for the RASC-AL Robo-Ops rover design challenge and it is our hope that this platform will be continually used in this competition in the years to come. It may also prove useful in other NASA competitions such as the Sample Return Challenge hosted by WPI.

REFERENCES

Andersen, H. J., & Kirk, K. (2004). Stereo vision based obstacle detection. *Univeristy of Aalborg,*

Astrobotic. (2011). *Scouting rovers.* Retrieved 10/10, 2011, from http://astrobotic.net/rovers/rover/

Bickler, D. (1989). In NASA (Ed.), *Articulated suspension system* (280/677 ed.). United States: B62D 21/00.

Broggi, A., Caraffi, C., Fedriga, R., & Grisleri, P. (2005). Obstacle detection with stereo vision for off-road vehicle navigation. *2005 IEEE Computer Society Conference on Computer Vision and Pattern Recognition,*

Chang, K. (2008, NASA delays next mars rover mission. doi:10/11/2011

Comstock, D. (2007). NASA's innovative partnerships program: Matching technology needs with technology capabilities. *High Fronteir: The Journal for Space and Missile Professionals, 3*(3)

Cornell University. (2005). *Geography of mars.* Retrieved 10/11, 2011, from http://athena.cornell.edu/mars_facts/geography.html

Dean, B., Hautaluoma, G., Humphries, K., Prucey, R., & Schierholz, S. (2008). *NASA tests lunar robots and spacesuits on earthly moonscape* (New Release No. 08-149)NASA. doi:10/11/2011

Flippo, D., & Miller, D. P. (2011). Suspension and wheel evaluation and experimentation testbed for planetary rovers. *International Journal of Mechatronics and Automation, 1*(1), 29-37.

Goldberg, S. B., Maimone, M. W., & Matthies, L. (2002). Stereo vision and rover navigation software for planetary exploration.

Harrington, B. D., & Voorhees, C. (2004). The challenges of designing the rocker-bogie suspension for the mars exploration rover. *37th Aerospace Mechanisms Symposium,* Johnson Space Center, Houston, Texas.

Hurlbert, K. M. (2010). *JSC rockyard.* Retrieved 10/11, 2011, from http://www1.nasa.gov/centers/johnson/engineering/test_facilities/space_analog_testing/jsc_rockyard/index.html

JPL & California Institute of Technology. (2009). *NASA's 2009 mars science laboratory.* Retrieved 10/12, 2011, from http://marsoweb.nas.nasa.gov/landingsites/msl/memoranda/MSL_overview_LS.pdf

Korsmeyer, D. *2008 mose lake sand dunes field test.* Retrieved 10/11, 2011, from http://ti.arc.nasa.gov/news/moses-lake-sand-dunes-field-test/

Lakdawalla, E. (2007). *Mars science lab at JPL MarsYard*

Lind, R. (2011). *NASA - about analog missions and field tests.* Retrieved 10/11, 2011, from http://www.nasa.gov/exploration/analogs/about.html

Lindemann, R. A., Reid, L., & Voorhees, C. J. (1999). Mobility sub-system for the exploration technology rover. *33rd Aerospace Mechanisms Symposium,* Pasadena, California. 125-140.

Lindemann, R. A., & Voorhees, C. J. (2005). Mars exploration rover mobility assembly design, test and performance. *2005 IEEE International Conference on Systems, Man and Cybernetics, , 1* 450-455.

Manning, R. M., & Adler, M. A. (2005). Landing on mars. Paper presented at the *AIAA Space 2005 Conference,*

Mars Institute. (2010). *Haughton mars project.* Retrieved 10/11, 2011, from http://www.marsonearth.org/

Mars Pathfinder Engineering Team. (1997). *Mars pathfinder frequently asked questions.* Retrieved October 9, 2011, from http://mars.jpl.nasa.gov/MPF/rover/faqs_sojourner.html

Meyer, C. (2003). *Lunar regolith* (Technical ReportNASA. doi:10/11/2011

Miller, D. P., Hunt, T., Roman, M., Swindell, S., & Winterholler, A. (2003). Experiments with a long-range planetary rover. *Proceedings of the 7th International Symposium on Artificial Intelligence, Robotics, and Automation in Space,* Nara, Japan.

Miller, D. P., & Lee, T. (2002). High-speed traversal of rough terrain using a rocker-bogie mobility system. *Proceedings of Robotics 2002: The 5th Internation Conference and Exposition on Robotics for Challenging Situations and Environments,* Albuquerque, New Mexico.

NASA. *Various photographs*

NASA. (2011). *NASA centennial challenges.*http://www.nasa.gov/offices/oct/early_stage_innovation/centennial_challenges/index.html

NASA JPL. (2011). *Mars exploration rovers.* Retrieved 10/8, 2011, from http://marsrover.nasa.gov/technology/

NASA JPL. (2011). *Mars science laboratory.* Retrieved 10/10, 2011, from http://marsprogram.jpl.nasa.gov/msl/

Neal, C. R. (2009). The moon 35 years after apollo: What's left to learn? *Chemie Der Erde-Geochemistry, 69*(1), 3-43.

Oggier, T., Becker, G., & Rüegg, B. (2006). SwissRanger SR3000 and first experiences based on miniaturized 3D-TOF cameras.

Petro, A. (2010). Open-door innovation. *Ask Magazine*, (38)

ProViScout. (2010). *Time of flight cameras.*http://www.proviscout.eu/index.php/science/industry/time-of-flight-cameras

Ringbeck, T. (2007). A 3D tiome of flight camera for object detection. *PMDTechnologies,*

Roman, M. (2005). Design and analysis of a four wheeled planetary rover. (Master's, University of Oklahoma).

Seybold, C. C. (1995). *Characteristics of the lunar enviroment.* Retrieved 10/11, 2011, from http://www.tsgc.utexas.edu/tadp/1995/spects/environment.html

Short, N. J. (2009). *3-D Point Cloud Generation from Rigid and Flexible Stereo Vision Systems,*

Viotti, M. *In-situ exploration and sample return: Autonomous planetary mobility.* Retrieved October 10, 2011, from http://marsrover.nasa.gov/technology/is_autonomous_mobility.html

Viotti, M. (2011). In-situ exploration and sample return: Autonomous planetary mobility. *NASA Jet Propulsion Laboratory,*

Volpe, R. *The MarsYard III.* Retrieved 10/11, 2011, from http://www-robotics.jpl.nasa.gov/facilities/facility.cfm?Facility=14

Watanabe, S. (2007). *MER spotlight: Wheels in the sky.* Retrieved October 10, 2011, from http://www.nasa.gov/vision/universe/roboticexplorers/rover_wheels.html

Wilcox, B. (2006). Low-cost propellant launch to earth orbit from a tethered balloon. Paper presented at the *Aerospace Conference, 2006 IEEE*, 17 pp.

Wilcox, B. H., & Nasif, A. K. (2000). In California Institute of Technology (Ed.), *High mobility vehicle* (180/345 ed.). United States: B60K 17/36.

Wilcox, B. H., & Nasif, A. K. (2001). In California Institute of Technology (Ed.), *High mobility vehicle* (180/347 ed.). United States: B60K 17/00.

Wilhelms, D. (1987). *Geologic history of the moon* (Professional Paper No. 1348)US Geological Survey. doi:10/11/2011

Zheng, Y., Ouyang, Z., & Blewett, D. (2008). Implanted helium-3 abundance distribution on the moon. Paper presented at the *Lunar and Planetary Institute Science Conference Abstracts, , 39* 1049.

Zhou, J., & Li, B. (2006). *Robust ground plane detection with normalized homography in monoculoar sequences from a robot platform*. Arizona State University:

APPENDIX A: Design Specification Sheet

ORYX 2.0

A PLANETARY EXPLORATION MOBILITY PLATFORM

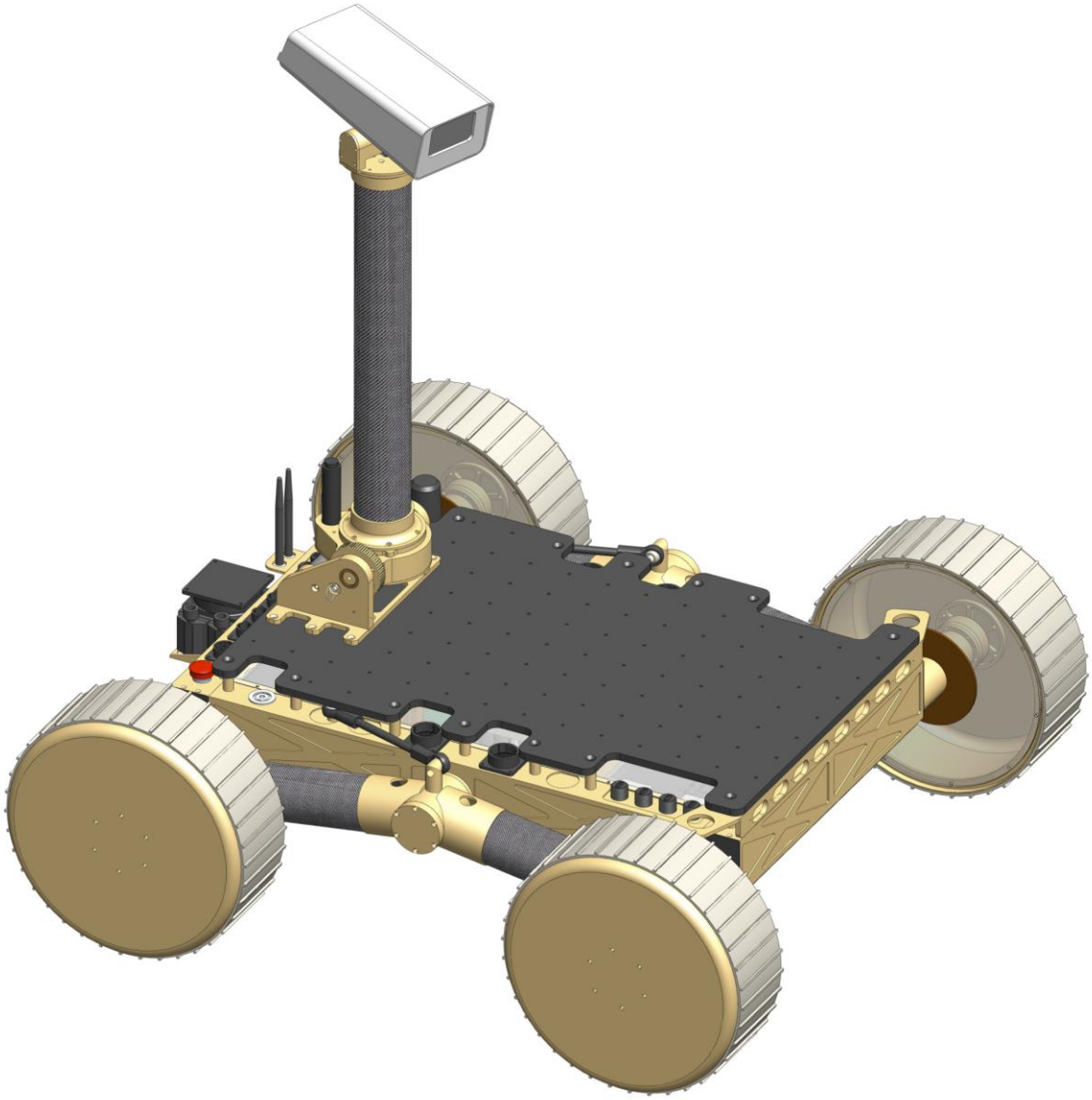

PROJECT OVERVIEW

ORYX 2.0 by Worcester Polytechnic Institute is a research mobility platform for evaluating planetary surface exploration technologies in extreme earth environments.

PROJECT FEATURES

Planetary exploration rovers are high cost partially due to their long development timelines and highly mission specific design. While specialized applications will always be necessary for space exploration, most planetary rovers are very similar from a mobility standpoint. The ORYX 2.0 is a research mobility platform aimed at tackling the mobility and situational awareness problems, allowing the user to focus on the development of mission specific technologies.

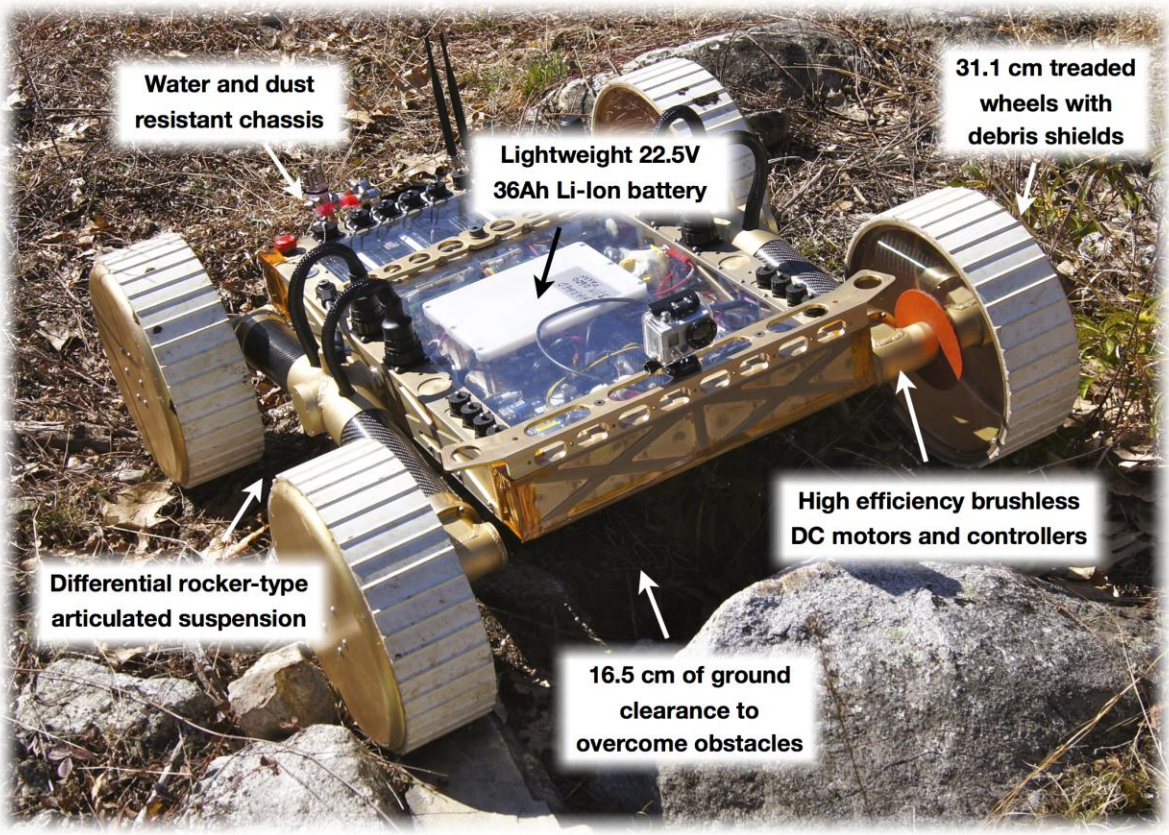

FOR MORE INFORMATION ON ORYX 2.0, VISIT **WWW.WPIROVER.COM**

TECHNICAL SPECIFICATIONS

TOP

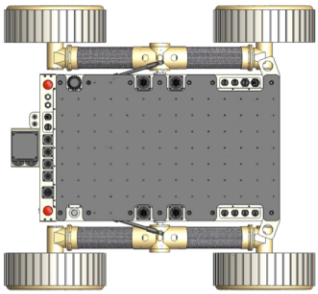

SIDE

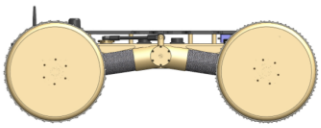

FRONT

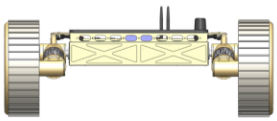

SPECIFICATION	
Dimensions (LxWxH)	96 x 89 x 31 cm 39.9 x 34.9 x 12.2 in
Mass	35 kg 77 lbs
Rated Payload	15 kg 33 lbs
Maximum Speed	1.2 m/s 3.9 ft/s
Maximum Obstacle Size	15 cm 5.9 in
Operating Time	3 hrs typ
Drive Power (Mechanical)	Up to 400 W continuous
Battery	22.5V 36Ah Lithium Ion w/BMS
On-Board Computer	Water-cooled Intel Quad-core i5 processor on Mini-ITX motherboard
Module Power Interface	Four accessible ports (5V / 12V / 24V)
Module Communications Interface	USB 2.0 (8) / Gigabit Ethernet (2) / Wi-Fi / 4G LTE
System Feedback and Sensing	Battery Voltages, System Temperatures, Rover Orientation, Odometry, Rocker Orientation, System Fault Handling
Software	ROS

FOR MORE INFORMATION ON ORYX 2.0, VISIT **WWW.WPIROVER.COM**

MODULE INTERFACE SPECIFICATION

ORYX 2.0 was designed specifically to accept modules that are created by both WPI and 3rd party sources.

Definition: **A MODULE is an assembly of mechanical, electrical, and/or software components which are not integral to the operation of the rover. All modules will adhere to a standard module specification (mechanical, electrical, communication) defined by the manufacturer.**

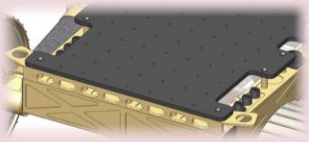

#10-32 tapped grid top plate and front rail

MECHANICAL

4 accessible ports each 5V / 12V / 24V

ELECTRICAL

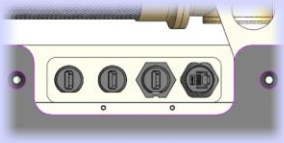

USB 2.0
IEEE 802.3 Gigabit
IEEE 802.11n (5dB)

COMMUNICATION

USER PAYLOAD DEVELOPER GUIDE AVAILABLE AT: WWW.WPIROVER.COM

EXAMPLE APPLICATIONS

SAMPLE RECOVERY AND SITE PREP
ORYX 2.0 is designed to accept user custom solutions for planetary sample recovery and excavation.

PERCEPTION & NAVIGATION
Navigation and mapping of planetary environments is a popular topic of research right now as many new technologies are emerging.

TELE-OPERATION
ORYX 2.0 is a complete mobility system that enables users to develop advanced control systems for tele-operation.

FOR MORE INFORMATION ON ORYX 2.0, VISIT WWW.WPIROVER.COM

APPENDIX B: Cost Report

Part Description	Module	Quantity	Source	Cost	Our Cost
Actuators					
4x drive motors with gear boxes and encoders	Wheel	4	Maxon	6000	1250
4x EPOS 70/10	Chassis	4	Maxon	3000	400
3x motors for pan/tilt/deploy	Vision	3	Maxon	800	300
3x EPOS 24/2	Vision	3	Maxon	1000	350
Sensors					
Axis M1114 IP camera	Vision	1	Axis	800	0
Temperature Sensors	All	8	Sparkfun	100	100
Arduino and connectors	Vision	1	many	100	100
InterSense IC3 IMU	Chassis	1	InterSense	1640	0
Rocker encoder	Chassis	1	US Digital	140	140
Computer and Electronics					
Power supply	Chassis	1	Mini-box	40	40
Ethernet switch	Chassis	1	Newegg	30	30
Water cooling parts	Chassis	1	Danger Den	200	200
RAM	Chassis	1	Newegg	50	50
i5 2405	Chassis	1	Newegg	219	219
motherboard	Chassis	1	Newegg	100	100
4G broadband card and antenna	Chassis	1	many	500	500
BMS	Chassis	1	Manzinita Micro	600	600
Main Contactor	Chassis	1	Gigavac	130	130
Misc. Electrical Materials	All	1	Misc	400	400
Solid state HD	Chassis	1	Newegg	70	70
Wireless card	Chassis	2	Radio labs	300	300
Battery Making Supplies	Chassis	1	many	150	150
Battery cells	Chassis	96	Tesla	1000	0
X-box controller	All	1		50	50
Wire and heat shrink			Powerwerx	400	400
Pins and connectors			Mouser	600	600
Water proof connectors			L-com	800	800
Label Printer	All	1	Amazon	100	100
Hardware					
Wheels	Wheel	6	Many	900	900
Chassis	Chassis	1	Many	750	750
Vision pan/tilt mast assembly	Vision	1	Many	400	400

Misc Hardware	All	1	McMaster	1500	1500
Carbon Fiber				300	300
Other stock			online metal	800	800
igus Hardware			igus	600	0
Manufacturing					
Vibrator and Supplies			Harbor Freight	220	220
Machining Parts for Camera payload			many	2000	2000
Chromate Conversion			Dav tech	$500	$500
Water jetting			hydro cutter	400	400
Carbide end mills			Lakeshore Carbide	200	200
Welding			Barnstorm cycles	500	0

Totals: $28,389 $15,349

APPENDIX C: Proposed Project Timeline

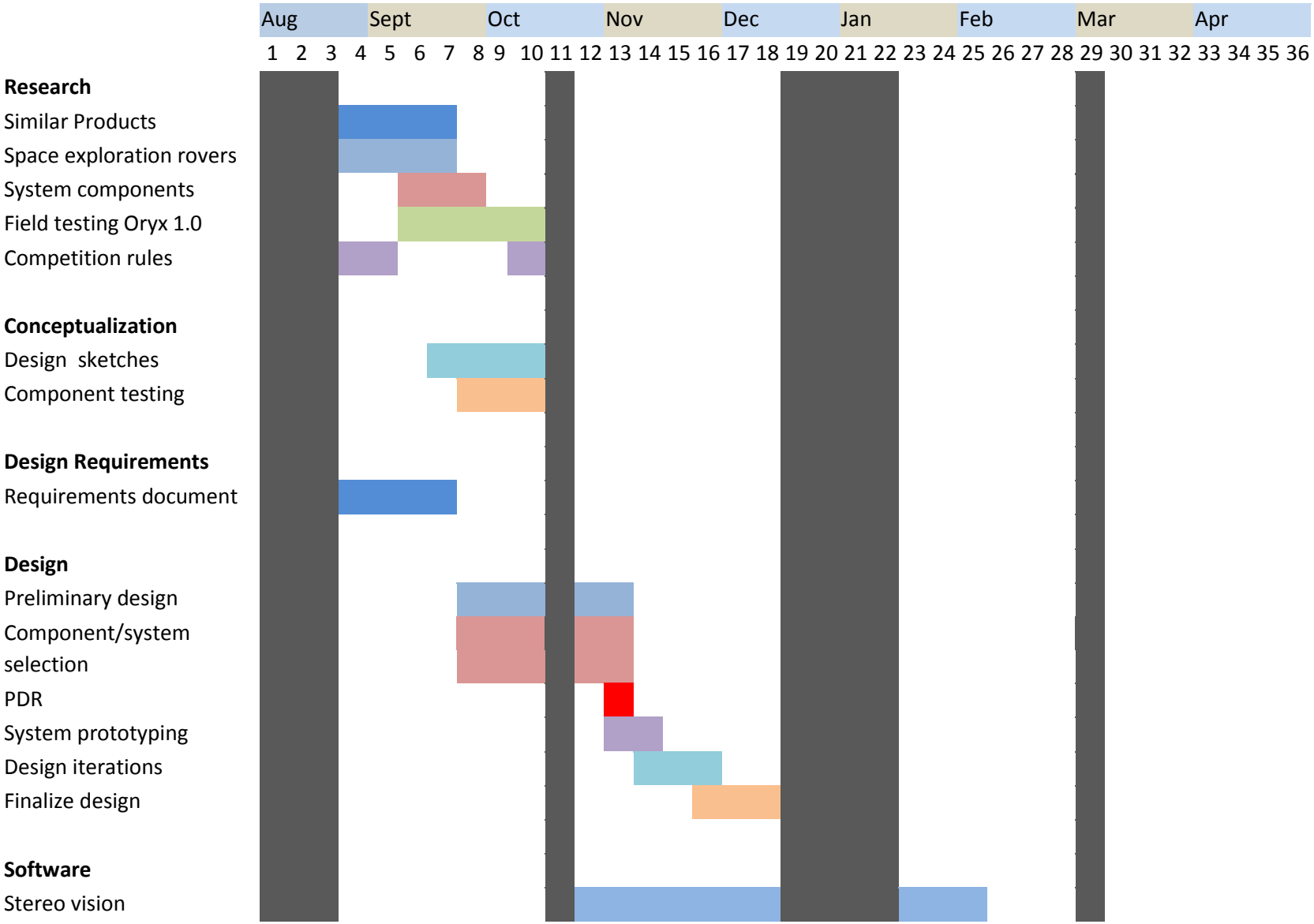

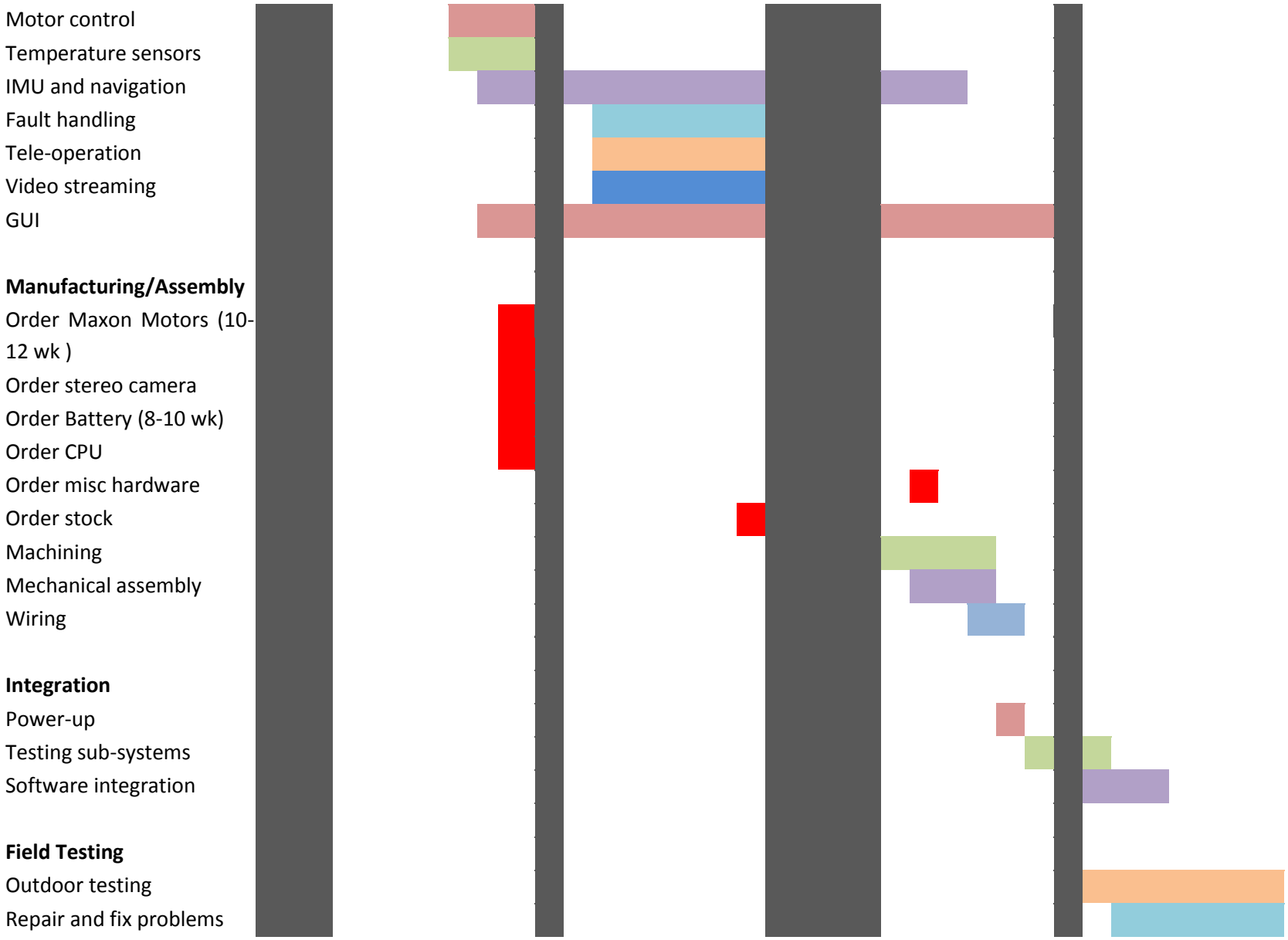
Motor control
Temperature sensors
IMU and navigation
Fault handling
Tele-operation
Video streaming
GUI
Manufacturing/Assembly
Order Maxon Motors (10-12 wk)
Order stereo camera
Order Battery (8-10 wk)
Order CPU
Order misc hardware
Order stock
Machining
Mechanical assembly
Wiring
Integration
Power-up
Testing sub-systems
Software integration
Field Testing
Outdoor testing
Repair and fix problems

Compete in Robo-Ops

CDR

APPENDIX D: RASC-AL Robo-Ops Design Specifications

2012 Planetary Rover Design Requirements

Requirements:

1. The rover must be no larger than 1m x 1m x 0.5m in a stowed configuration.
2. The rover must have a mass less than or equal to 45kg.
    a. The rovers will be weighed in at the beginning of the competition. They need to be fully assembled with all equipment prior to the weigh-in.
    b. Teams will be penalized 5% of their total score for every kg over the 45kg weight limit.
    c. After the weigh-in at the beginning of the competition, no additional mass can be added to the rover.
3. The rover must be able to traverse over obstacles up to 10cm in height.
4. The rover must be able to negotiate upslopes and downslopes of 33% grades.
5. The rover must be capable of selectively picking up irregularly shaped rocks with maximum diameters ranging from 2 to 8 cm and masses ranging from 20 to 150 gm. The rover must be capable of picking up a minimum of five of these rocks and transporting them using the rover throughout the course.
6. The rover must be capable of determining the color (red, purple, blue, green, yellow, or orange) of each of the rocks.
7. The Rover must be capable of traversing sand with no appreciable slope for a distance of at least 20 feet.
8. Each Team will have at most an hour to complete the course and required tasks.
    a. The rover cannot be charged, nor can batteries be swapped out during this time.
    b. The rover may not be actively operating for this entire time.
    c. The total amount of operational time will vary depending on the strategy used by each Team.
9. The rover cannot be powered by an internal combustion engine.
10. The rover must be able to operate in light rain, but the competition can be halted at the judges' discretion due to heavier rain.
11. The rover will be controlled remotely based solely on data, including video, gathered from the rover itself.
12. If the rover needs to be repaired after initial operation begins, judges will allow one human intervention lasting up to five minutes.
    a. The five minutes will be considered part of the overall time limit.
13. The rover will be controlled from the home campus of the university, with the video from the rover capable of being streamed through a web site.
    a. The Robo-Ops website will play the video streamed from your rover during the competition. Windows Media-enabled Code for the streaming link will need to

be submitted to NIA prior to the competition (cannot require an Applet, a separate Java App, or be Flash-based).

14. Communication with the rover will be through use of a Verizon broadband card, and each team is required to supply their own broadband cards. Typical data rates at the site are ~0.6Mb/s download and ~0.4Mb/s upload, and latency of 150-300ms. 3G or 4G are both are supported in the JSC Rock Yard area. Multiple Verizon cards can be used, if desired.
15. GPS devices can be used on a stationary base on the rover, but any "GPS base" needs to be packaged with the rover in the same volume and count in its total mass.

APPENDIX E: Drive Motor Comparative Analysis

Parameters		Resulting Requirements	
Wheel Diameter (m)	0.311	Speed of wheels (rpm)	73.69
Max speed (m/sec)	1.2	Speed of wheels (rads/sec)	7.72
Max slope (degrees)	30	Torque per motor (N-m)	8.57
Robot mass (kg)	45	Expect Accel on level ground (m/s^2)	4.90
		Time to max speed (sec)	0.24
		Total power (W)	264.55
		Total power at each wheel (W)	66.14

Motor: EC-4pole 30 Ø30 mm, brushless, 200 Watt

Motor Parameters

Nominal speed (rpm)	12500
Nominal torque (mNm)	124
Gear reduction	156
Gear box efficiency	0.62
Stall torque (mNm)	3220
Motor mass (grams)	300
Gearbox mass (grams)	460
Cost of motor	800
Cost of gear box	374

Expected Results

Speed (m/s)	1.30
Torque per wheel (Nm)	11.99
Continuous pushing force (N)	308.51
Stall pushing force (N)	8011.28
Max continuous incline (deg)	44.39
Max incline (degrees)	NA
Total mechanical power (W)	402.47
Total power at each wheel (W)	100.62
Total weight (grams)	3040.00
Power/mass ratio (W/kg)	132.39
Total cost	4696.00

Motor: EC-4pole 30 Ø30 mm, brushless, 100 Watt

Motor Parameters

Nominal speed (rpm)	12500
Nominal torque (mNm)	64.6
Gear reduction	156
Gear box efficiency	0.62
Stall torque (mNm)	1240
Motor mass (grams)	210
Gearbox mass (grams)	460
Cost of motor	620
Cost of gear box	374

Expected Results

Speed (m/s)	1.30
Torque per wheel (Nm)	6.25
Continuous pushing force (N)	160.72
Stall pushing force (N)	3085.09
Max continuous incline (deg)	21.37
Max incline (degrees)	NA
Total mechanical power (W)	209.67
Total power at each wheel (W)	52.42
Total weight (grams)	2680.00
Power/mass ratio (W/kg)	78.24
Total cost	3976.00

Motor: EC-4pole 22 Ø22 mm, brushless, 120 Watt

Motor Parameters

Nominal speed (rpm)	12500
Nominal torque (mNm)	61.8
Gear reduction	159
Gear box efficiency	0.6
Stall torque (mNm)	954
Motor mass (grams)	175
Gearbox mass (grams)	213
Cost of motor	800
Cost of gear box	374

Expected Results

Speed (m/s)	1.28
Torque per wheel (Nm)	5.90
Continuous pushing force (N)	151.66
Stall pushing force (N)	2341.13
Max continuous incline (deg)	20.11
Max incline (degrees)	NA
Total mechanical power (W)	194.11
Total power at each wheel (W)	48.53
Total weight (grams)	1552.00
Power/mass ratio (W/kg)	125.07
Total cost	4696.00

APPENDIX F: User Payload Development Guide

ORYX 2.0

A PLANETARY EXPLORATION MOBILITY PLATFORM

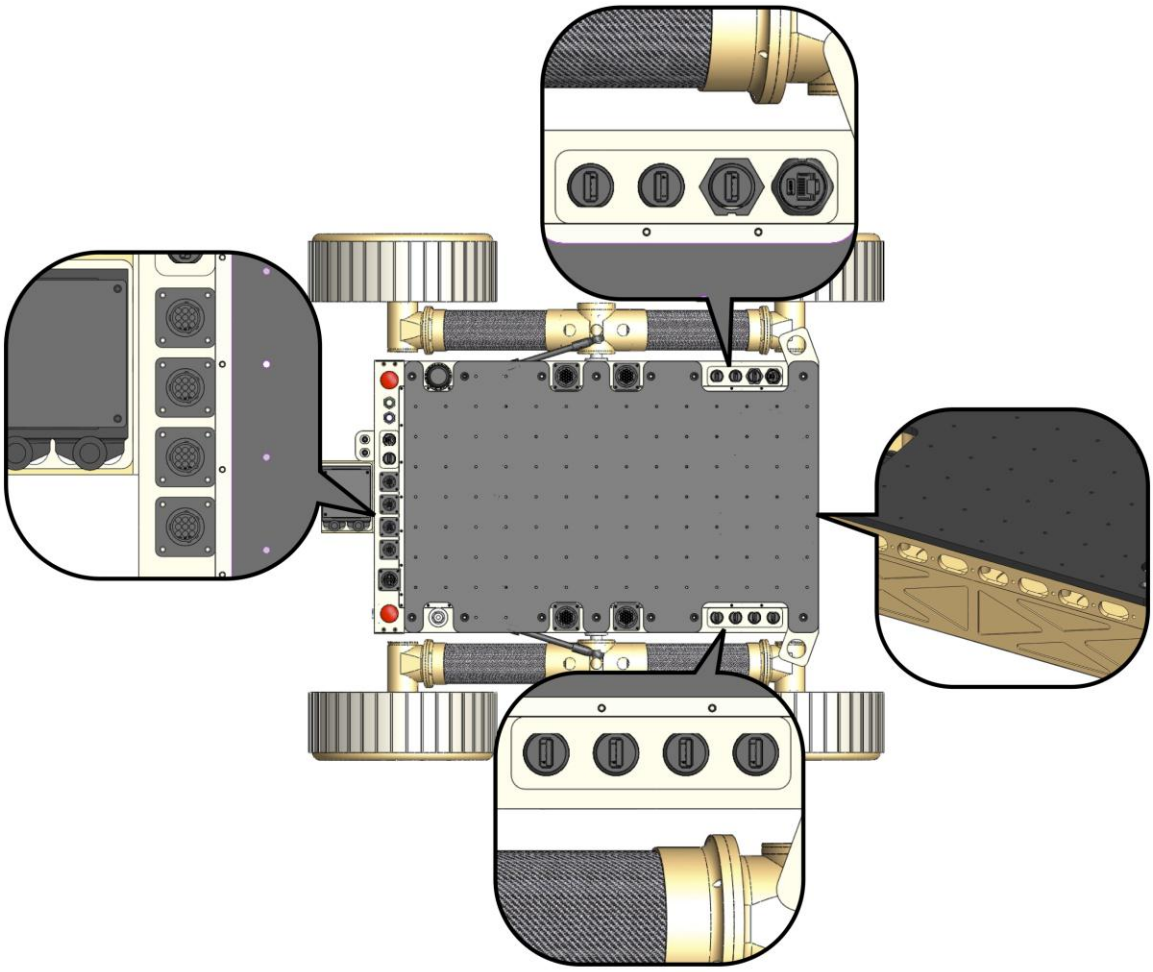

USER PAYLOAD DEVELOPMENT GUIDE

This document provides all the relevant information for those looking to develop custom payloads for ORYX 2.0. The mechanical, electrical, and software interfaces to the rover are discussed in detail.

PAYLOAD ARCHITECTURE

The primary purpose of space exploration rovers is to safely transport scientific instruments between sites of interest. Payload integration is often done in parallel with rover development resulting in highly specialized systems for a given mission.

ORYX 2.0 is a planetary exploration mobility platform that is low cost and accessible to smaller organizations. It was specifically designed for mission scenario testing in analog Martian and lunar environments. ORYX 2.0 includes mechanical, electrical, and software features that foster the development and integration of custom payloads.

MECHANICAL INTERFACE

To physically attach custom payloads to ORYX 2.0 there is a series of #10-32 tapped holes on the front and top of the rover much like an optics table.

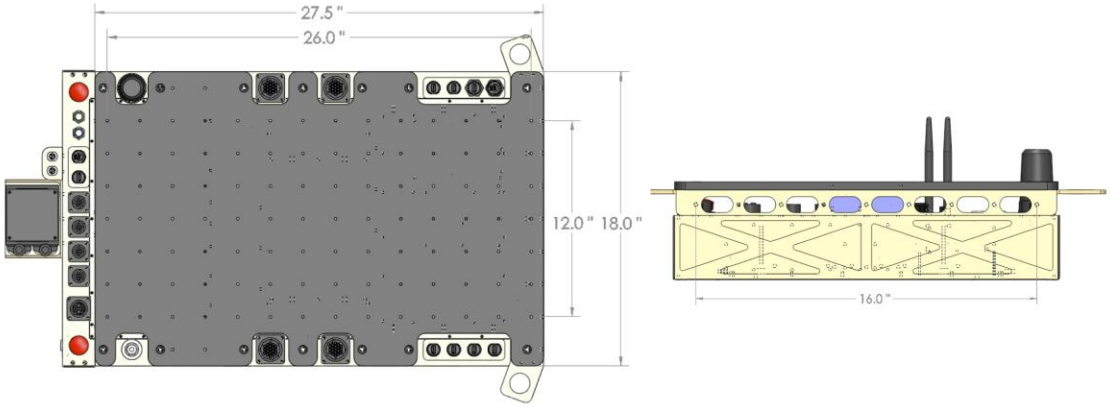

LOCATION	DESCRIPTION	PAYLOAD CAPACITY
Top Plate	27.5” x 18” x 3/8” Aluminum, 2” x 2” grid of #10-32 holes	15 kg
Front	16”, 2” spaced #10-32 holes	3 kg

FOR MORE INFORMATION ON ORYX 2.0, VISIT **WWW.WPIROVER.COM**

ELECTRICAL INTERFACE

In order to provide power to user payloads ORYX 2.0 was designed with 4 identical TE Connectivity Circular Plastic Connectors (TE PN: 206705-3) that each provide access to 5V / 12V / 24V busses. The user payload power pinout, current limit, and mating component list is tabulated below.

TE PIN #	PURPOSE	
1	24V+	
2	24V GND	
3	-	
4	12V+	
5	12V GND	
6	OneWire Temp +	
7	5V+	
8	5V GND	
9	OneWire Temp GND	

VOLTAGE	CURRENT PER PORT*
24V	10 AMPS
12V	3 AMPS
5V	2.5 AMPS

TE PART #	DESCRIPTION
206708-1	9-Pin Circular Plug
66592-1	Socket 22-18 AWG
1-66109-7	Socket 26-22 AWG
54123-1	9-Pin Heat Shrink Boot
58495-1	AMP PRO-CRIMPER III

* 24V bus connections fused at 10 amps, 12V 150W and 5V 50W current-limiting DC-DC converters

ORYX 2.0 has (8) accessible USB 2.0 ports and (2) accessible Ethernet ports that use L-Com IP67 waterproof connectors. These connectors will accept both standard cables (USB Type A, CAT-5E RJ45) as well as IP67 cable assemblies from L-Com.

L-COM PART #	DESCRIPTION
WPUSBAB-2M	IP67 USB Type A to USB Type B Cable Assembly, 2.0m
TRD5WP-1	IP67 RJ45 to RJ45 Cable Assembly, 1.0m

SOFTWARE INTERFACE

ORYX 2.0 has an on-board computer with a Intel Quad-core i5 processor that runs Linux Ubuntu 11.04. All of the software for the rover was developed using Robot Operation System (ROS) Electric Emys. All payload software should be developed on a similar system.

ROS

FOR MORE INFORMATION ON ORYX 2.0, VISIT WWW.WPIROVER.COM

EXAMPLE: DEPLOYABLE PAN TILT CAMERA

As an example payload a deployable pan tilt camera module was developed. This module can be attached or detached from the rover in the field with a single tool in approximately 5 minutes.

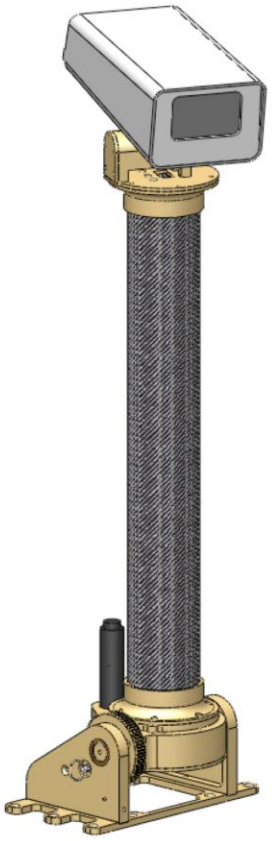

CATEGORY	INTERFACE
Mechanical	Attached to the top plate with (10) #10-32 x 1/2" fasteners
Electrical Power	24V power via user power connector to both the motor controllers and the camera
Electrical Communication	Camera interfaced to computer using Ethernet, Motor controllers interfaced using USB 2.0
Software	Custom ROS packages developed for controlling pan and tilt; accessing the IP camera video; colored rock detection

Clearpath Husky A100 upgrade to provide payload cross compatibility is available

FOR MORE INFORMATION ON ORYX 2.0, VISIT **WWW.WPIROVER.COM**